Electrocatalytic Ammonia Oxidation Mediated by a Cu(II) Complex: A Hydrazine Pathway to Hydrogen Generation

Thillai Natarajan M,[a] Deewan S. Teja,[b] Sk Samim Akhter,[a] Prabhakar Bhardwaj,[c] Pankaj Kumar,[c] Bhabani S. Mallik,[b] and Sumanta Kumar Padhi*[a]

[a] Artificial Photosynthesis Laboratory, Department of Chemistry and Chemical Biology, Indian Institute of Technology (Indian School of Mines), Dhanbad, Jharkhand 826004, India.

[b] Department of Chemistry, Indian Institute of Technology Hyderabad, Sangareddy, Telangana 502284, India.

[c] Department of Chemistry, Indian Institute of Science Education and Research (IISER), Tirupati, Andhra Pradesh 517507, India.

Supporting Information

Table of Contents

1. Materials and General Instrumentation.

Materials

All the reagent-grade chemicals and salts were procured from Alfa Aesar, Sigma Aldrich, and SRL chemicals, respectively, and were utilized as it was delivered. All the analytical-grade solvents were procured from Finar Chemicals Limited, double-distilled, and dried before use. For the electrocatalytic ammonia oxidation, aqueous ammonia (28%) and deuterated ammonia (ND_4OD) have been procured from Finar chemicals and CIL, respectively. The ammonia cylinder has been acquired from commercial sources. The pentadentate $^tBuN_2Py_3$ ligand has been synthesized by a modified procedure (described below). Some starting materials were purchased commercially, and some were synthesized according to the literature unless specified. The preparation of the complex is described below. All the starting materials and complexes were well-characterized by NMR, HR-MS, SC-XRD, and FT-IR. All the CV experiments used commercially available 28% aqueous ammonia and NH_3-CH_3CN (bubbled ammonia gas at a flow rate of 1 kg/cm^2 in dry acetonitrile). Gaseous products N_2 and H_2 were detected using gas chromatography. Before the controlled potential electrolysis, the reaction mixture was sparged with Argon to remove air, and then ammonia was added.

General Instrumentation

The NMR spectroscopy of ligand and starting materials was recorded in $CDCl_3$ on an ASCEND 400 BRUKER NMR spectrometer (298 K) at 400 MHz (for ^1H) and 100 MHz (for ^{13}C). The high-resolution mass spectrometry was recorded on a Waters XEVO G2-XS QTOF High-Resolution Mass Spectrometer. Rigaku SuperNova G8910B EosS2 single-crystal X-ray diffractometer equipped with an EosS2 CCD detector and having Mo Kα radiation (λ = 0.71073 Å) was used to

collect the X-ray diffraction data from suitable **[Cu1]** single crystals at 293 K. The elemental analysis (C, H, N) of **[Cu1]** was analysed using the UNICUBE Elementar Analysensysteme. UV-vis spectra of the complex before and after adding ammonia were recorded on an Agilent Technologies Cary 8454 photodiode array UV–visible spectrophotometer. FT-IR spectra were recorded on a PerkinElmer spectrometer. The EPR spectra of the paramagnetic **[Cu1]** complex before and after adding ammonia and after controlled potential electrolysis were made using the EMX MICROX, Bruker instrument. The UV-vis spectroelectrochemical studies were performed simultaneously using a Cary 8454 UV-vis spectrophotometer and a mSTAT300 DropSens Metrohm, respectively. The Quartz cuvette holding 1.0 mM analyte solution with the addition of 0.84 M aqueous and NH_3-CH_3CN (0.87 M) was employed. For CPE, the electrolytic solution was well sparged with argon before adding ammonia with a glassy carbon plate working, platinum plate counter, and saturated calomel reference electrodes where 0.1 M $[^nBu_4N]ClO_4$ was used as the supporting electrolyte. The gaseous products N_2 and H_2 were detected through GC-1310RJ gas chromatography through a molecular sieve column with a TCD detector, and argon was used as a carrier gas (flow rate: 5 kg/cm^2). Field Emission-Scanning Electron Microscope Supra 55 (Carl Zeiss) and SDD X MAX 50 EDS instrument were used for FE-SEM and EDX analyses, respectively, to analyze the surface morphology of the glassy carbon working electrode after the controlled potential electrolysis process. Formation of D_2 and N_2 from ND_4OD was detected using an online MS with OmniStarTM Gas Analysis System GSD 320 (Pfeiffer) quadrupole mass spectrometer apparatus. Raman analysis of the reaction mixture was performed in a LabRAM HR Evolution Raman microscope (HR UV-Open) using the cuvette method. To determine the concentration of NH_3 in CH_3CN, ^1H NMR spectra of an aliquot of gas-bubbled solution were recorded in CD_3CN in a 400 NMR spectrometer at 298 K.

2. Synthetic Procedures.

Scheme S1. Synthesis of 2-methyl-N-(pyridin-2-ylmethyl)propan-2-amine:

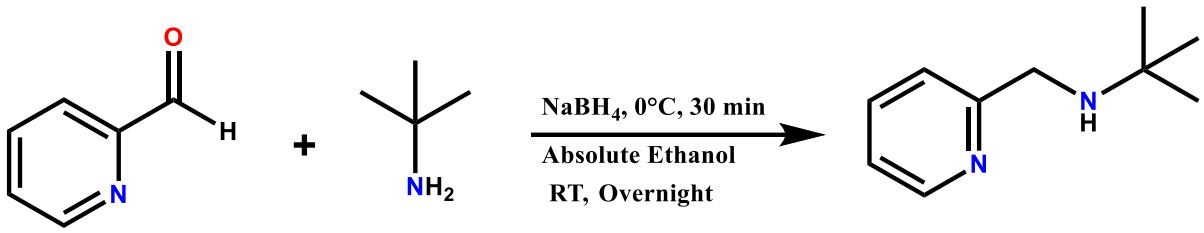

Pyridine-2-carboxaldehyde (1.5 g, 14 mmol) was dissolved in 20 mL dry ethanol, and then tertiary butylamine (1.766 mL, 19.7 mmol) was added. At 0 °C, inert atmosphere sodium borohydride (1.589 g, 42 mmol) was added portion-wise and stirred at room temperature overnight. After confirming with TLC that full consumption of the aldehyde, the reaction mixture was concentrated under a vacuum, the product was extracted using dichloromethane, washed with brine, dried by using sodium sulphate, and then filtered and concentrated under a vacuum to produce a yellowish oil. Yield: (2.12 g, 92 %). ^{1}H NMR (400 MHz, $CDCl_3$): δ (ppm) 8.40 (d, J = 4.5 Hz, 1H), 7.47 (td, J = 7.6, 1.7 Hz, 1H), 7.19 (d, J = 7.7 Hz, 1H), 7.02 – 6.92 (m, 1H), 3.75 (s, 2H), 1.69 (bs, 1H), 1.06 (s, 9H). ^{13}C NMR (100 MHz, $CDCl_3$): δ (ppm) 160.40, 149.08, 136.48, 122.52, 121.77, 50.54, 48.50, 29.04.

Scheme S2. Synthesis of dimethyl pyridine-2,6-dicarboxylate:

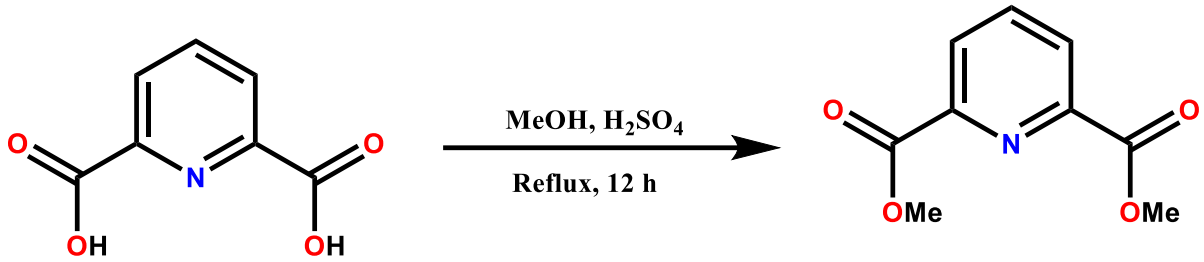

After the dissolution of pyridine-2,6-dicarboxylic acid (2 g, 12 mmol) in methanol (80 mL), 98 % H_2SO_4 (10 mL) was added at room temperature. The reaction mixture was refluxed for 12 h, and after it reached room temperature, the mixture was neutralized (pH = 7) by a saturated sodium bicarbonate solution. The product was extracted using dichloromethane, washed with brine, dried using sodium sulphate then concentrated in vacuo to produce a white crystalline solid. Yield: (2.3 g, 98 %). ^{1}H NMR (400 MHz, $CDCl_3$): δ (ppm) 8.33 (d, J = 7.8 Hz, 2H), 8.04 (t, J = 7.8 Hz, 1H), 4.04 (s, 6H). ^{13}C NMR (100 MHz, $CDCl_3$): δ (ppm) 165.08, 148.19, 138.46, 128.11, 53.28.

Scheme S3. Synthesis of pyridine-2,6-diyldimethanol:

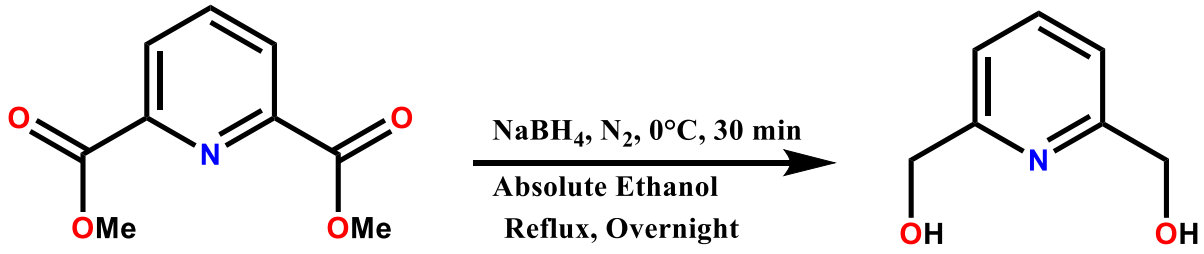

Pyridine-2,6-dicarboxylate (2.04 g, 10.5 mmol) was dissolved in dry ethanol (30 mL), and subsequently, under a nitrogen atmosphere, sodium borohydride (1.186 g, 31.3 mmol) was slowly added to the above solution at 0 °C. The reaction mixture was stirred for 2 h at room temperature followed by refluxing overnight, anhydrous potassium carbonate (2.89 g, 21 mmol) was added to quench the reaction further continued the reflux for 2 h. The reaction mixture was concentrated

under a vacuum, filtered using a sintered funnel, washed with dry THF, and again concentrated under a vacuum to produce an off-white powder. Yield: (0.93 g, 64 %). ^{1}H NMR (400 MHz, $CDCl_3$): δ (ppm) 7.73 (t, *J* = 7.7 Hz, 1H), 7.22 (d, *J* = 7.7 Hz, 2H), 4.81 (s, 4H), 3.43 (s, 2H. ^{13}C NMR (100 MHz, $CDCl_3$): δ (ppm) 158.34, 137.57, 119.22, 64.29.

Scheme S4. Synthesis of 2,6-bis(bromomethyl)pyridine:

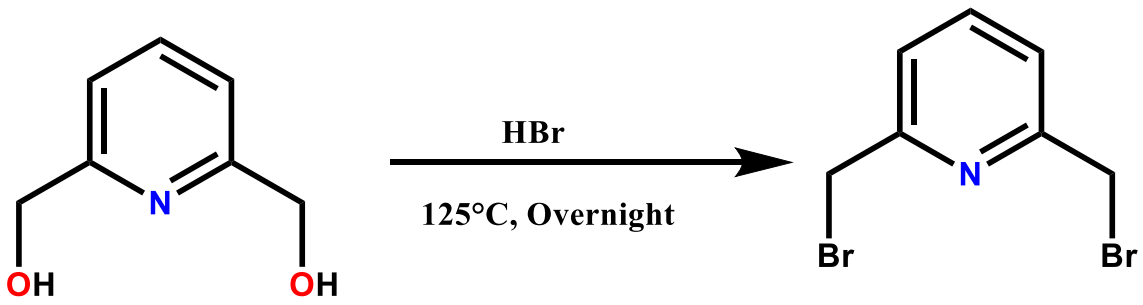

To a pyridine-2,6-dimethanol (1 g, 7.19 mmol) was added 15 mL of HBr (33% in glacial acetic acid), refluxed at 120 °C overnight. After it had reached room temperature, the mixture was neutralized (pH = 7) by a saturated sodium bicarbonate solution. The product was extracted using dichloromethane, washed with brine, dried using sodium sulphate then concentrated in vacuo to produce a brownish oil. Then, the reaction mixture was triturated using dichloromethane: petroleum ether (1:3, v/v) produced a precipitate, which was centrifuged, and the filtrate portion concentrated in vacuo produced a brownish solid. Yield: (1.78 g, 94 %). ^{1}H NMR (400 MHz, $CDCl_3$): δ (ppm) 7.71 (t, *J* = 7.7 Hz, 1H), 7.37 (d, *J* = 7.7 Hz, 2H), 4.54 (s, 4H). ^{13}C NMR (100 MHz, $CDCl_3$): δ (ppm) 156.75, 138.16, 122.84, 33.47.

Scheme S5. Synthesis of $^{t}BuN_2Py_3$:

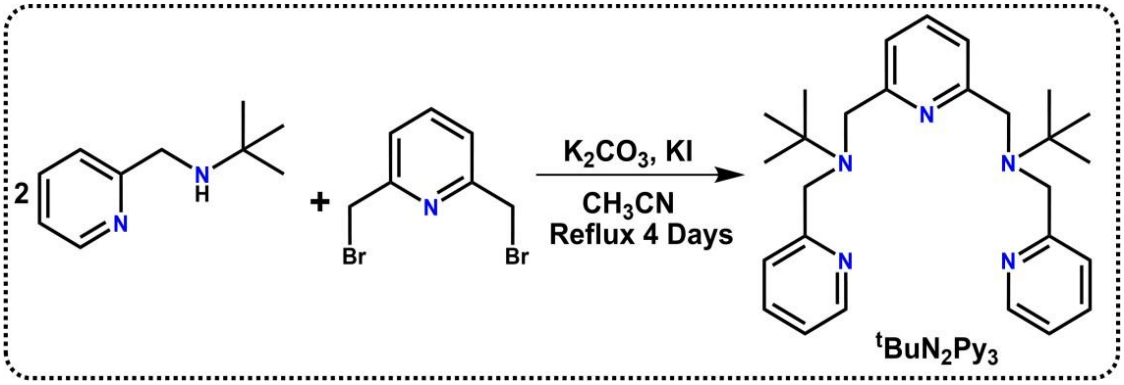

Stepwise reactions synthesized the pentadentate $^{t}BuN_2Py_3$ ligand. Initially, 2-methyl-N-(pyridin-2-ylmethyl)propan-2-amine was prepared using a modified procedure from the literature (**Scheme S1, Fig. S1 and S2**).[1] Next 2,6-bis(bromomethyl)pyridine was synthesized by a three-step reaction starting from pyridine-2,6-dicarboxylic acid (**Scheme S2−S4, Fig. S3−S8**).[2–4] 2,6-bis(bromomethyl)pyridine (1.5 g, 5.66 mmol) was dissolved in 30 mL acetonitrile, and potassium carbonate (3.130 g, 22.6 mmol) and potassium iodide (0.470 g, 2.83 mmol) were added to the reaction mixture while stirring. Pre-dissolved 2-methyl-N-(pyridin-2-ylmethyl)propan-2-amine (2.139 g, 13.02 mmol) in 10 mL acetonitrile was added dropwise into the reaction mixture and refluxed at 83 °C for 48 h, after confirming the consumption of limiting reagent through TLC, filtered the reaction mixture using the sintered funnel, washed with ethyl acetate for several times, the filtrate was concentrated in vacuo produces brown solid. The product was purified by trituration with dichloromethane: petroleum ether (1:10 v/v), precipitate was centrifuged, and the filtrate was concentrated in vacuo, producing a yellowish solid as a product. Yield: (1.976 g, 81%). ^{1}H NMR (400 MHz, $CDCl_3$): δ (ppm) 8.30 (d, J = 4.8 Hz, 1H), 7.39 – 7.38 (m, 2H), 7.36 – 7.26 (m, 1H), 7.19 (d, J = 7.7 Hz, 1H), 6.89 (dd, J = 8.6, 4.8 Hz, 1H), 3.86 (s, 2H), 3.81 (s, 2H), 1.09 (s, 9H). ^{13}C NMR (100 MHz, $CDCl_3$): δ (ppm) 162.51, 160.90, 148.26, 135.71, 135.67, 123.06,

121.14, 120.51, 56.62, 56.54, 55.81, 27.25. ESI-MS: The *m/z* calcd. for $[M+H]^+$ 432.3127; $[M+Na]^+$ 454.2942; found: 432.3112 and 454.2943 for $[M+H]^+$ and $[M+Na]^+$ respectively. FT-IR (KBr, cm^{-1}): 3042 (w), 2969 (m), 1467 (s), 1192 (s).

3. NMR Spectral Data.

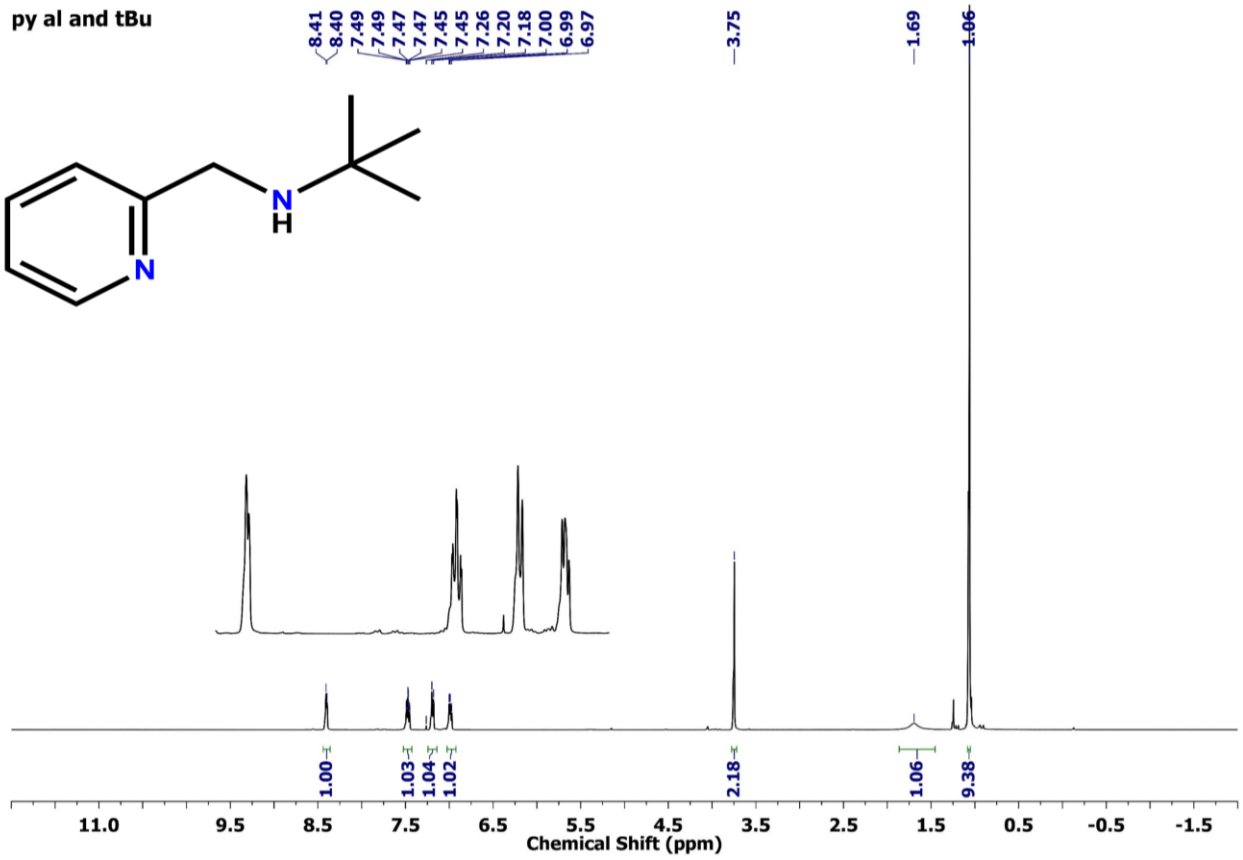

Fig. S1 ^1H NMR (400 MHz) spectrum of 2-methyl-N-(pyridin-2-ylmethyl)propan-2-amine in $CDCl_3$.

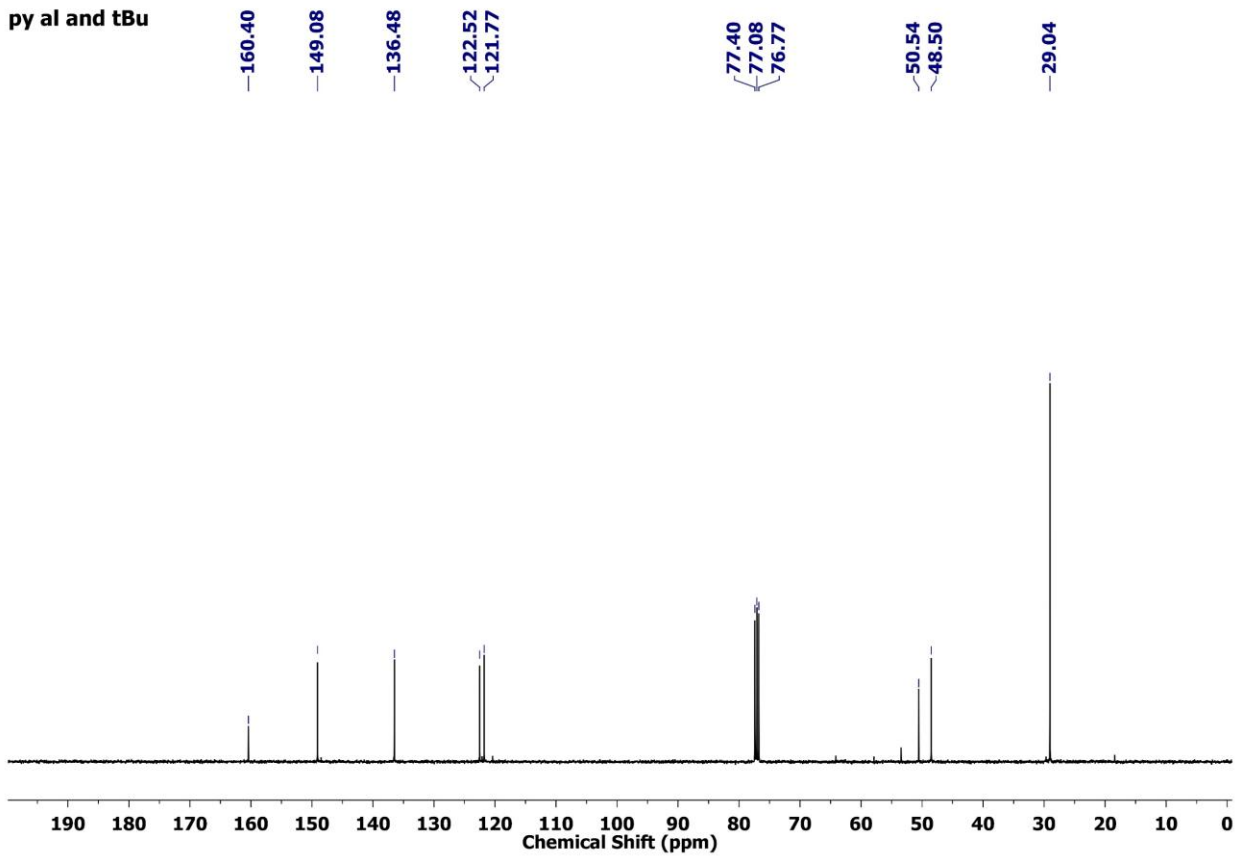

Fig. S2 $^{13}C\{^{1}H\}$ NMR (100 MHz) spectrum of 2-methyl-N-(pyridin-2-ylmethyl)propan-2-amine in $CDCl_3$.

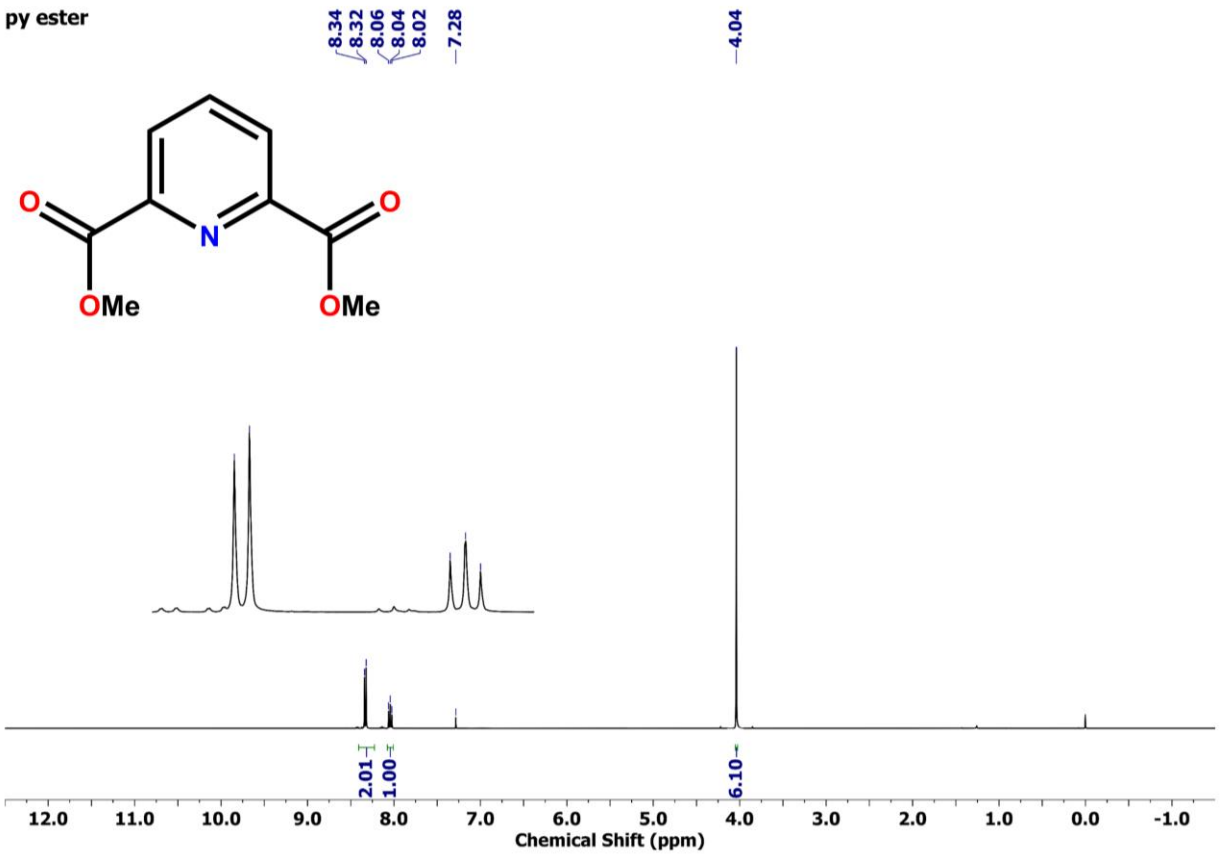

Fig. S3 ^{1}H NMR (400 MHz) spectrum of dimethyl pyridine-2,6-dicarboxylate in $CDCl_3$.

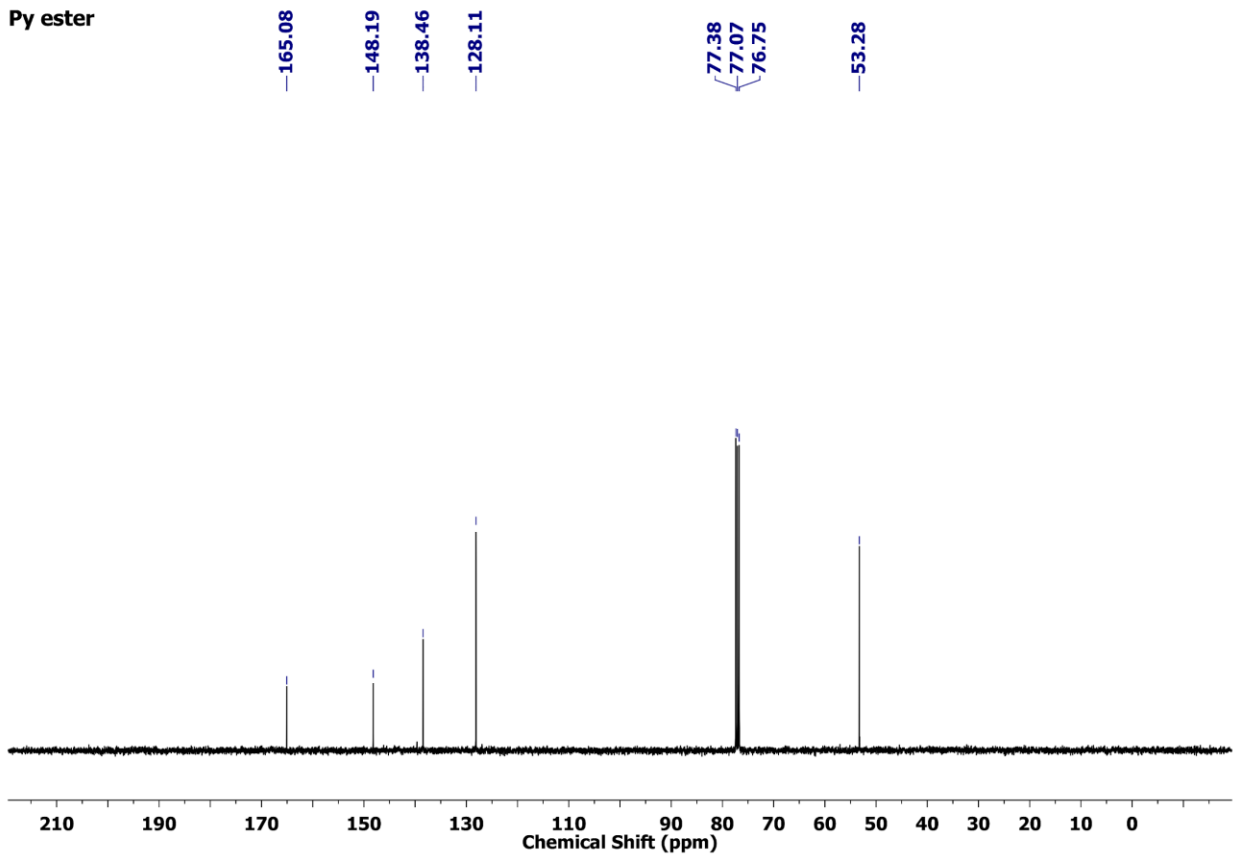

Fig. S4 $^{13}C\{^{1}H\}$ NMR (100 MHz) spectrum of dimethyl pyridine-2,6-dicarboxylate in $CDCl_3$.

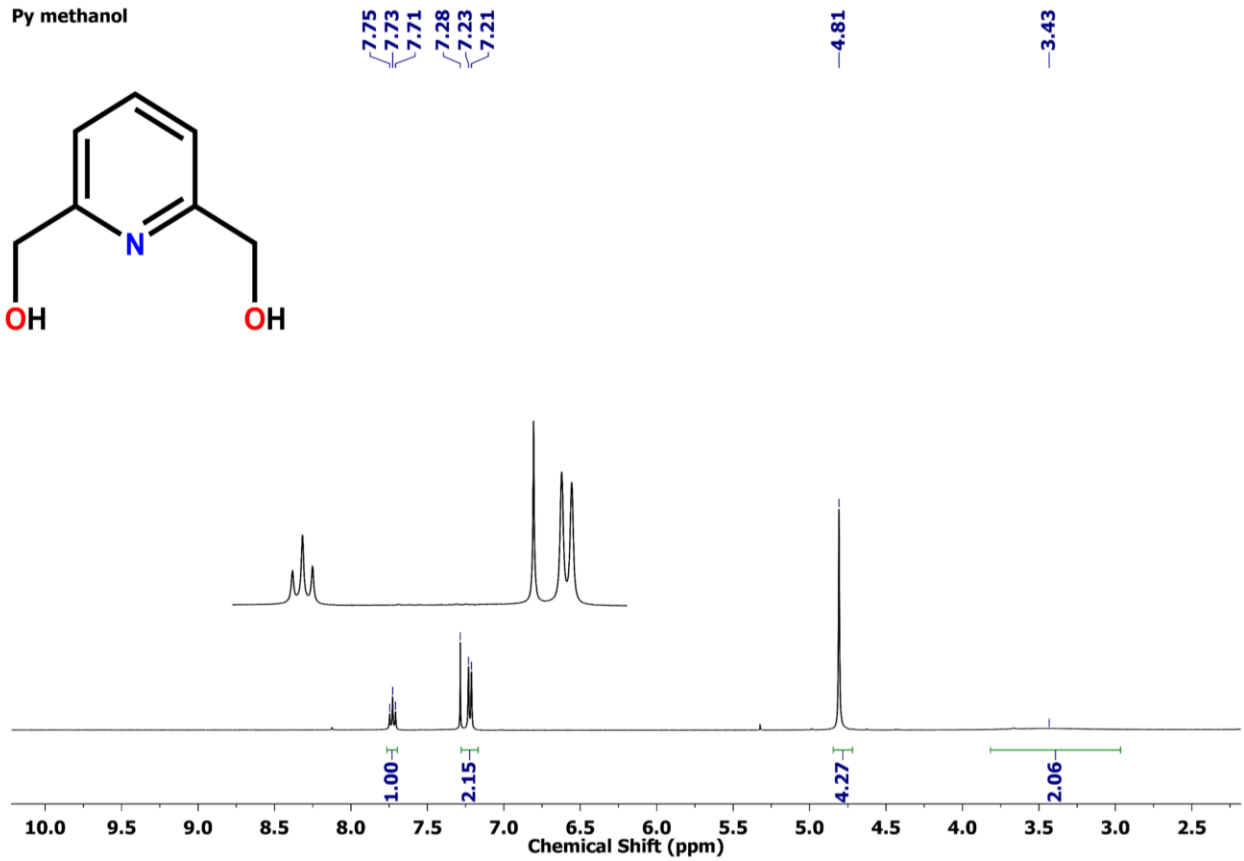

Fig. S5 ^{1}H NMR (400 MHz) spectrum of pyridine-2,6-diyldimethanol in $CDCl_3$.

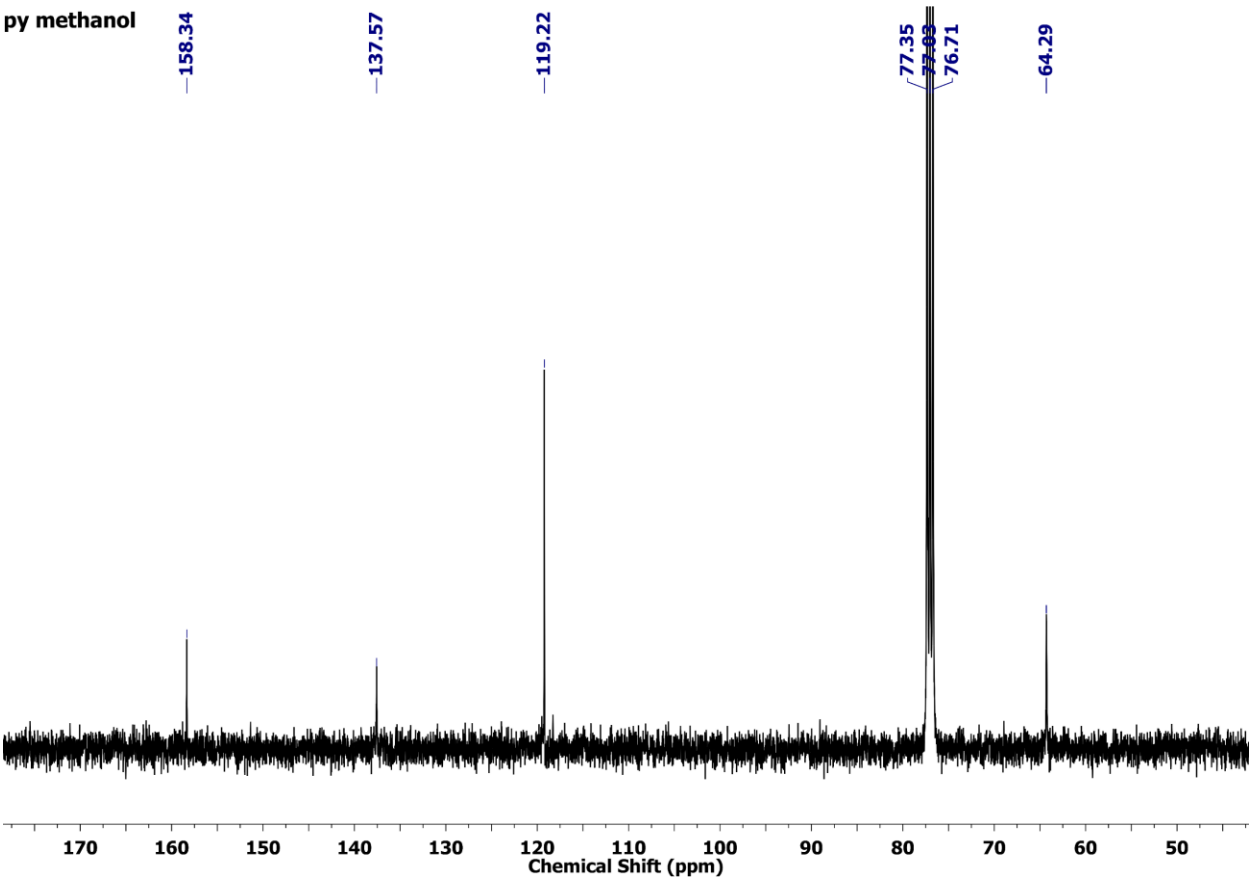

Fig. S6 $^{13}C\{^{1}H\}$ NMR (100 MHz) spectrum of pyridine-2,6-diyldimethanol in $CDCl_3$.

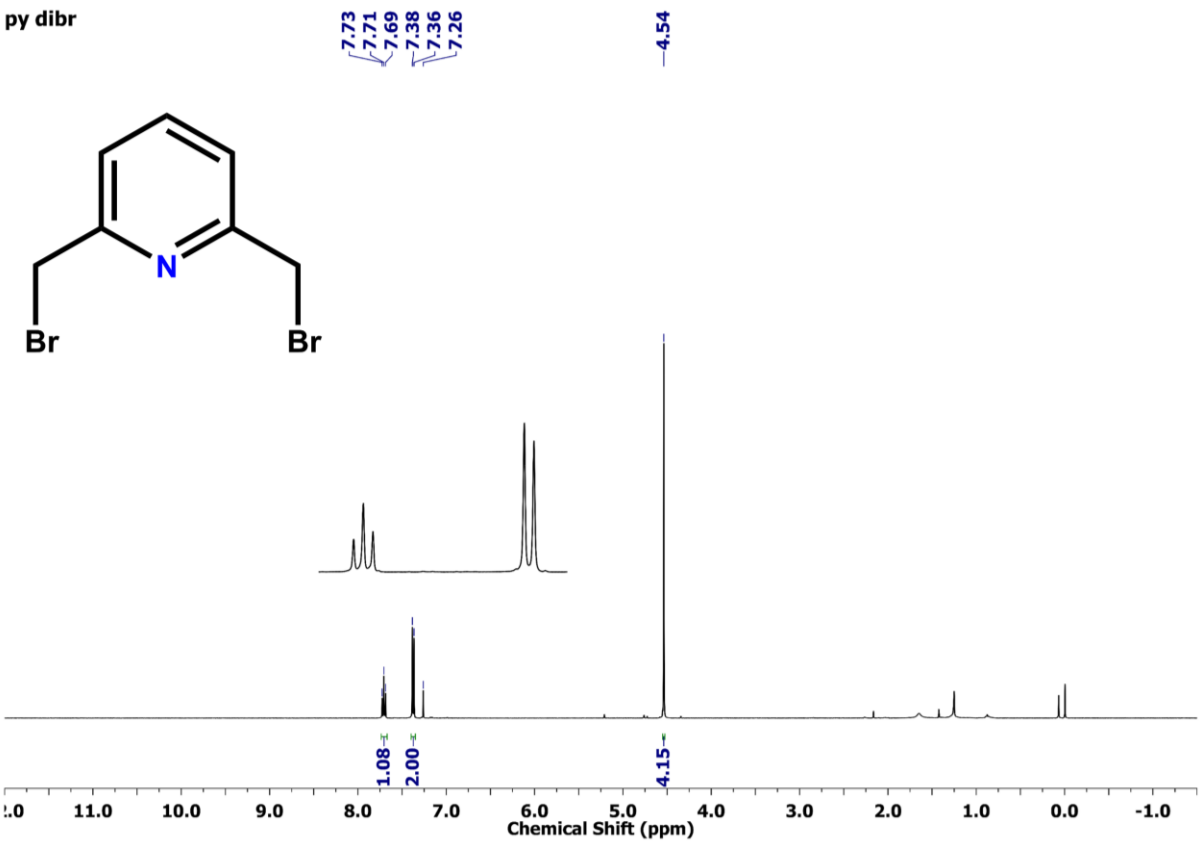

Fig. S7 ^{1}H NMR (400 MHz) spectrum of 2,6-bis(bromomethyl)pyridine in $CDCl_3$.

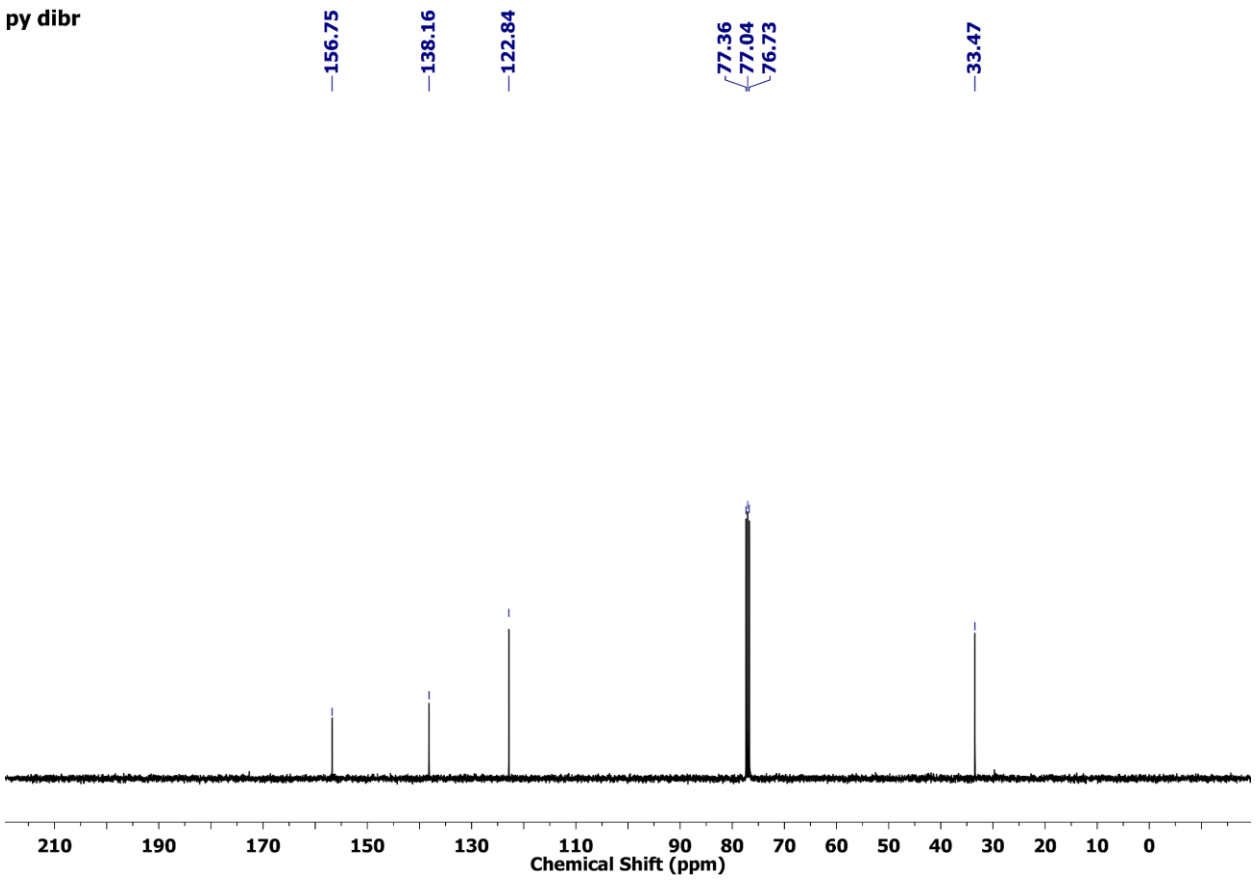

Fig. S8 $^{13}C\{^{1}H\}$ NMR (100 MHz) spectrum of 2,6-bis(bromomethyl)pyridine in $CDCl_3$.

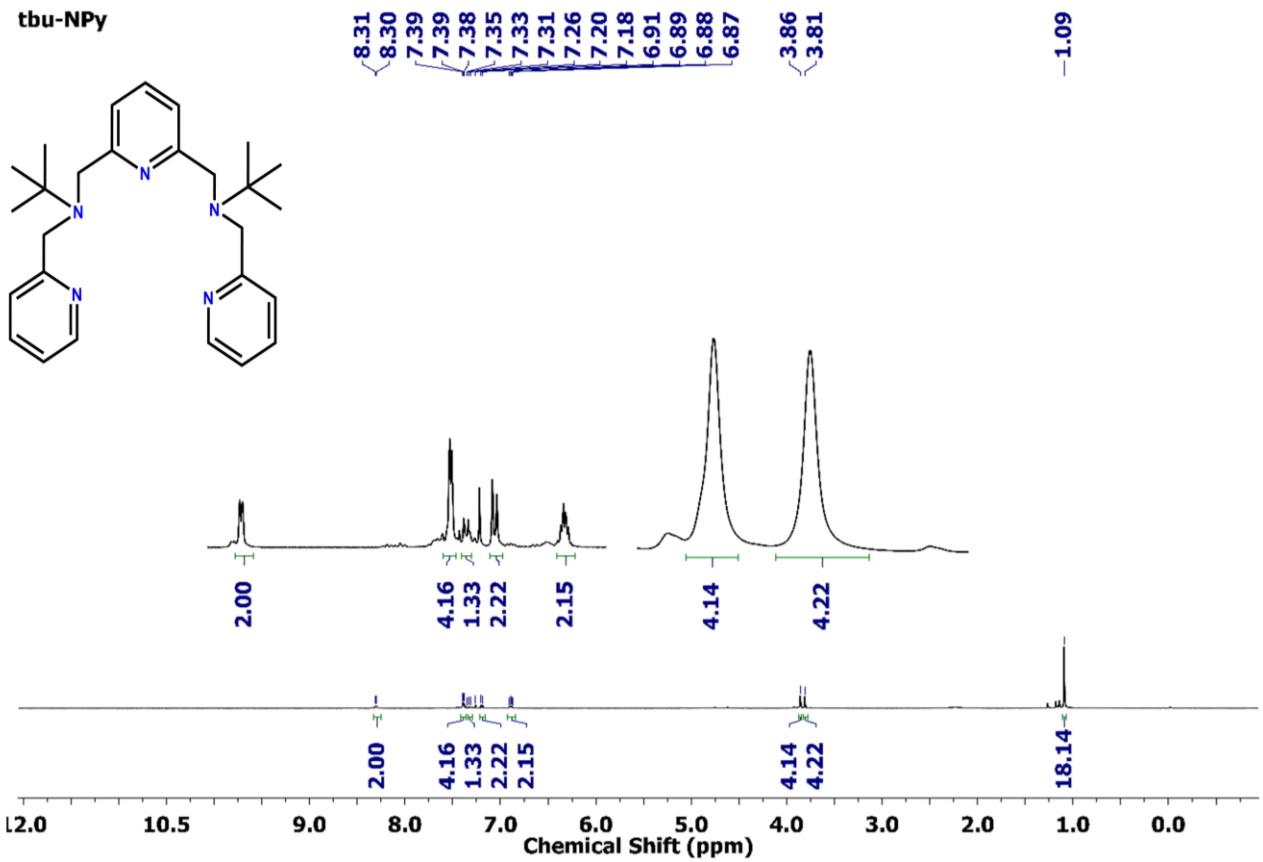

Fig. S9 ^{1}H NMR (400 MHz) spectrum of $^{t}BuN_2Py_3$ in $CDCl_3$.

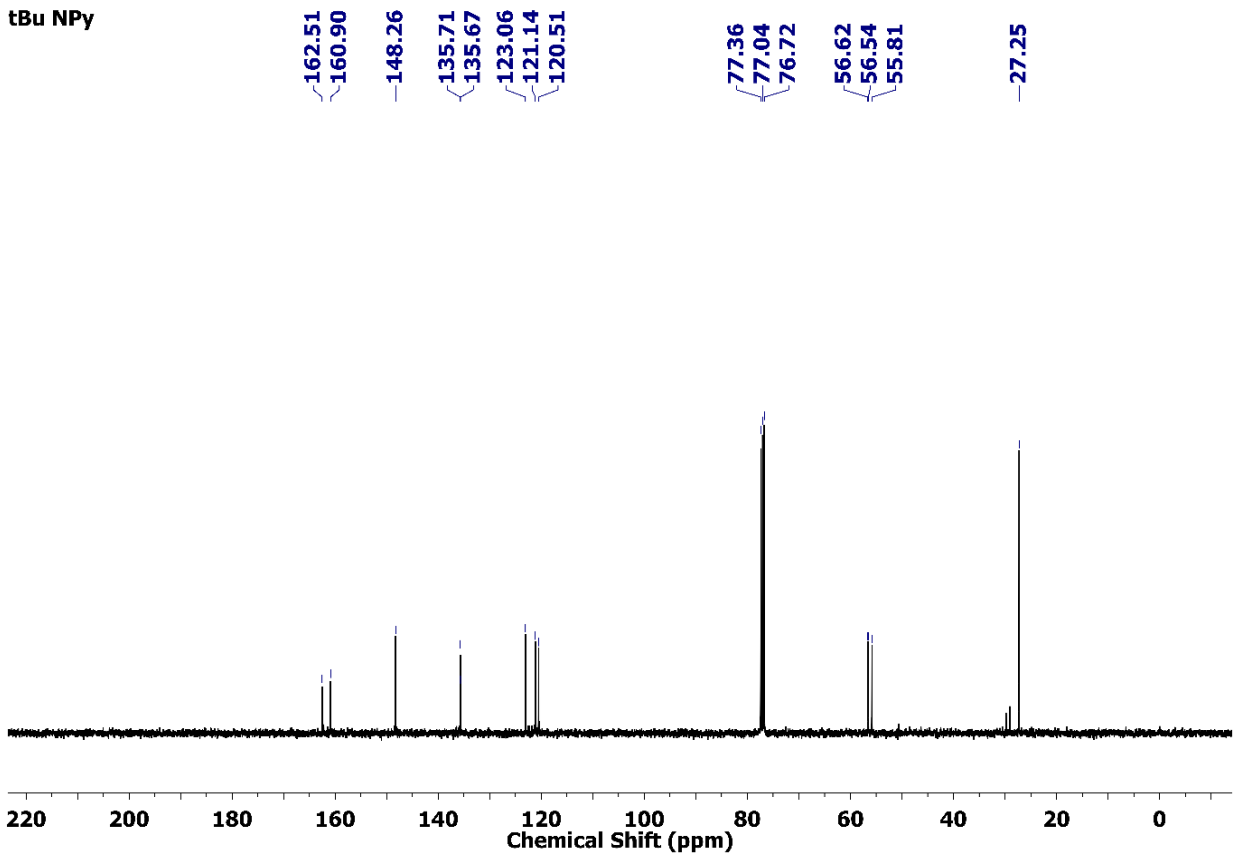

Fig. S10 $^{13}C\{^{1}H\}$ NMR (100 MHz) spectrum of $^{t}BuN_2Py_3$ in $CDCl_3$.

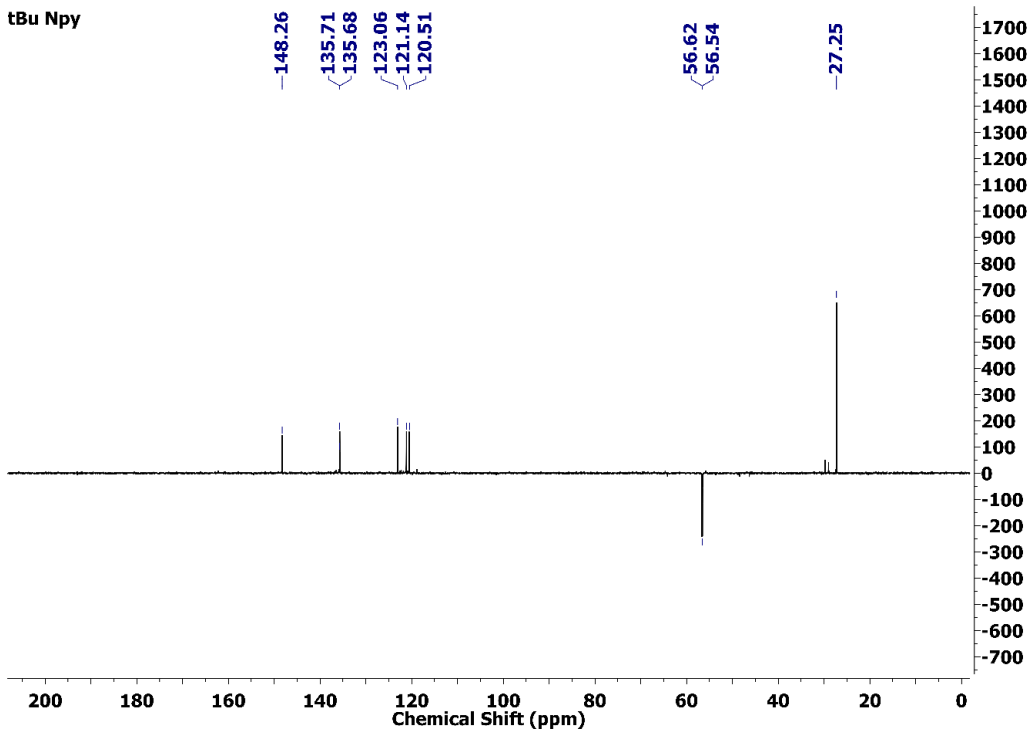

Fig. S11 $^{13}C\{^{1}H\}$ DEPT-135 NMR (100 MHz) spectrum of $^{t}BuN_2Py_3$ in $CDCl_3$.

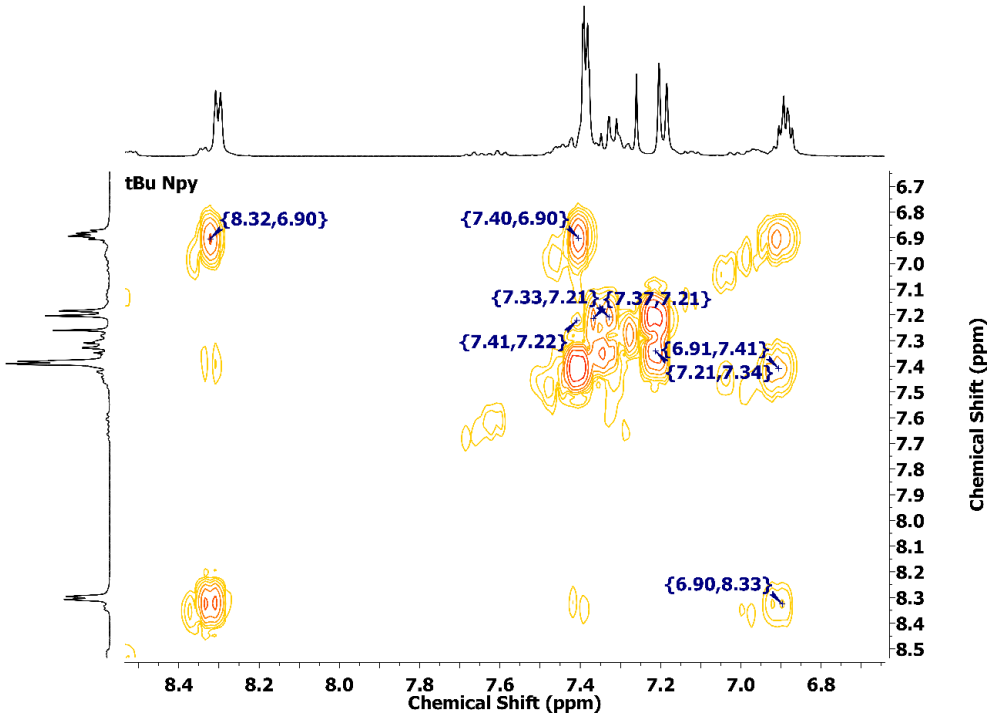

Fig. S12 ^{1}H-^{1}H NMR COSY (400 MHz) spectrum of $^{t}BuN_2Py_3$ in $CDCl_3$.

4. FT-IR and UV-vis Spectra.

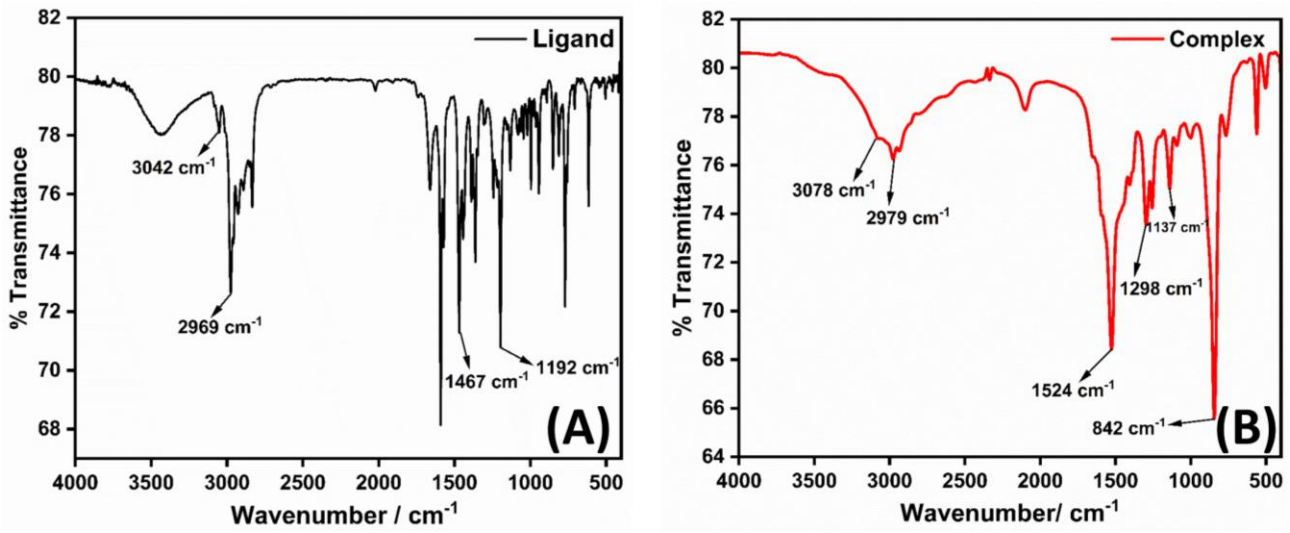

Fig. S13 FT-IR spectra of (A) $^{t}BuN_2Py_3$ (black trace), and (B) [Cu($^{t}BuN_2Py_3$) (red trace) recorded in KBr pellet at 298 K.

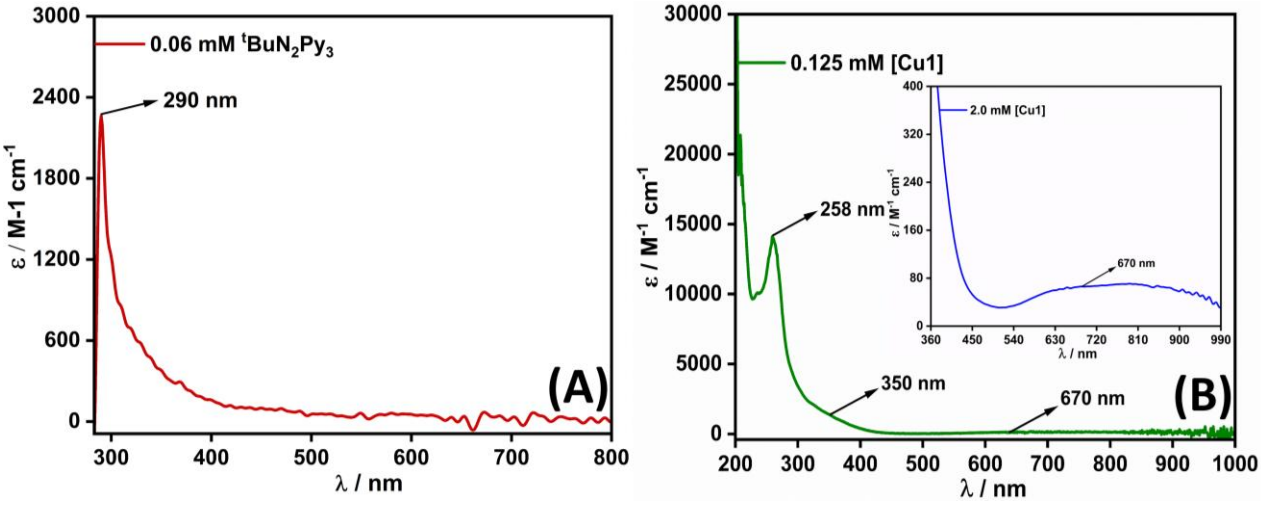

Fig. S14 The UV-vis spectra of (A) $^{t}BuN_2Py_3$ (0.06 mM) in CH_3CN (optical length: 10 mm), and (B) [Cu($^{t}BuN_2Py_3$)] (0.125 mM) in CH_3CN (optical length: 10 mm). (Inset) magnified view of [Cu($^{t}BuN_2Py_3$)] (2.0 mM) in the d-d band region of 600-900 nm.

5. Mass Spectral Data.

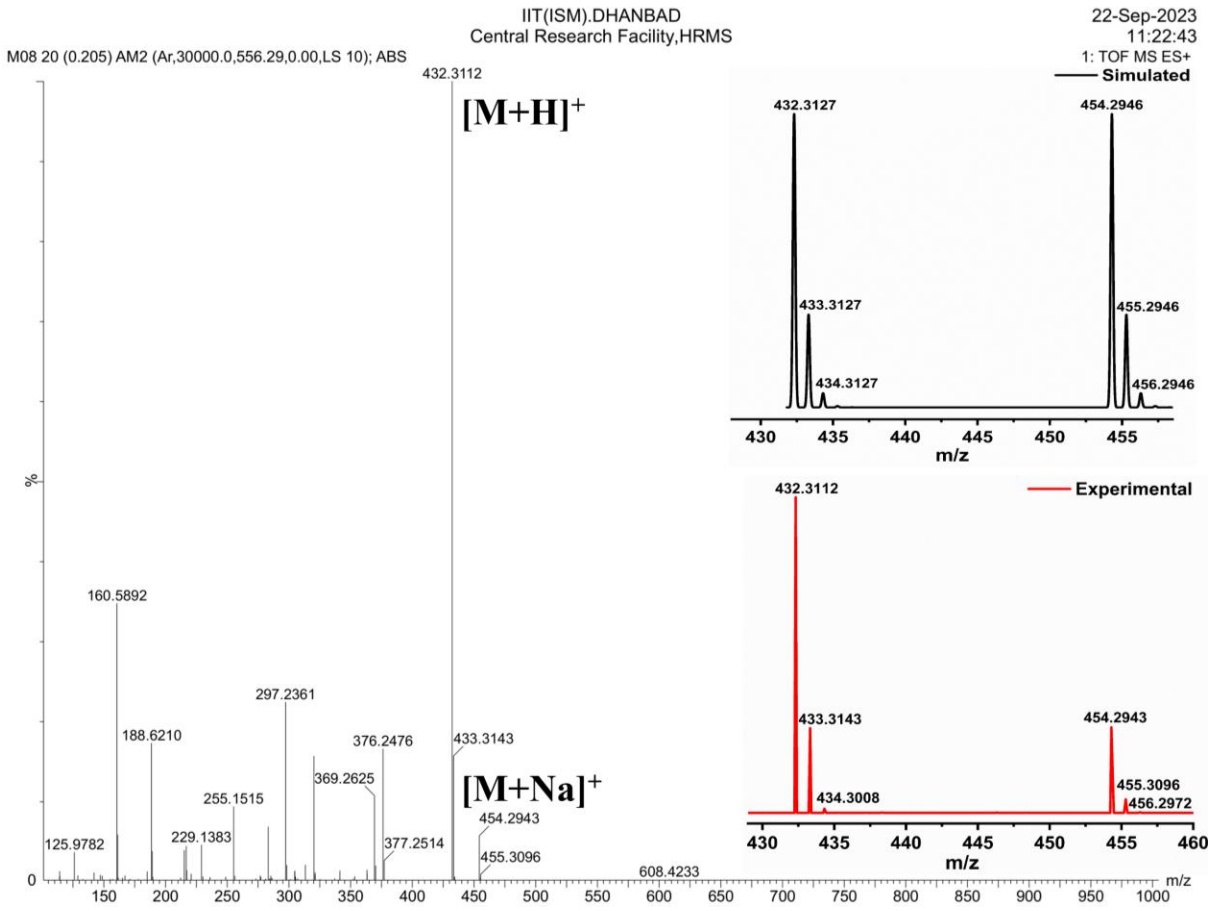

Fig. S15 ESI-MS spectrum of $^{t}BuN_2Py_3$ in acetonitrile. Inset: isotopic distribution patterns for $^{t}BuN_2Py_3$ (black trace: simulated, red trace: experimental).

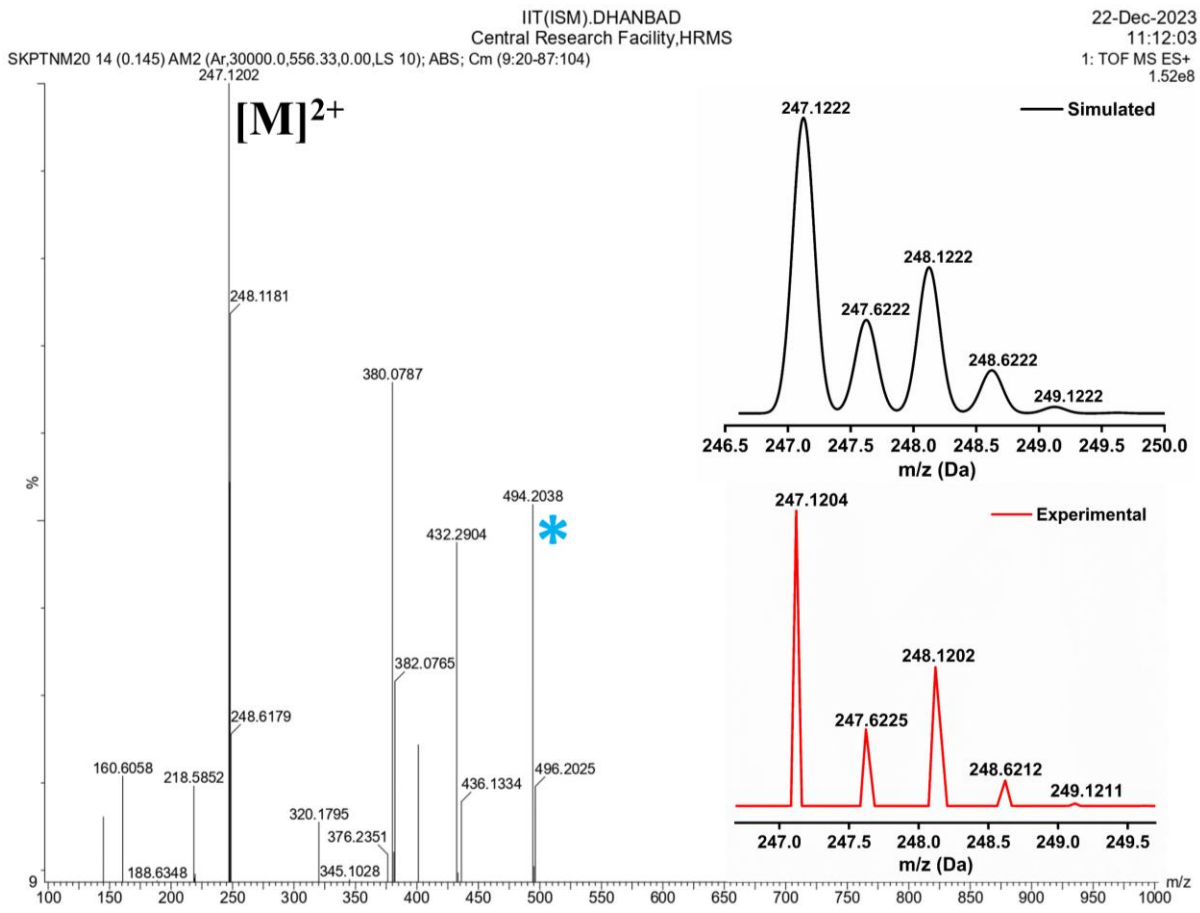

Fig. S16 ESI-MS spectrum of [Cu(^{t}BuN$_2$Py$_3$)] **[Cu1]** in acetonitrile (calcd, $[M]^{2+}$ = 247.1222; found, $[M]^{2+}$ = 247.1202). The peak at *m/z* 494.2038, marked with an asterisk is assigned to be $[M]^{+}$ pattern for **[Cu1]** (calcd, *m/z* = 494.2445). Inset: isotopic distribution patterns for **[Cu1]** (black trace: simulated, red trace: experimental).

6. CHN(S) Analysis of [Cu1].

Table S1 CHN(S) analysis of [Cu(^{t}BuN$_2$Py$_3$)].

[Cu(^{t}BuN$_2$Py$_3$)]	% Carbon	% Nitrogen	% Hydrogen
Theoretical	41.96	8.44	5.10
Experimental	**41.74**	**8.57**	**5.43**
Deviation	−0.22	+0.13	+0.33

7. Crystallographic Details.

A single-crystal X-ray diffraction experiment was performed to study the structural aspects of **[Cu1]** in depth. The crystal suitable for X-ray analysis was isolated by vapor diffusion of diethyl ether into a methanolic solution of **[Cu1],** yielding 74% concerning copper center (greenish block). The asymmetric unit consists of the **[Cu(^{t}BuN$_2$Py$_3$)]$^{2+}$** cation in the primary coordination sphere of the complex and two PF_6 counter ions. The X-ray analysis revealed that **[Cu1]** exhibits a monoclinic crystal system with a C2/c space group, the overall complex is neutral and displays a square pyramidal geometric configuration as evidenced by the value (0.065) of structure parameter, τ_5.

$$\boldsymbol{\tau_5 = \frac{\beta - \alpha}{60^\circ} \approx -0.01667\alpha + 0.01667\beta}$$

Table S2 Crystallographic data and processing parameters for **[Cu1]**

Identification code	CCDC 2449918
Empirical formula	$C_{54}H_{74}Cu_2F_{18}N_{10}P_3$
Formula weight	1425.241
Temperature (K)	293(2)
Crystal system	monoclinic
Space group	C2/c
a (Å)	17.5811(11)
b (Å)	22.9896(14)
c (Å)	17.8190(12)
α (°)	90
β (°)	93.358(6)
γ (°)	90
Volume ($Å^3$)	7189.8(8)
Z	4
ρ_{calc} (g/cm^3)	1.317
μ (mm^{-1})	0.744
F (000)	2938.5
Crystal size (mm^3)	0.22 × 0.2 × 0.18
Radiation	Mo Kα (λ = 0.71073)
2θ range for data collection (°)	3.62 to 50
Index ranges	$-23 \le h \le 23$, $-31 \le k \le 31$, $-24 \le l \le 22$
Reflections collected	17908
Independent reflections	6305 [R_{int} = 0.0547, R_{sigma} = 0.1349]
Data/restraints/parameters	6305/0/400
Goodness-of-fit on F^2	1.000
Final R indexes [I>=2σ (I)]	R_1 = 0.0691, wR_2 = 0.1590
Final R indexes [all data]	R_1 = 0.1176, wR_2 = 0.1808
Largest diff. peak/hole (e $Å^{-3}$)	0.94/-0.73

Table S3 Selected Bond Lengths for **[Cu1]**

Atom	**Atom**	**Length / Å**
Cu1	N1	1.913 (4)
Cu1	N2	1.972 (4)
Cu1	N3	2.122 (4)
Cu1	N4	2.230 (4)
Cu1	N5	2.238 (4)

Table S4 Selected Bond Angles for **[Cu1]**

Atom	**Atom**	**Atom**	**Angle / °**
N1	Cu1	N2	160.09 (18)
N3	Cu1	N2	83.86 (16)
N3	Cu1	N1	82.90 (16)
N3	Cu1	N4	156.19 (16)
N4	Cu1	N2	108.74 (16)
N4	Cu1	N1	79.17 (16)
N5	Cu1	N2	93.43 (16)
N5	Cu1	N1	106.35 (17)
N5	Cu1	N4	75.44 (16)
N5	Cu1	N3	125.10 (17)

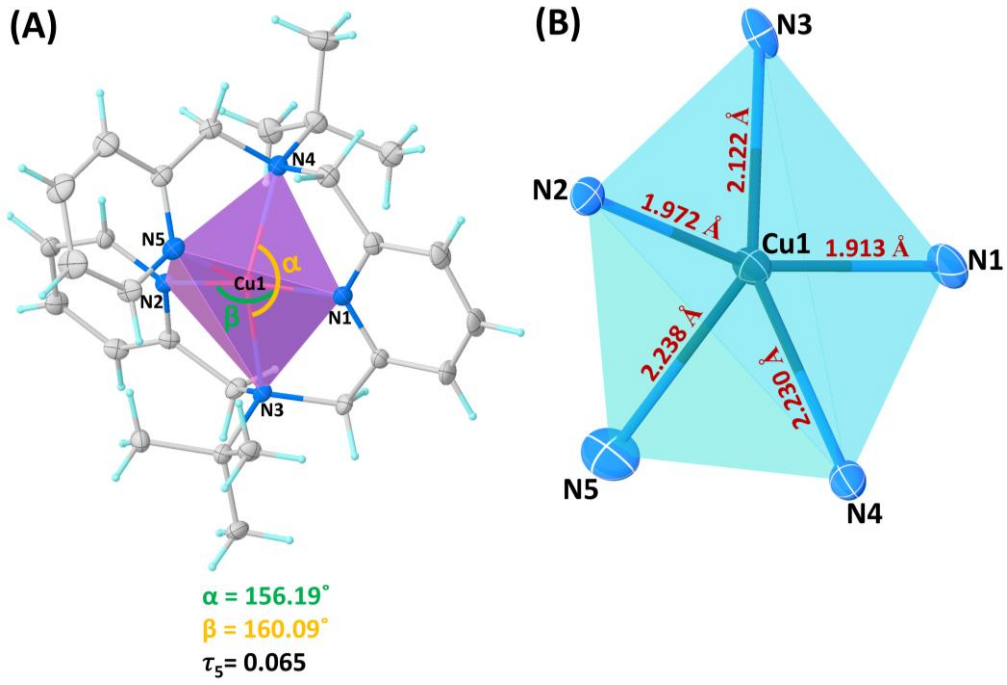

Fig. S17 (A) The structural parameter τ_5 in [Cu(^{t}BuN$_2$Py$_3$)], (B) The square pyramidal polyhedron of [Cu(^{t}BuN$_2$Py$_3$)] and bond distances at centers.

8. EPR Spectrum and Its Simulated Parameters.

The EPR spectra were recorded at X-band 9.32 GHz frequencies for the [Cu(^{t}BuN$_2$Py$_3$)](PF$_6$)$_2$ at various conditions. The details of simulated parameters are listed in **Table S5**. To investigate the catalyst stability, after performing controlled potential electrolysis of **[Cu1]** in 0.84 M NH$_{3(aq)}$ at 1.0 V for 1 h, the X-band EPR spectrum was recorded (**Fig. S18**). The spectrum was simulated with $g_x = 2.094$, $g_y = 2.047$, and $g_z = 2.255$ exhibits clearly resolved hyperfine splitting for $^{65/63}$Cu, I = 3/2, S = 1/2 ($A_x = 15$, $A_y = 30$, $A_z = 162$ G), it confirms the presence of Cu(II) center and stable after the ammonia oxidation reaction, the small bump on the lowest field part of the experimental spectrum at $g_y = 2.047$ indicates the anisotropic splitting.[5]

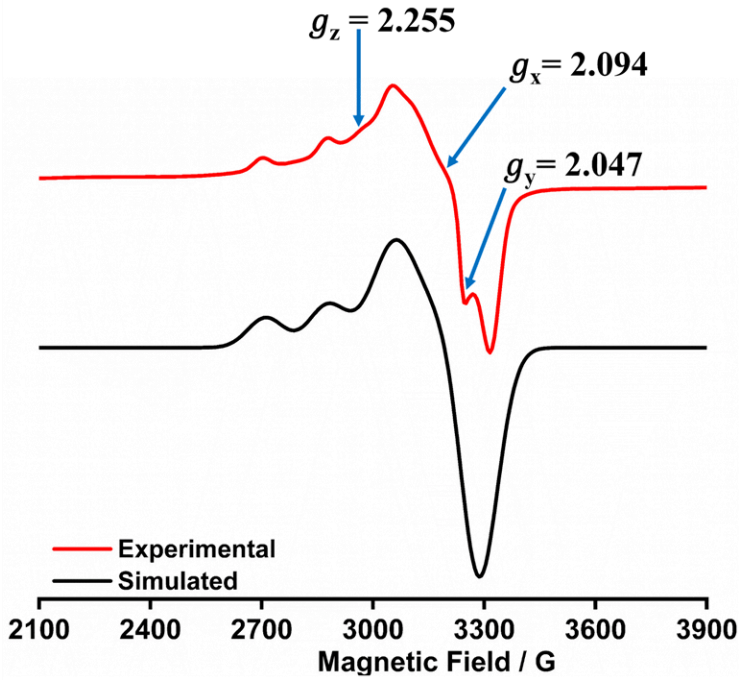

Fig. S18 The X-Band EPR Spectrum (red trace) was recorded at 100 K in a frozen glass of acetonitrile: toluene mixture after 1 h of CPE in 0.84 M $NH_{3(aq)}$ at 1.0 V and its simulation (black trace).

Table S5 Simulated EPR parameters of **[Cu1]**

	g-Matrix			**A-Matrix / G**			**D and E-Matrix / G**	
	g_x	**g_y**	**g_z**	**A_x**	**A_y**	**A_z**	**D**	**E**
[Cu1] in CH_3CN	2.077	2.077	2.225	3	5	141	0	0
[Cu1] in NH_4OH	2.067	2.067	2.264	5	40	165	0	0
[Cu1] after CPE	2.094	2.047	2.255	15	30	162	0	0

9. Determination of Magnetic Susceptibility of [Cu1] by the Evans' Method and SQUID.

The mixture of ^{t}BuOH/DMSO-d_6 (1:9, v/v) was made for 0.6 mL, where 50 µL of ^{t}BuOH solution was used as the standard for the paramagnetic shift and transferred into a capillary tube. In the remaining solution, 20 µmol of **[Cu1]** was added and transferred into an NMR tube. Subsequently, a capillary tube was also inserted. A ^{1}H NMR spectrum was recorded on an ASCEND 400 BRUKER NMR spectrometer (400 MHz) at 298 K, and the chemical shift of the ^{t}BuOH peak was 1.11 ppm. The effective magnetic moment (μ_{eff}) was calculated by Evans' method[6–9] according to the following equation:

$$\mu_{eff} = 798\sqrt{(\chi_m)T}$$

Using the Quantum Design MPMS SQUID (Superconducting Quantum Interference Device) VSM DC magnetometer, the Cu complex's variable-temperature magnetic susceptibility was determined. To investigate how the magnetic characteristics of the samples varied with temperature, the experiments were carried out over a wide temperature range, from 10 to 300 Kelvin. To keep the data consistent, the Cu complex was subjected to a continuous magnetic field of 1000 Oe.

Calculation:

(I) Diamagnetic Susceptibility (χ_D):

The following expression determined the diamagnetic susceptibility of a complex,

$$\chi_D = \frac{\text{Molecular weight of the complex}}{2} \times 10^{-6}\ \text{cm}^3\ \text{mol}^{-1}$$

$$\chi_D = -247.59 \times 10^{-12}\ \text{m}^3\ \text{mol}^{-1}$$

(II) Magnetic Susceptibility (χ_m) by Evans' method:

The following expression determined the magnetic susceptibility of a paramagnetic complex:

$$\chi_m = \frac{6}{1000} \times \frac{1}{c} \times \frac{\Delta f}{f}$$

Where,

c = Concentration of paramagnetic complex (mol L^{-1})

Δf = The shift in frequency of a reference compound (^{t}BuOH)

f = Frequency of NMR spectrometer (Hz)

For [Cu1]:

c = 33.6 $\times 10^{-3}$ mol L^{-1}

Δf = [1.11−1.01] $\times$400 Hz

(Or), Δf = 40 Hz

f = 400 $\times 10^{6}$ Hz

Now, χ_m (Cu1) = 0.0178 $\times 10^{-6}$ m^3 mol^{-1}

(III) Determination of effective magnetic moment (μ_{eff}):

$$\chi_p = \chi_m - \chi_D$$

For [Cu1]:

$\chi_p = \chi_m(\mathrm{Cu1}) - \chi_D(\mathrm{Cu1}) = (0.0178 \times 10^{-6} - (-247.59 \times 10^{-12}))$ m^3 mol^{-1}

(Or), $\chi_p(\mathrm{Cu1}) = 0.018 \times 10^{-6}$ m^3 mol^{-1}

Now, μ_{eff} (Cu1) = 798 $\sqrt{(\chi_m)T}$

$\mu_{eff} = 1.85\ \mu_B$

μ_{eff} for [Cu1] = 1.85 μ_B refers to the one unpaired electron present in the complex.

The experimental value for μ_{eff} is slightly higher than the spin-only value ($\mu_s = 1.73\ \mu_B$), and is typical for copper (II)-d^9 (S = 1/2) systems.[10]

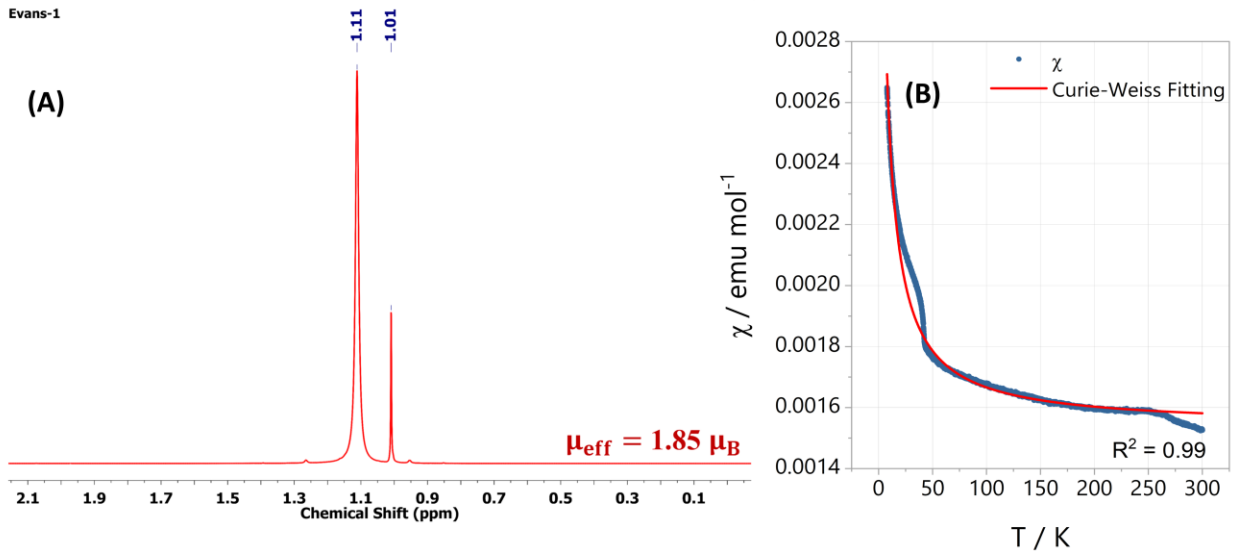

Fig. S19 (A) ^{1}H NMR spectrum (400 MHz, DMSO-d_6, 298 K) of tertiary butanol used for Evans' method of [Cu(^{t}BuN$_2$Py$_3$)] to determine magnetic susceptibility in solution. **[Cu1]** = 33.6 ×10^{-3} mol L^{-1}, Δf = 40 Hz, μ_{eff} = 1.85 μ_B. (B) χ_M vs. T plot unlocked from SQUID data.

10. Cyclic voltammograms.

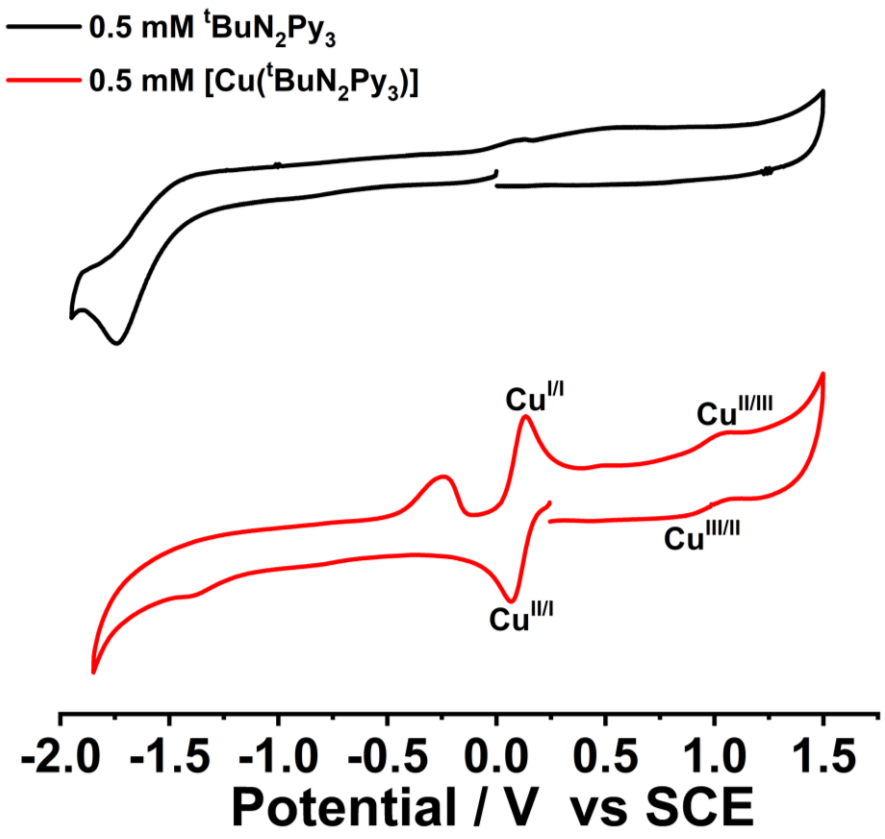

Fig. S20 Cyclic voltammograms of 0.5 mM $^{t}BuN_2Py_3$ (black trace) and 0.5 mM [Cu($^{t}BuN_2Py_3$)], **[Cu1]** (red trace) in acetonitrile referenced vs SCE. Conditions: 0.1 M [$^{n}Bu_4N$]ClO_4 supporting electrolyte, with GC working, platinum wire counter, and saturated calomel reference electrodes. Scan rate: 100 mV s^{-1}.

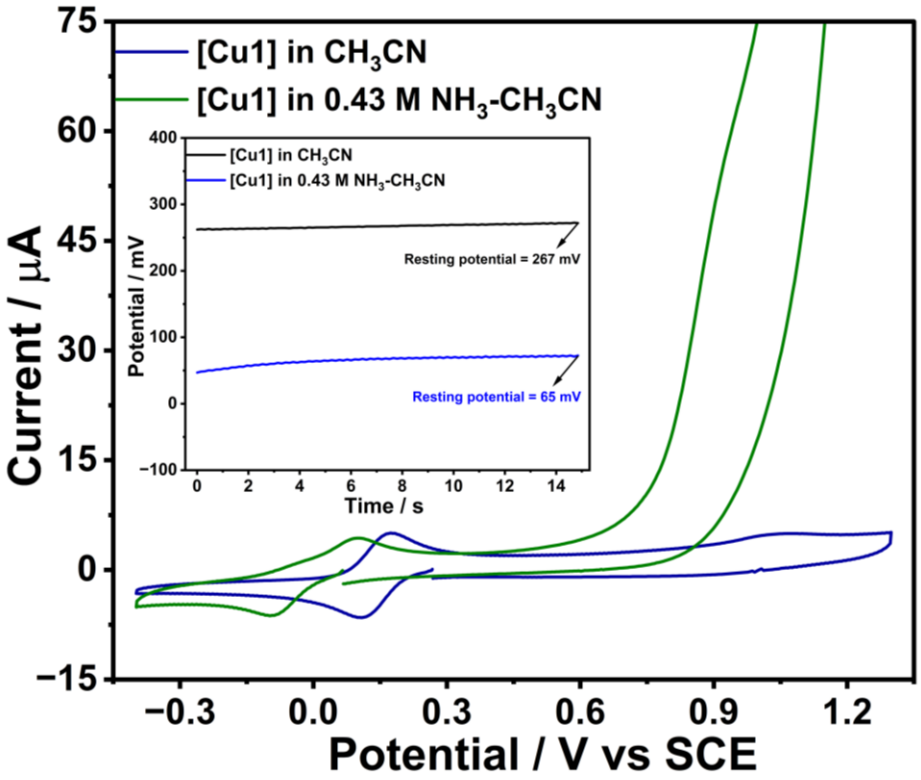

Fig. S21 Overlay of cyclic voltammograms of 0.5 mM **[Cu1]** in the absence (royal blue trace) and presence (olive trace) of 0.43 M NH_3-CH_3CN (Inset: resting potential in the presence and absence of ammonia in acetonitrile). Conditions: 0.1 M $[^nBu_4N]ClO_4$ supporting electrolyte, with GC working, platinum wire counter, and saturated calomel reference electrodes. Scan rate: 100 mV s^{-1}.

11. Determination of Diffusion Coefficient of [Cu1] by Cyclic Voltammetry in CH_3CN.

According to the Randles-Sevcik equation, the peak current of a redox process is given by

$$\mathbf{I_p = 0.4463\ n^{3/2}\ FA\ D^{1/2}\ [C_0]\ \upsilon^{1/2}\ (F/RT)^{1/2}}$$

Where, I_p is the peak current of the redox couple, n is the number of electrons participating in the redox reaction (n = 1 for $Cu^{II/I}$ redox couple of **[Cu1]**), F is the Faraday constant (96500 C mol^{-1}),

A is the surface area of the glassy carbon electrode (A = 0.07 cm^2), D is the diffusion coefficient of **[Cu1]** in the solution (cm^2 s^{-1}), C_0 is the concentration of **[Cu1]** in the bulk solution (10^{-6} mol/cm^3), υ is the scan rate (V s^{-1}), R is the gas constant (R = 8.314 J K^{-1} mol^{-1}), and T is the temperature (298 K). The diffusion coefficient (D) was calculated from the slope of I_p versus the square root of the scan rate ($\upsilon^{1/2}$) plot.

From the I_p vs $\upsilon^{1/2}$ plot, the slope for the anodic and cathodic waves was calculated to be 47.55 × 10^{-6} and −40.11× 10^{-6} $AV^{-1/2}$ s^{-1} respectively. Using the above equation, the diffusion coefficient for anodic and cathodic waves was determined to be D_a = 6.39 × 10^{-6} and D_c = 4.55 × 10^{-6} cm^2 s^{-1} respectively.[11]

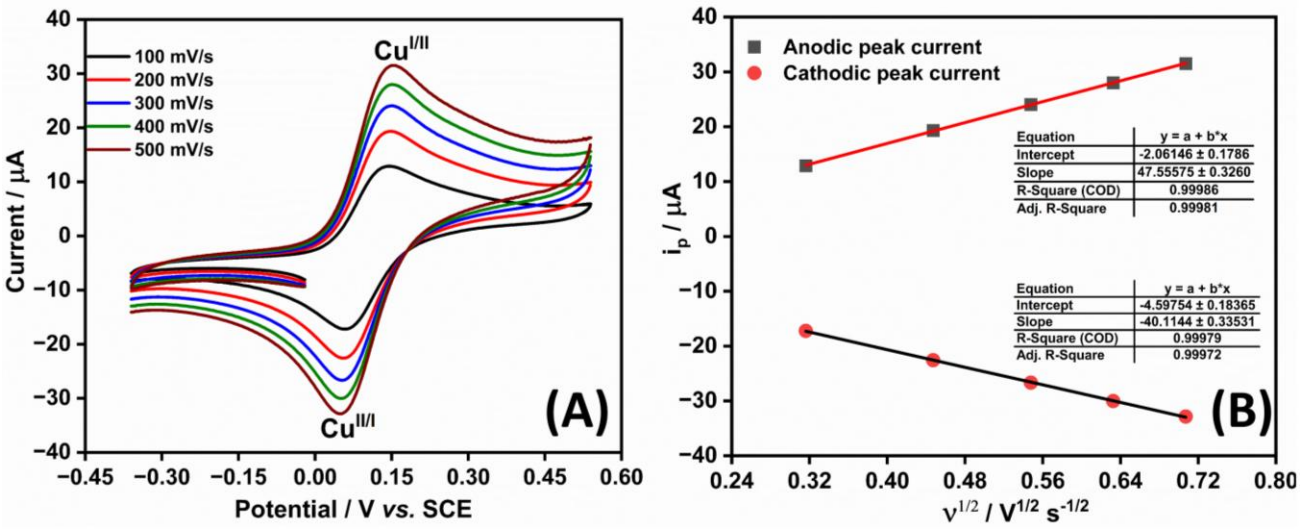

Fig. S22 (A) Cyclic voltammograms of $Cu^{II/I}$ redox couple in acetonitrile referenced vs SCE at scan rates 100−500 mV s^{-1}. Conditions: 0.1 M [^{n}Bu$_4$N]ClO$_4$ supporting electrolyte, with GC working, platinum wire counter, and saturated calomel reference electrodes. (B) The linear plot of I_p vs $\upsilon^{1/2}$ of $Cu^{II/I}$ redox couple (red line: anodic segment, black line: cathodic segment).

12. Determination of Ammonia Concentration by ^{1}H NMR Experiment.

A solution of tertiary butyl alcohol (30.0 µL, 3.1×10^{-4} mol) in 0.5 mL CD_3CN was added to a 3 mL vial. Dry acetonitrile was well-sparged with argon for 10 mins, 5 mL of the solution was transferred into a 15 mL vial, well closed with a septum, and then the dry acetonitrile solution was bubbled with $NH_{3\,(g)}$ for 2 mins (flow rate: 1 kg/cm^2). An aliquot (20 µL) of the saturated ammonia solution was added to the ^{t}BuOH-CD_3CN mixture. Further, to protonate ammonia, perchloric acid (70.0 µL, 1.16×10^{-3} mol) was added and the solution was analysed by ^{1}H NMR spectroscopy recorded in a 400 MHz NMR spectrometer (298 K). The concentration of ammonia was determined by integrating the ammonium proton of ammonium perchlorate resonance δ (ppm) 6.12 (0.76 H, $^1J_{H\text{-}N}$ = 53.27 Hz due to coupling with ^{14}N, 1:1:1 triplet) relative to the integration of internal standard δ (ppm) 1.38 (s, 9 H).[12–14]

$$[NH_3] = \frac{integration\ of\ NH_4^+}{integration\ of\ t_{BuOH}} \times [t_{BuOH}]$$

$$= \frac{0.76}{9} \times 10.3\ M$$

$$\mathbf{[NH_3] = 0.87\ M}$$

The experiments were repeated three times, and the concentration of ammonia was found to be 0.87 M $\pm$ 0.05 M. Keeping the same method, the concentrations of ammonia were calculated when lower concentrations of NH_3-CH_3CN were used for the CV experiments.

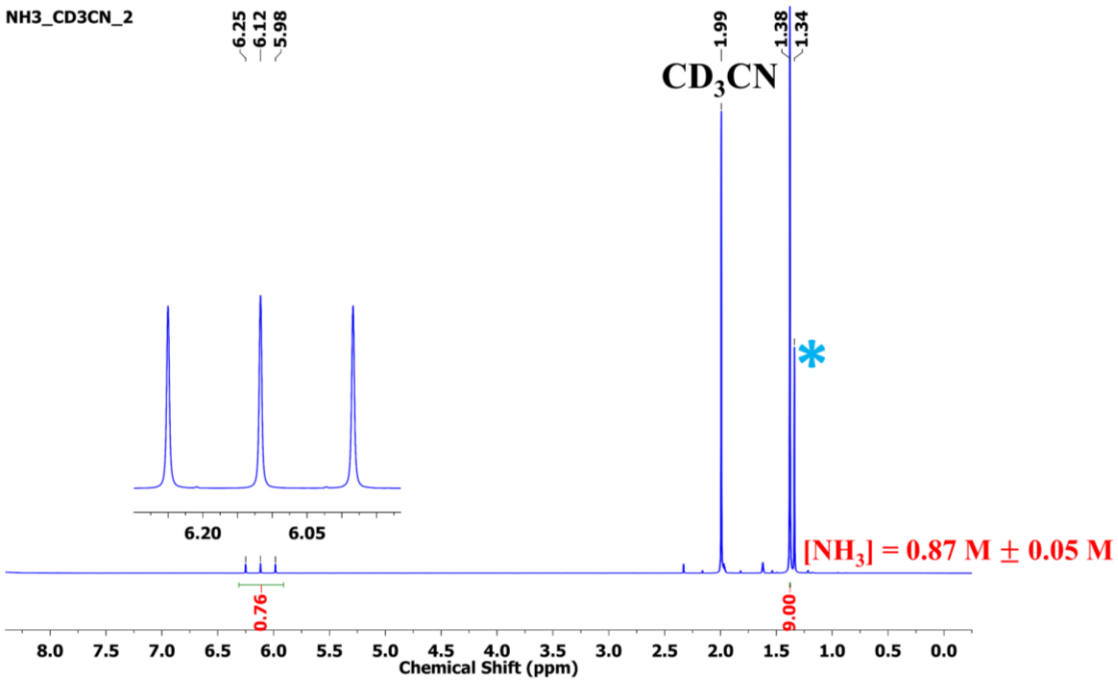

Fig. S23 ^{1}H NMR spectrum (400 MHz, CD_3CN, 298 K) of an aliquot of ammonia-bubbled solution in dry acetonitrile. Condition: bubbling of ammonia gas (flow rate: 1 kg/cm^2) for 2 mins in dry acetonitrile, tertiary butyl alcohol δ (ppm) 1.38 (s, 9H) was used as an internal standard, and perchloric acid was used as a proton source, * denotes the O-H peak of tertiary butanol.

13. Electrochemical Oxidation of Ammonia.

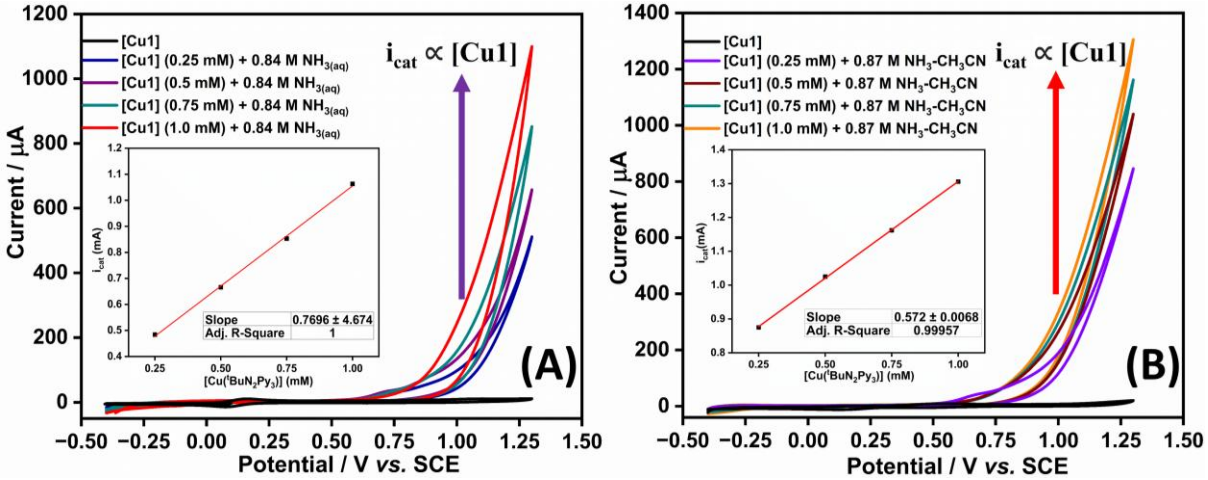

Fig. S24 Electrocatalytic oxidation of ammonia. (A) cyclic voltammograms of 0.25−1.0 mM **[Cu1]** in the presence of 0.84 M aqueous ammonia in acetonitrile. (B) cyclic voltammograms of 0.25−1.0 mM **[Cu1]** in the presence of 0.87 M NH_3-CH_3CN (ammonia gas bubbled in dry acetonitrile). Conditions: 0.1 M $[^nBu_4N]ClO_4$ supporting electrolyte, with GC working, platinum wire counter, and saturated calomel reference electrodes. Scan rate: 100 mV s^{-1}. (Inset: Corresponding I_{cat}, measured at 1.30 V vs SCE (mA) vs catalyst concentration (mM) plot for the rate dependence of **[Cu1]**.

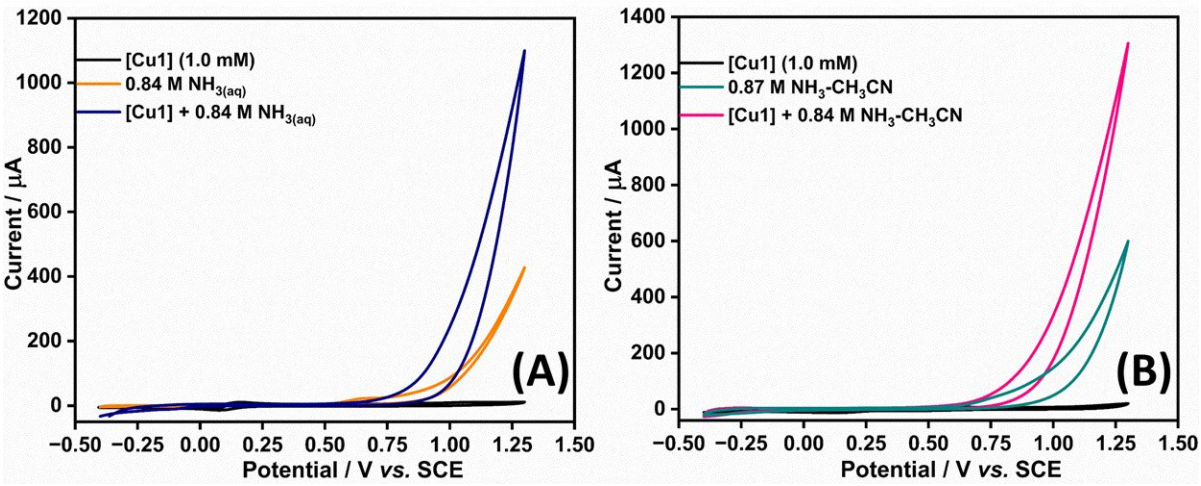

Fig. S25 (A) CVs of 1.0 mM of **[Cu1]** in acetonitrile (black trace), 0.84 M aqueous ammonia (orange trace), and **[Cu1]** (1.0 mM) in the presence of 0.84 M aqueous ammonia (navy blue trace). (B) CVs of 1.0 mM of **[Cu1]** in acetonitrile (black trace), 0.87 M NH_3-CH_3CN (ammonia gas bubbled in dry acetonitrile) (dark cyan trace), and **[Cu1]** in the presence of 0.87 M NH_3-CH_3CN (pink trace). Conditions: 0.1 M $[^nBu_4N]ClO_4$ supporting electrolyte, with GC working, platinum wire counter, and saturated calomel reference electrodes. Scan rate: 100 mV s^{-1}.

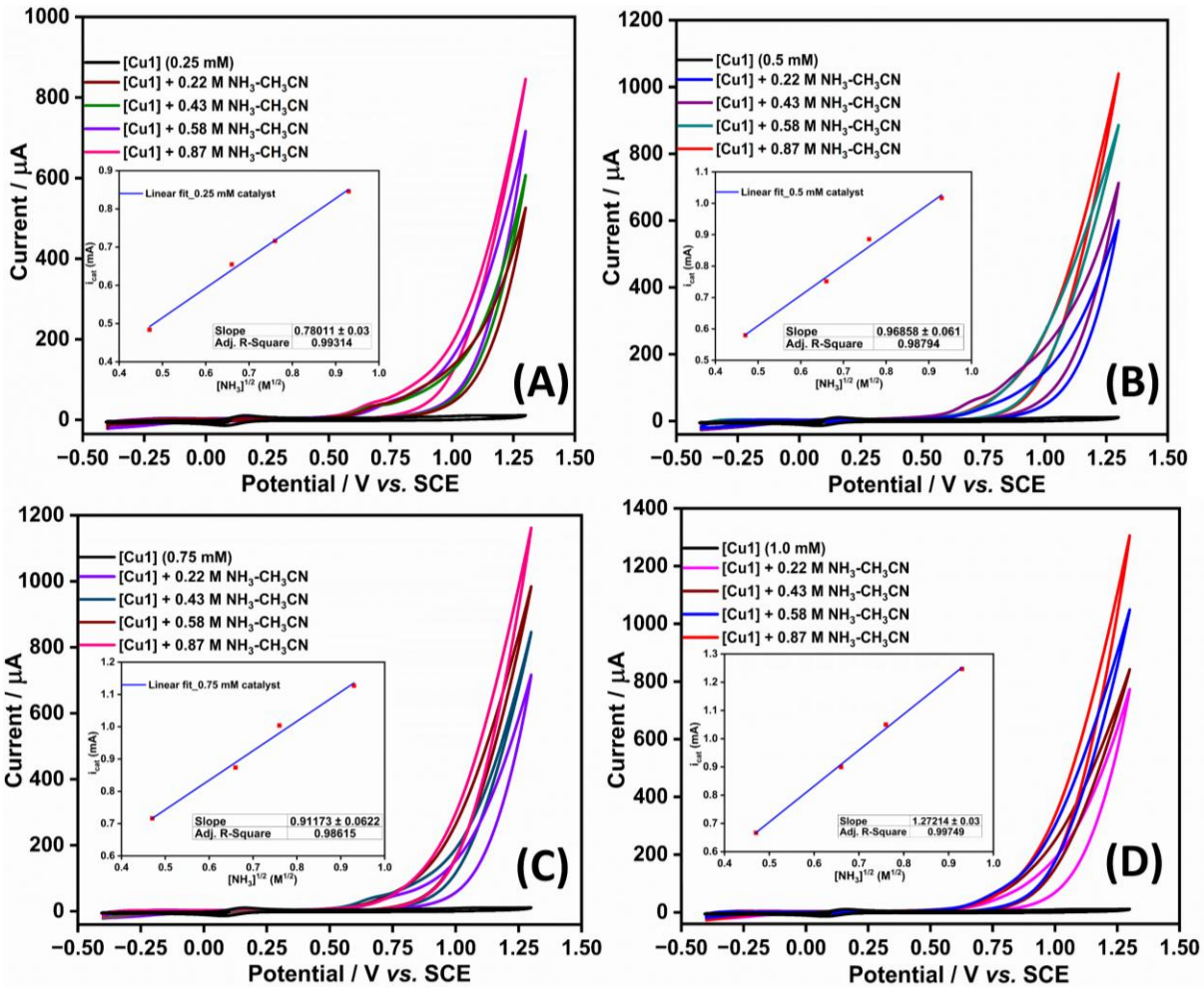

Fig. S26 Electrocatalytic ammonia oxidation by (A) 0.25 mM (B) 0.5 mM (C) 0.75 mM, and (D) 1.0 mM of [Cu(^{t}BuN$_2$Py$_3$)] at different concentrations of NH_3-CH_3CN (0.22 to 0.87 M) with 0.1 M [^{n}Bu$_4$N]ClO_4 supporting electrolyte at a scan rate of 100 mV s^{-1}. (Inset) Catalytic current, measured at 1.30 V vs SCE (mA), vs $[NH_3]^{1/2}$ ($M^{1/2}$) plot showing linearity.

14. UV-SEC of [Cu1] at 1.4 V and UV-vis spectra by varying concentrations of ammonia.

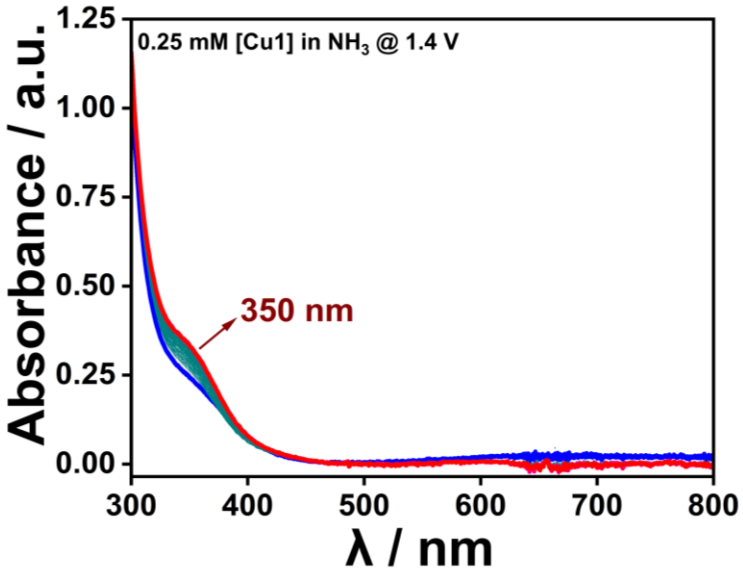

Fig. S27 UV–vis spectral changes of **[Cu1]** (0.25 mM) in 0.36 M NH_3-CH_3CN under an applied potential of 1.4 V vs SCE, using 0.1 M $[nBu_4N]ClO_4$ as the supporting electrolyte.

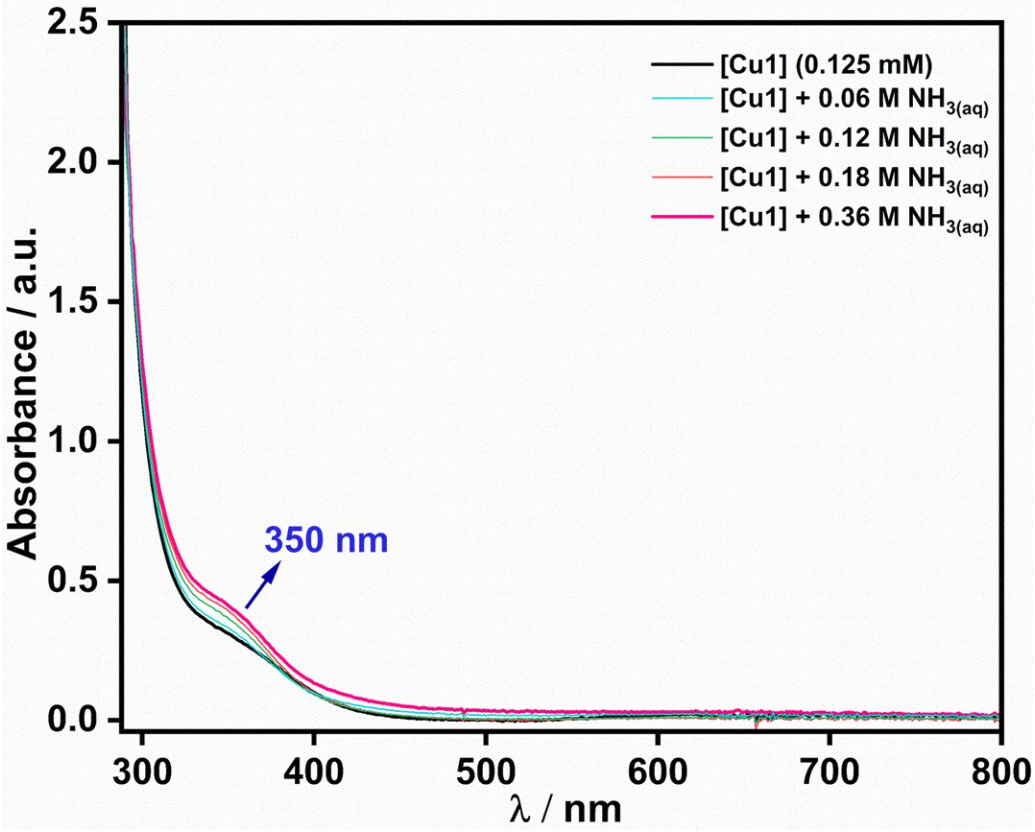

Fig. S28 UV-vis spectrum of **[Cu1]** (0.125 mM) by varying the concentrations of aqueous ammonia (0.06−0.36 M), around 350 nm rise in peak while increasing the concentration of ammonia.

15. Displaying of Color Change after CPE & Spectro electrochemical Setup.

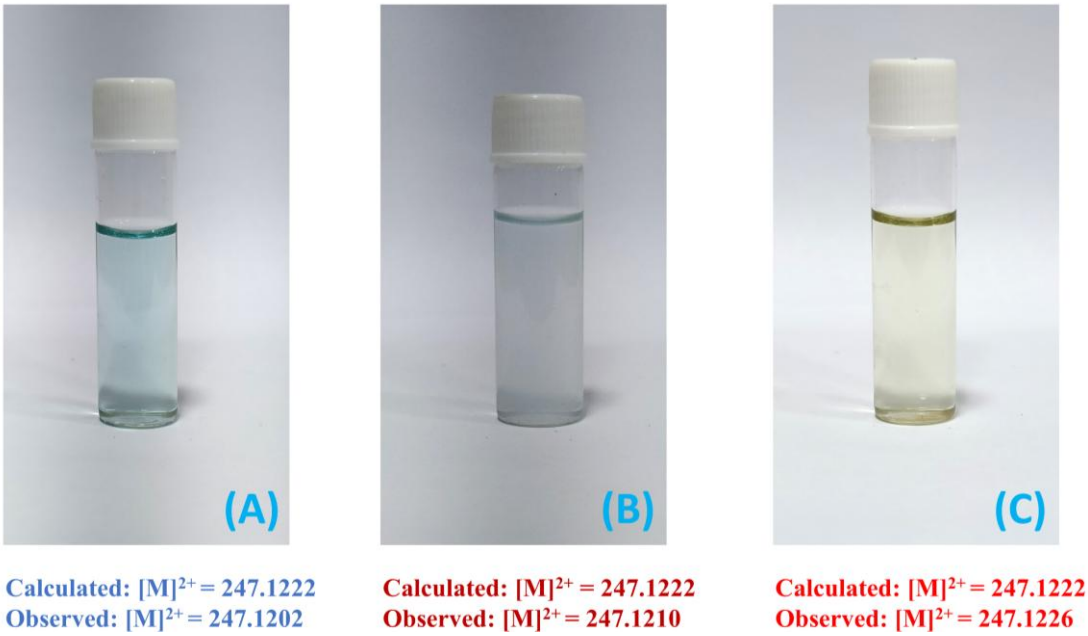

Fig. S29 The **[Cu1]** (0.5 mM) (A) In acetonitrile (B) after addition of aqueous ammonia (before CPE) (C) **[Cu1]** after 1 h CPE at 1.4 V vs SCE (recorded after two days).

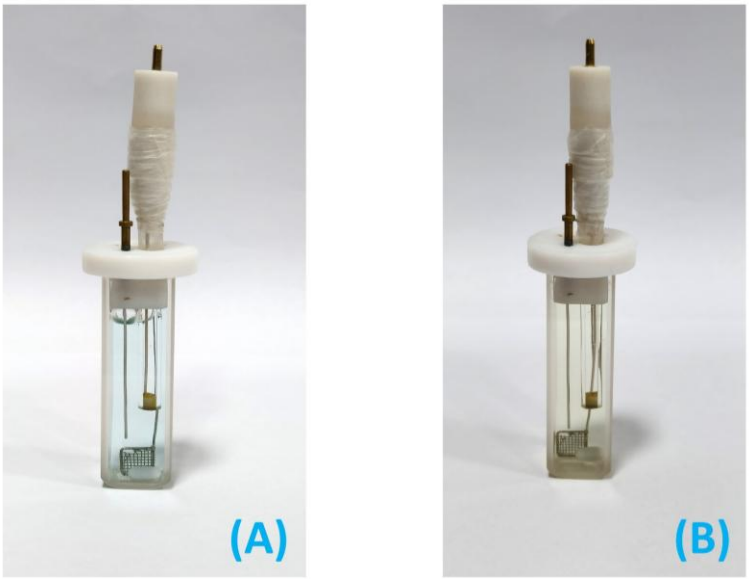

Fig. S30 UV-Spectro electrochemical electrode setup of (A) 0.5 mM **[Cu1]** in acetonitrile (B) after 1 h CPE at 1.4 V vs SCE.

16. Solution FT-IR Spectra.

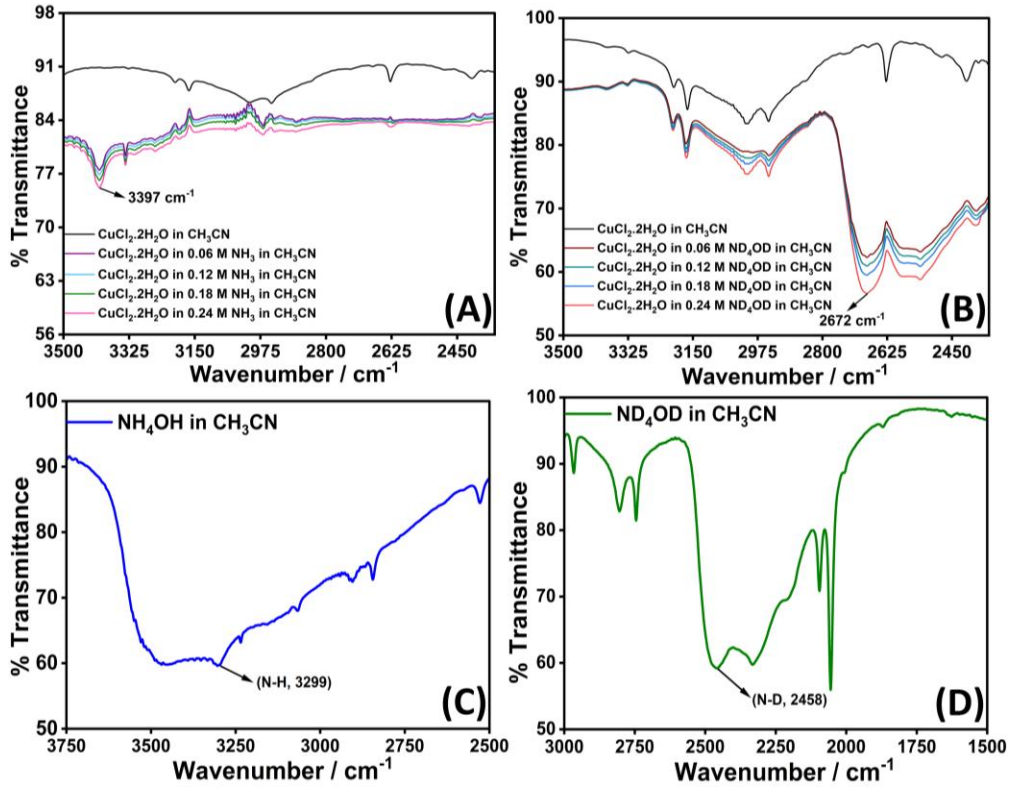

Fig. S31 Solution FT-IR spectra of (A) $CuCl_2.2H_2O$ in NH_3, (B) $CuCl_2.2H_2O$ in ND_4OD, (C) Blank NH_4OH and (D) Blank ND_4OD in CH_3CN recorded using a high-sealing OTTLE cell equipped with CaF_2 windows at 298 K.

Fig. S32 Solution FT-IR OTTLE cell (OMNI-CELL, SPECAC) equipped with CaF_2 window.

17. Controlled Potential Electrolysis (CPE) for NH_3 oxidation.

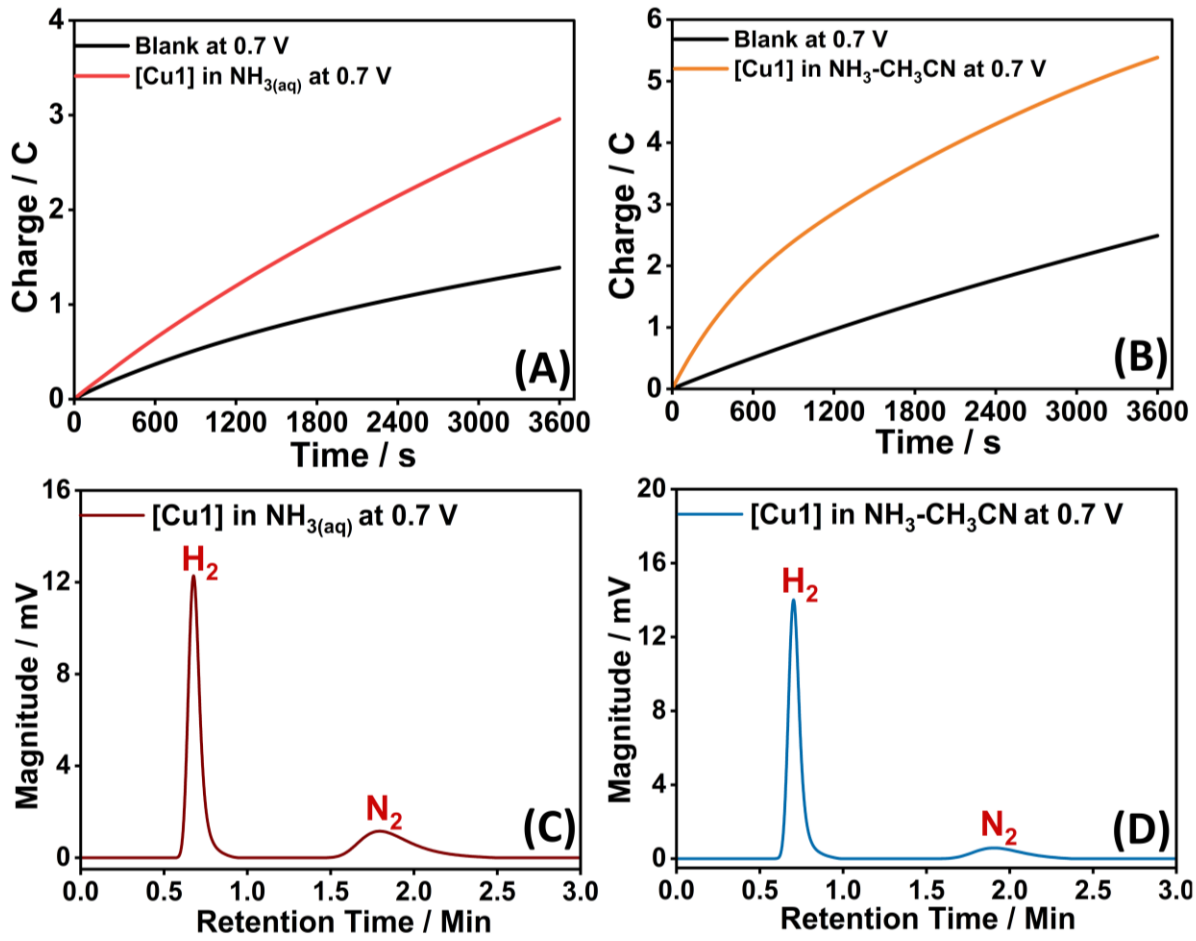

Fig. S33 Controlled potential electrolysis (CPE) was performed at 0.7 V vs SCE for 1 h in the absence and presence of [Cu1] (0.5 mM) in (A) $NH_{3(aq)}$ and (B) NH_3-CH_3CN, using a glassy carbon plate (1 × 1 cm^2) as the working electrode, a platinum plate as the counter electrode, and a saturated calomel electrode (SCE) as the reference electrode in acetonitrile under an argon atmosphere. Gas chromatograms recorded after 1 h of CPE using a thermal conductivity detector (TCD) for (C) [Cu1] in $NH_{3(aq)}$ and (D) [Cu1] in NH_3-CH_3CN at 0.7 V vs. SCE.

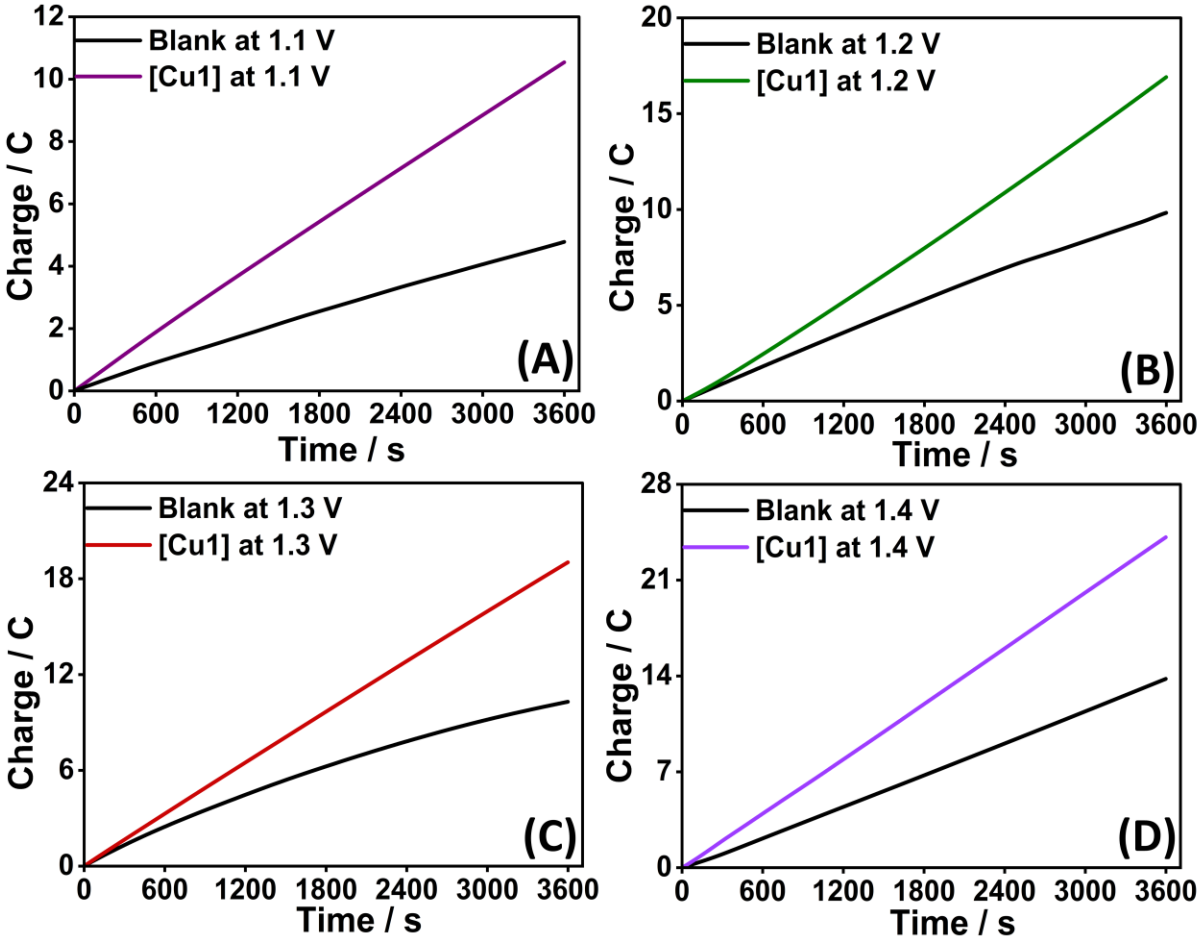

Fig. S34 Controlled potential electrolysis (CPE) was performed for 1 h in the absence and presence of [Cu1] (0.5 mM) in $NH_{3(aq)}$ at (A) 1.1 V, (B) 1.2, (C) 1.3 V, (D) 1.4 V using a glassy carbon plate (1 × 1 cm^2) as the working electrode, a platinum plate as the counter electrode, and a saturated calomel electrode (SCE) as the reference electrode in acetonitrile under an argon atmosphere.

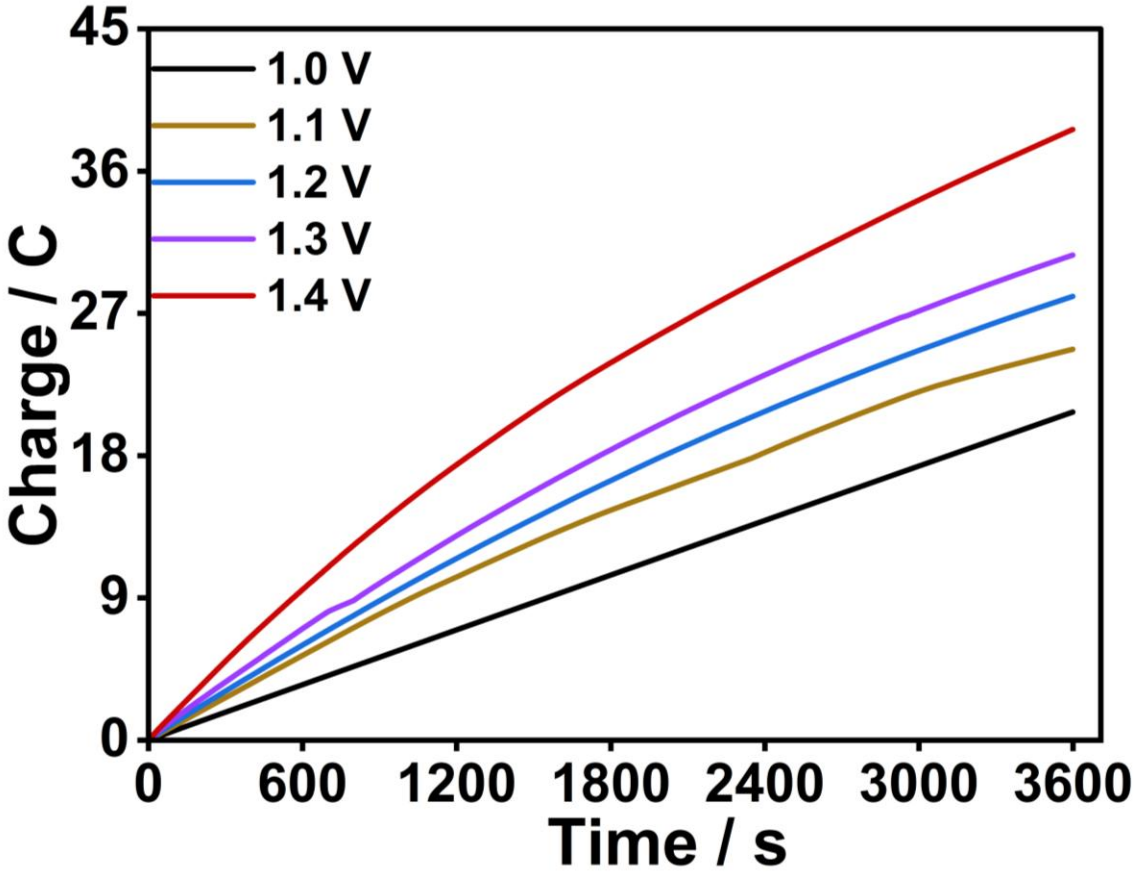

Fig. S35 The controlled potential electrolysis of **[Cu1]** (0.5 mM) at an applied potential of 1.0 to 1.4 V (vs SCE) for 1 h in the presence of 0.87 M NH_3-CH_3CN under an argon atmosphere.

18. GC-TCD Detection of N_2 and H_2.

STD H2_3.hw

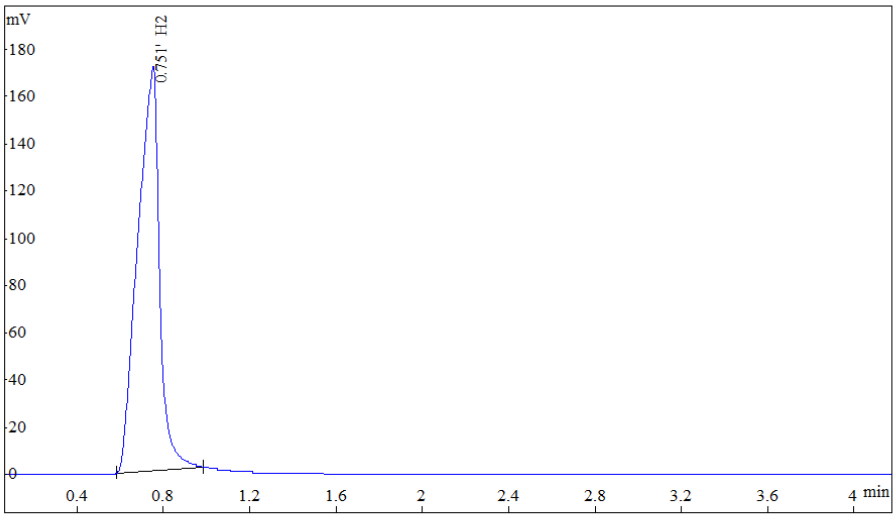

Rank	Time	Name	Area%	Area	Resolution
1	0.751	H_2	100	302570	0.00

Fig. S36 The gas chromatogram of standard H_2 injection using a gas-tight syringe through the GC headspace. Conditions: argon carrier; 5 kg/cm^2 flow rate; molecular sieve column; TCD detector.

STD N2_4.hw

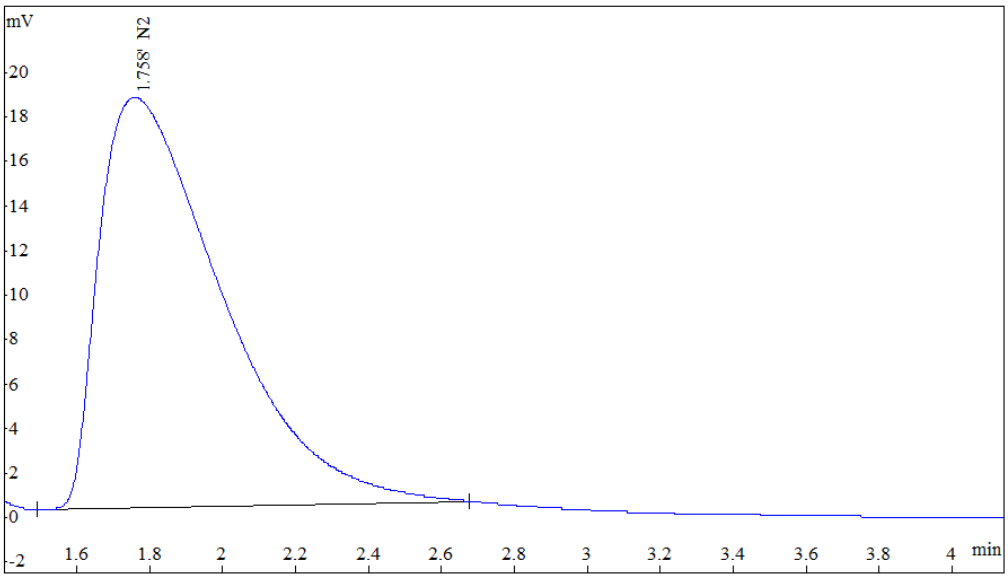

Rank	Time	Name	Area%	Area	Resolution
1	1.758	N_2	100.00	25654	0.00

Fig. S37 The gas chromatogram of standard N_2 injection using a gas-tight syringe through the GC headspace. Conditions: argon carrier; 5 kg/cm^2 flow rate; molecular sieve column; TCD detector.

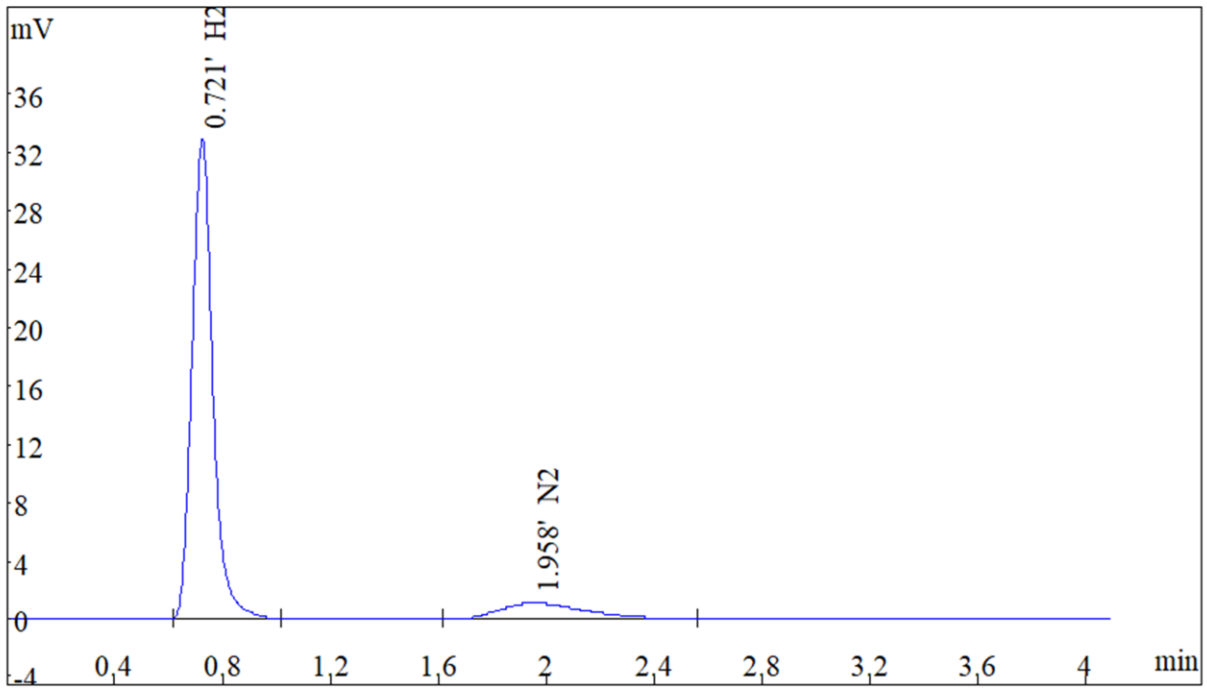

Rank	Time	Name	Area%	Area	Resolution
1	0.721	H2	87.69	171938	3.38
2	1.958	N2	12.31	24842	0.00

Fig. S38 The gas chromatogram illustrates an evolution of H_2 and N_2 from the cell headspace after CPE for 1 h at an applied potential of 1.0 V vs SCE. Electrolysis conditions: 0.5 mM **[Cu1]** in the presence of 0.84 M aqueous ammonia in dry acetonitrile under an argon atmosphere.

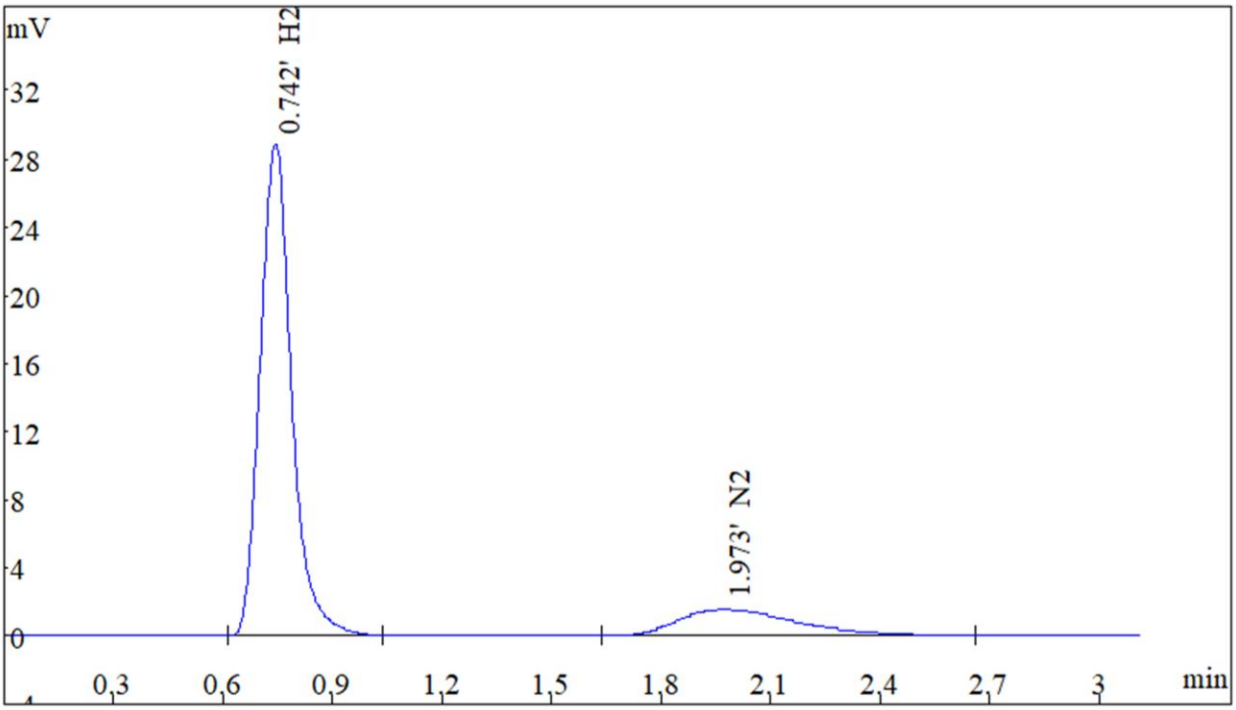

Rank	Time	Name	Area%	Area	Resolution
1	0.742	H2	82.04	171780	3.15
2	1.973	N2	17.96	24042	0.00

Fig. S39 The gas chromatogram illustrates an evolution of H_2 and N_2 from the cell headspace after CPE for 1 h at an applied potential of 1.0 V vs SCE. Electrolysis condition: 0.5 mM **[Cu1]** in 0.87 M NH_3-CH_3CN under an argon atmosphere.

19. Determination of Faradaic Efficiency from CPE Measurements.

$$\textbf{Faradaic efficiency} = \frac{Qexp}{Qtheo} \times 100\ \%$$

Q_{theo} is the number of moles of product formed during controlled potential electrolysis, and Q_{exp} is the number of moles of product detected by gas chromatography.

$$\mathbf{Q_{theo}} = \frac{\Delta C}{nF}$$

Where, ΔC is the charge difference between controlled potential electrolysis in the presence of catalyst and blank solution, n is the number of electrons involved in the electrocatalytic oxidation of ammonia (n = 6), and F is the Faraday constant.[15]

At 1.0 V [Cu1] (0.5 mM) in 0.84 M NH_3:

- During the controlled potential electrolysis (CPE) at 1.0 V vs SCE, the total charge consumed 5.53 C in 1 h (ΔC) therefore, theoretical moles (Q_{theo}) = 9.55×10^{-6} moles. Q_{theo} for N_2 = 2.39×10^{-6} moles, Q_{theo} for H_2 = 7.16×10^{-6} moles.
- Gas chromatography yields (Q_{exp}) of evolved products have been calculated by using response factor,

$$\textbf{Response Factor (RF)} = \frac{(\textbf{peak area})_{\textbf{unknown}} \times (\textbf{number of moles of } N_2 \textbf{ or } H_2)_{\textbf{known}}}{(\textbf{Peak area})_{\textbf{known}}}$$

- For H_2, 0.25 mL of gas injected into GC, the average peak area of known H_2 is 302513, and the peak area of H_2 detected after CPE is 171938. From this number of moles of H_2 is calculated to be 6.34×10^{-6} moles.
- For standard N_2, 0.05 mL of gas injected into GC, the average peak area of known N_2 is 25507, and the peak area of N_2 detected after CPE is 24842. From this number of moles of N_2 is calculated to be 2.17×10^{-6} moles.

Faradaic efficiency of H_2 = $\frac{6.34 \times 10^{-6}\ \text{moles}}{7.16 \times 10^{-6}\ \text{moles}} \times 100$ = 89 %

Faradaic efficiency of N_2 = $\frac{2.17 \times 10^{-6}\ \text{moles}}{2.39 \times 10^{-6}\ \text{moles}} \times 100$ = 91 %

At 1.0 V [Cu1] (0.5 mM) in NH_3-CH_3CN (0.87 M):

- During the controlled potential electrolysis (CPE) at 1.0 V vs SCE, the total charge consumed 5.98 C in 1 h (ΔC) therefore, theoretical moles (Q_{theo}) = 10.33 × 10^{-6} moles. Q_{theo} for N_2 = 2.58 × 10^{-6} moles, Q_{theo} for H_2 = 7.75 × 10^{-6} moles.
- Gas chromatography yields (Q_{exp}) of evolved products have been calculated by using response factor,

Response Factor (RF) = $\frac{(\boldsymbol{peak\ area})_{\boldsymbol{unknown}} \times (\boldsymbol{number\ of\ moles\ of\ N_2\ or\ H_2})_{\boldsymbol{known}}}{(\boldsymbol{Peak\ area})_{\boldsymbol{known}}}$

- For standard H_2, 0.25 mL of gas injected into GC, the average peak area of known H_2 is 302513, and the peak area of H_2 detected after CPE is 171780. From this number of moles of H_2 is calculated to be 6.34 × 10^{-6} moles.
- For standard N_2, 0.05 mL of gas injected into GC, the average peak area of known N_2 is 25507, and the peak area of N_2 detected after CPE is 24042. From this number of moles of N_2 is calculated to be 2.1 × 10^{-6} moles.

Faradaic efficiency of H_2 = $\frac{6.34 \times 10^{-6}\ \text{moles}}{7.75 \times 10^{-6}\ \text{moles}} \times 100$ = 82 %

Faradaic efficiency of N_2 = $\frac{2.1 \times 10^{-6}\ \text{moles}}{2.58 \times 10^{-6}\ \text{moles}} \times 100$ = 81 %

Table S6 The Faradaic efficiencies of H_2 and N_2, produced during the oxidation of ammonia by adding 0.84 M aqueous ammonia and 0.5 mM **[Cu1]** as the catalyst.

E_{app} (V) *vs.* SCE	Experimental (H_2/N_2) in µmol	Theoretical (H_2/N_2) in µmol	Faradaic Efficiency of H_2 (%)	Faradaic Efficiency of N_2 (%)	Molar ratio (H_2:N_2)
0.7	1.26/0.49	2.02/0.67	62	73	2.57:1
1.0	6.34/2.17	7.16/2.39	89	91	2.92:1
1.1	6.49/2.22	7.46/2.49	87	89	2.92:1
1.2	7.61/2.71	9.17/3.06	83	89	2.81:1
1.3	9.41/3.65	11.31/3.77	83	97	2.58:1
1.4	10.87/3.88	13.41/4.47	81	87	2.8:1

Table S7 The Faradaic efficiencies of H_2 and N_2 were produced during the oxidation of ammonia in the presence of 0.87 M NH_3-CH_3CN and 0.5 mM **[Cu1]** as the catalyst.

E_{app} (V) *vs.* SCE	Experimental (H_2/N_2) in µmol	Theoretical (H_2/N_2) in µmol	Faradaic Efficiency of H_2 (%)	Faradaic Efficiency of N_2 (%)	Molar ratio (H_2:N_2)
0.7	2.64/0.98	3.74/1.25	71	78	2.69:1
1.0	6.34/2.1	7.75/2.58	82	81	2.99:1
1.1	7.36/2.94	9.35/3.12	79	94	2.5:1
1.2	8.82/3.12	10.4/3.47	85	90	2.83:1
1.3	9.87/3.55	11.81/3.94	84	90	2.78:1
1.4	11.81/4.01	14.27/4.76	83	84	2.94:1

20. Determination of turnover number (TON).[16,17]

$$\textbf{TON} = \frac{\textit{moles of } N_2/H_2 \textit{ produced}}{\textit{moles of catalyst used}}$$

The controlled potential electrolysis experiment was performed in a custom-made electrolysis cell consisting of a GC plate working, platinum plate counter, and saturated calomel reference electrodes.

Catalyst concentration = 1.2 mg (0.5 mM) = 2.4 µmol

After 7 h CPE at a potential of 1.0 V vs SCE, the total charge consumed was 212.45 C.

The amount of N_2 produced = 8.46 µmol

Therefore, **TON (N_2)** after 7 h CPE experiment = $\frac{8.46\ \mu mol}{2.4\ \mu mol}$ = **3.5**.

The amount of H_2 produced = 47.38 µmol

Therefore, **TON (H_2)** after 7 h CPE experiment = $\frac{47.38\ \mu mol}{2.4\ \mu mol}$ = **20**.

21. Determination of Kinetic Isotope Effect (NH_3/ND_3).

To investigate the kinetic isotope effect on the ammonia oxidation reaction, cyclic voltammetric experiments were performed in 0.5 mM of **[Cu1]** in the presence of NH_3 and ND_3 (0.12 to 0.84 M) in CH_3CN with 0.1 M $[NBu_4]ClO_4$ as the supporting electrolyte. The CV data shows that ammonia oxidation is first order with respect to $[NH_3]$ and $[ND_3]$. The slope obtained from the plot of I_{cat} (mA) vs $[NH_3/ND_3]^{1/2}$ ($M^{1/2}$) was used for calculating the kinetic isotopic effect (k_H/k_D).

$$\text{KIE} = \frac{k_{NH_3}}{k_{ND_3}} = \frac{slope_{NH_3}}{slope_{ND_3}} = \frac{0.714}{0.687} = \mathbf{1.04}.$$

The NH_3 and ND_3 ($k_H/k_D = 1.04$) show no kinetic isotope effect, indicating the proton transfer step is not involved in this catalytic reaction's rate-determining step.

22. Determination of the Onset Overpotential of Ammonia Oxidation Reaction in CH_3CN.

The electrocatalytic ammonia oxidation by $[Cu(^tBuN_2Py_3)]$ (0.5 mM) was performed in 0.84 M NH_3-CH_3CN, and the cyclic voltammogram plot shows the onset potential for AO reaction is 0.60 V vs SCE. The thermodynamic potential for ammonia oxidation reaction is −0.94 V vs Fc^+/Fc (−0.56 V vs SCE).

$$\eta_{onset} = E_{onset} - E°_{AO} = 0.60 - (-0.56)\ V = 1.16\ V \text{ vs SCE}.$$

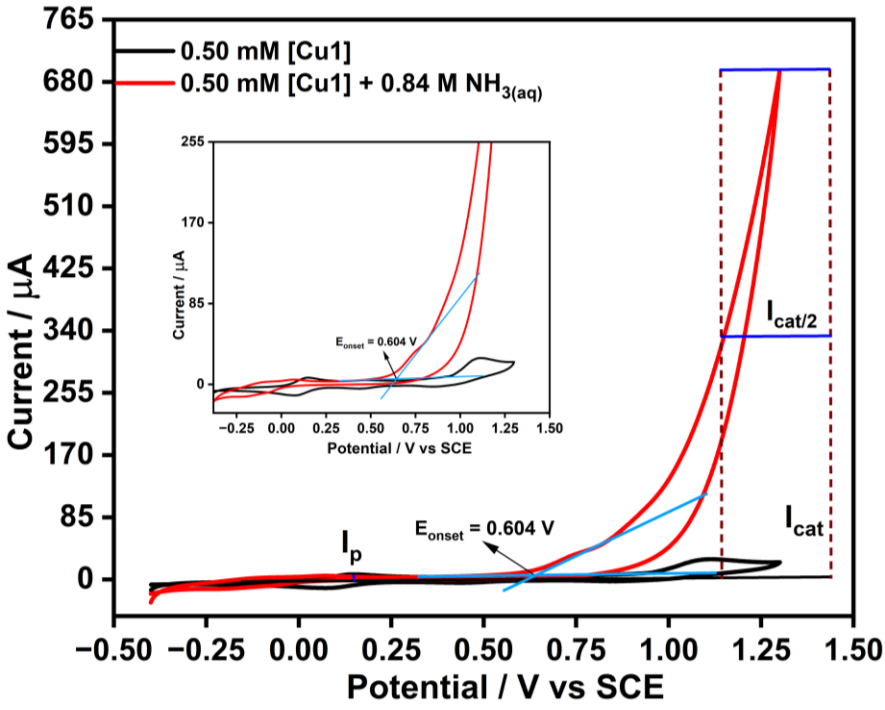

Fig. S40 Overlay of cyclic voltammograms of 0.5 mM **[Cu1]** in the absence and presence of 0.84 M $NH_{3(aq)}$ showing the onset potential (Inset: magnified view).

23. Kinetics from the Cyclic Voltammetry Experiment.

Fig. S23 displays varying catalyst concentrations ranging from 0.25 to 1.0 mM at a fixed ammonia concentration of 0.84 M. As the catalyst concentration increases, the catalytic current also rises, as shown in the foot-of-the-wave plot (**Fig. S42**) where k_{obs} versus **[Cu1]** (mM) follows a linear trend, confirming first-order kinetics with respect to the catalyst.

By varying the ammonia concentrations between 0.12 and 0.84 M at a fixed catalyst concentration (0.25 mM), we observed that the catalytic current increases linearly with an increase in the ammonia concentration. The first order with respect to ammonia is confirmed by the linear trend in the i_{cat} (mA) versus $[NH_3]^{1/2}$ plot. A similar trend was observed for the different catalyst concentrations, ranging from 0.5 to 1.0 mM.

24. Foot-of-the-wave analysis (FOWA).

A foot-of-the-wave analysis14 was performed to understand the kinetic process and calculate the rate constant (k_{obs}), by the following equation:

$$\frac{i}{i_p} = \frac{2.24\sqrt{\frac{RT}{nF\upsilon}}\sqrt{k_{obs}}}{[1+\exp\{\frac{nF}{RT}(E^{\circ}_{ap}-E)\}]}$$

Where F is the Faraday constant (96500 C mol^{-1}), T is the temperature (298 K), n is the number of electrons (n = 6) involved in the electrocatalytic oxidation of ammonia into dinitrogen and dihydrogen, R is the gas constant (8.314 J K^{-1} mol^{-1}), υ is the scan rate (0.1 V s^{-1}), E°_{ap} is apparent potential (1.3 V), E = $E_{cat/2}$ (half-wave potential for the catalytic process). The plot of i/i_p versus $1/[1+\exp\{(nF/RT)\ (E_{ap} - E)\}]$ for various concentrations of catalyst in 0.87 M NH_3-CH_3CN is shown in **Fig. S38** (where i represents catalytic current increased after the addition of NH_3 and i_p represents the peak current corresponds to $Cu^{II/I}$ one electron redox wave. FOWA was performed for varying ranges of catalyst concentration, ammonia concentration, and scan rates to allow a fair comparison when conditions change. A linear plot of i/i_p versus $1/[1+\exp\{(nF/RT)\ (E_{ap} - E)\}]$ has been selected as the foot of the wave regions ($R^2 > 0.98$). Then from the slope of that plot, the first-order rate constant in the case of aqueous ammonia (0.84 M) and NH_3-CH_3CN (0.87 M) is calculated to be approximately 4×10^6 and $3 \times 10^6\ s^{-1}$ respectively. The FOWA confirmed the appropriateness of the presumed first-order EC_{cat} mechanism.

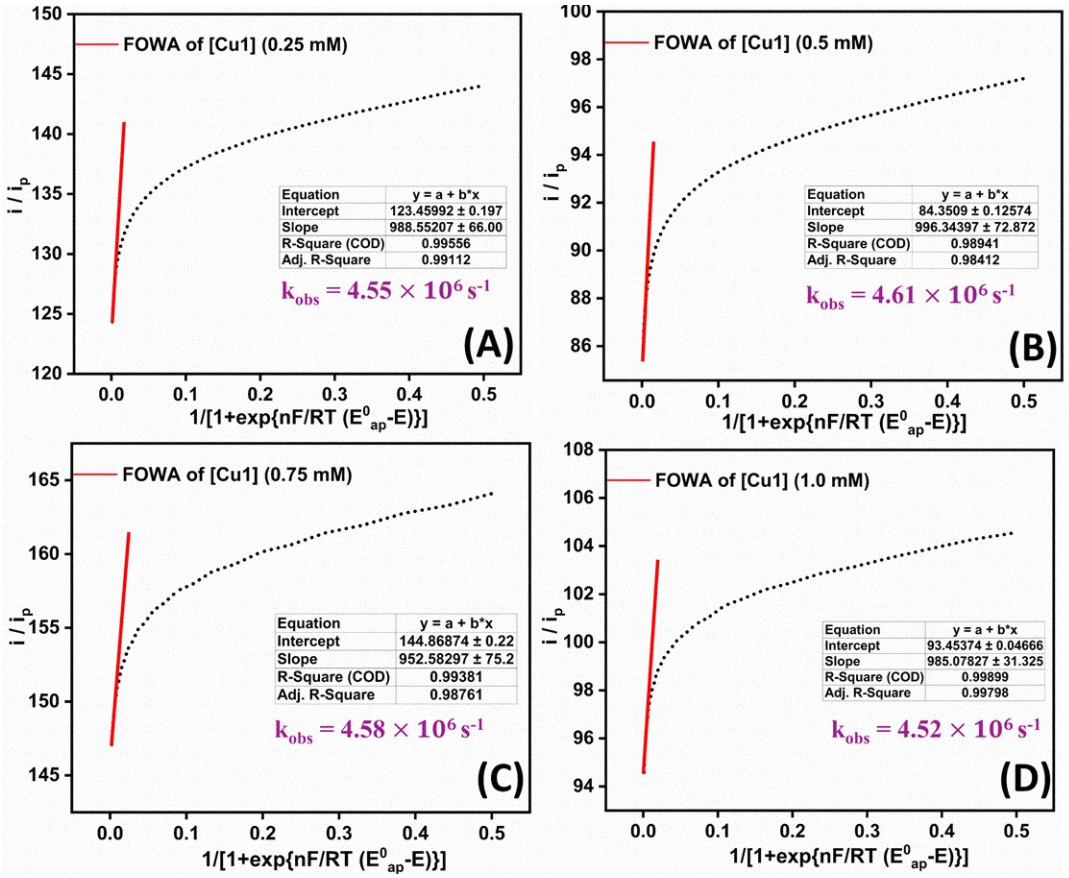

Fig. S41 FOWA (using Savéant's foot of the wave methodology) for an ammonia oxidation reaction by (A) 0.25 mM (B) 0.5 mM (C) 0.75 mM (D) 1.0 mM [Cu(^{t}BuN$_2$Py$_3$)] after the addition of 0.84 M aqueous ammonia, CV recorded at 100 mV s^{-1} in a CH_3CN solution containing 0.1 M [^{n}Bu$_4$N]ClO$_4$.

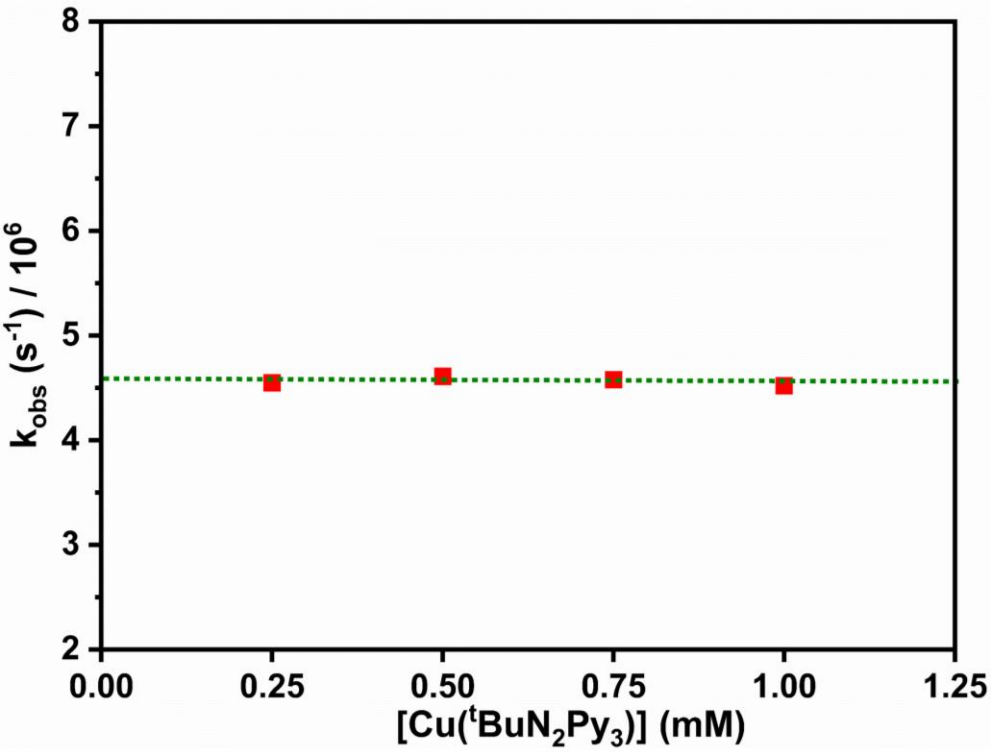

Fig. S42 The plot of k_{obs} vs [Cu(^{t}BuN$_2$Py$_3$)] (0.25 to 1.0 mM) calculated by FOWA from CV after the addition of 0.84 M aqueous ammonia and 0.1 M [^{n}Bu$_4$N]ClO$_4$ in CH$_3$CN at 100 mV s^{-1}. The linear trend indicates that homogeneous electrocatalytic oxidation of ammonia follows a first-order behaviour with regard to **[Cu1].**

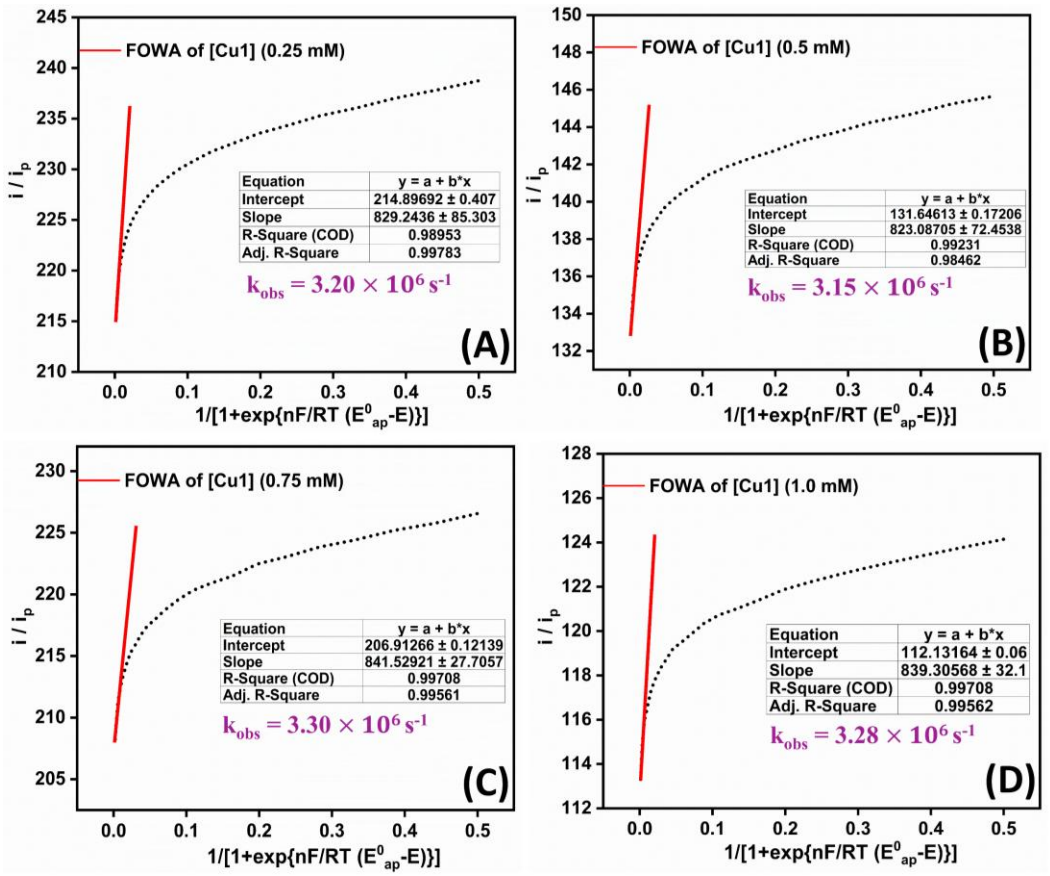

Fig. S43 FOWA (using Savéant's foot of the wave methodology) for an ammonia oxidation reaction by (A) 0.25 mM (B) 0.5 mM (C) 0.75 mM (D) 1.0 mM [Cu(^{t}BuN$_2$Py$_3$)] in the presence of 0.87 M NH_3-CH_3CN at 100 mV s^{-1} with 0.1 M [^{n}Bu$_4$N]ClO_4 as supporting electrolyte.

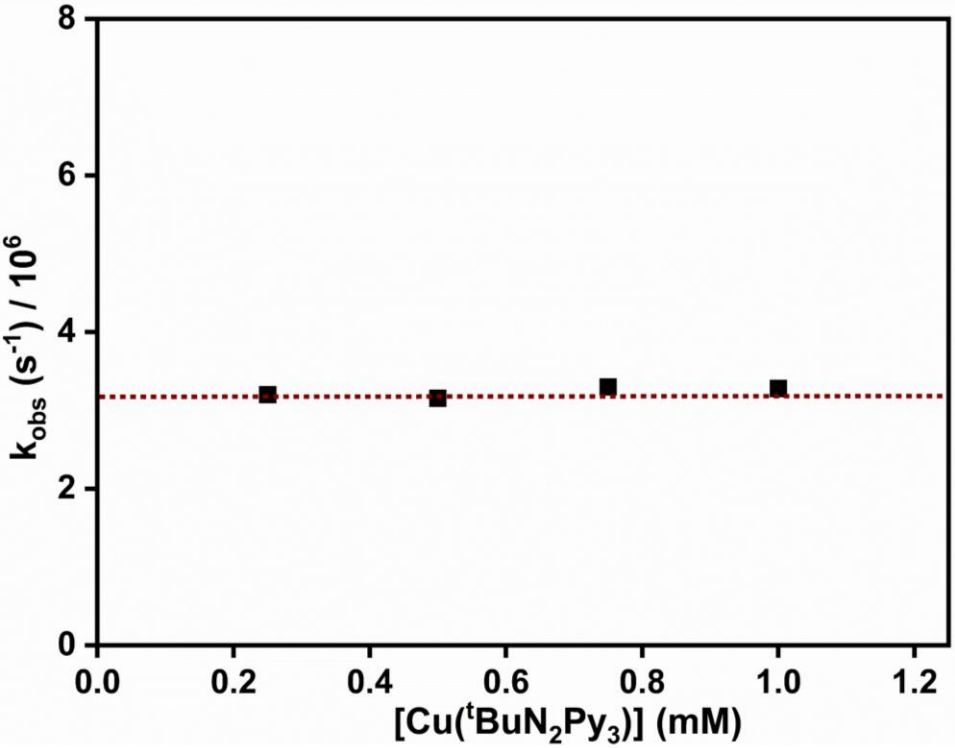

Fig. S44 The plot of k_{obs} vs [Cu(^{t}BuN$_2$Py$_3$)] (0.25 to 1.0 mM) calculated by FOWA from a CV in the presence of 0.87 M NH_3-CH_3CN and 0.1 M [^{n}Bu$_4$N]ClO_4 at 100 mV s^{-1}. The linear trend indicates that homogeneous electrocatalytic oxidation of ammonia follows a first-order behaviour with regard to **[Cu1]**.

25. Stability and Homogeneity Studies.

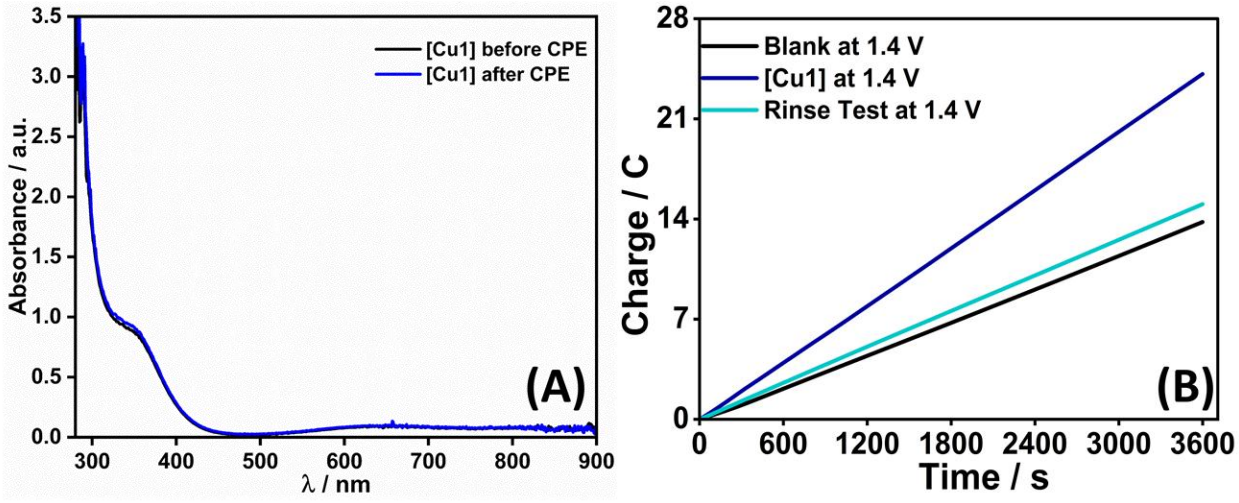

Fig. S45 (A) The UV-vis spectra of complex [Cu1] (0.5 mM) in acetonitrile before and after the controlled potential electrolysis for 1 h at 1.4 V vs SCE. (B) Rinse Test after CPE for 1 h with [Cu1] in $NH_{3(aq)}$ at 1.4 V.

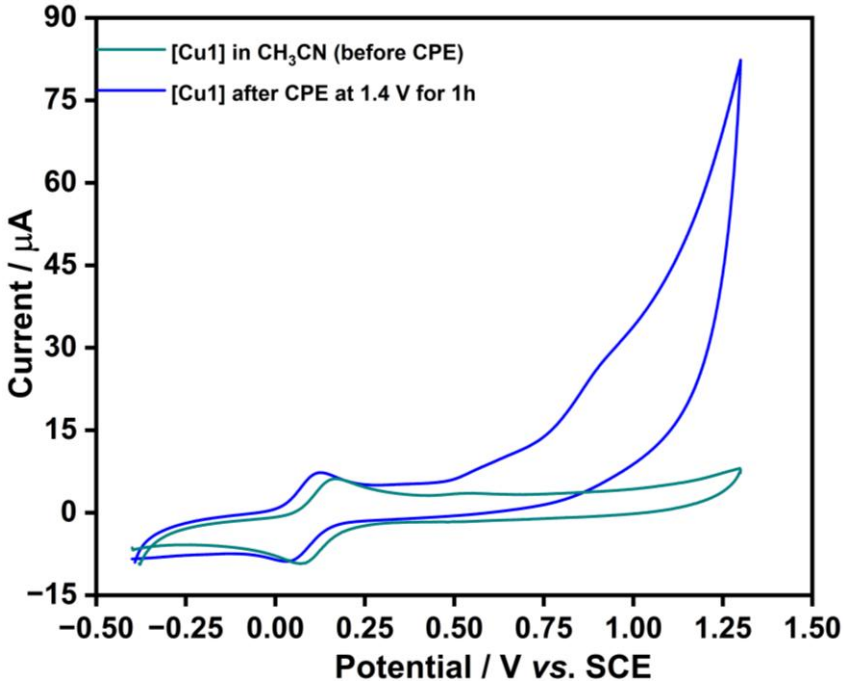

Fig. S46 The cyclic voltammogram (anodic scan) of complex [Cu1] (0.5 mM) in acetonitrile before and after the controlled potential electrolysis for 1 h at 1.4 V vs SCE.

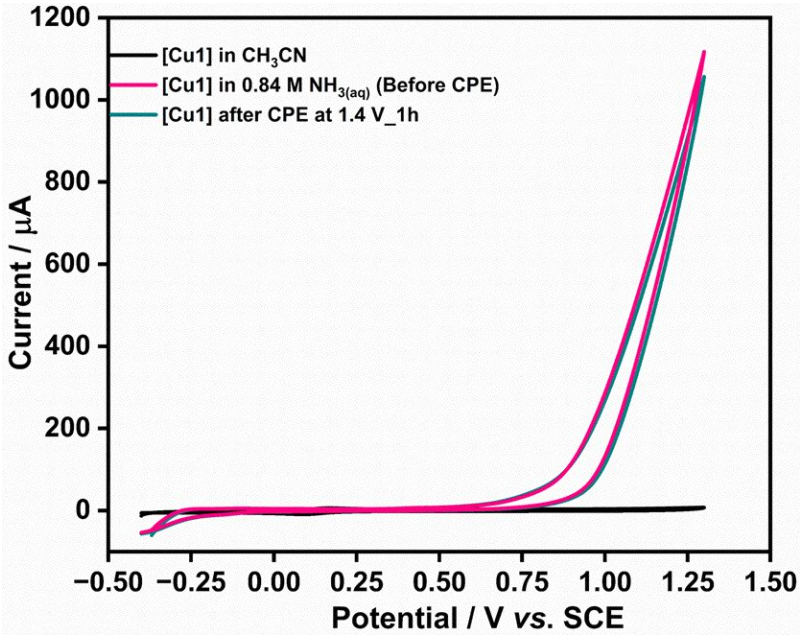

Fig. S47 The cyclic voltammogram of complex **[Cu1]** in acetonitrile, before and after the controlled potential electrolysis for 1 h at 1.4 V vs SCE.

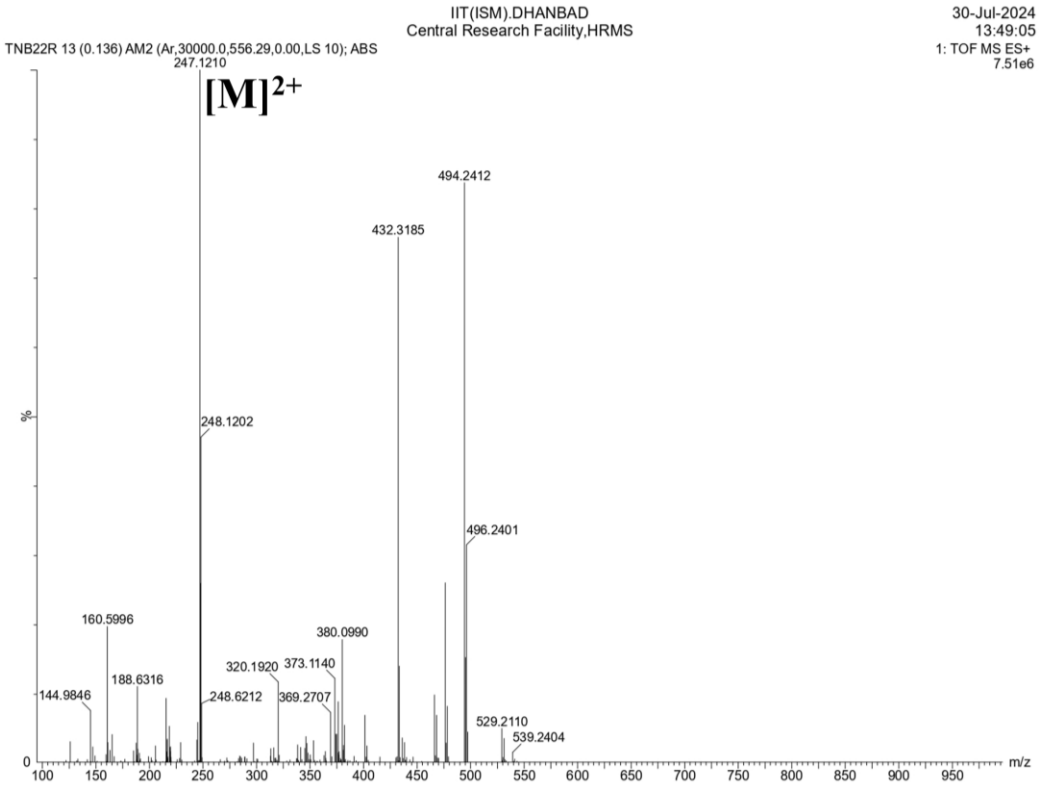

Fig. S48 ESI-MS spectrum of **[Cu1]** in acetonitrile after the addition of aqueous ammonia (calcd, $[M]^{2+}$ = 247.1222, found, $[M]^{2+}$ = 247.1210).

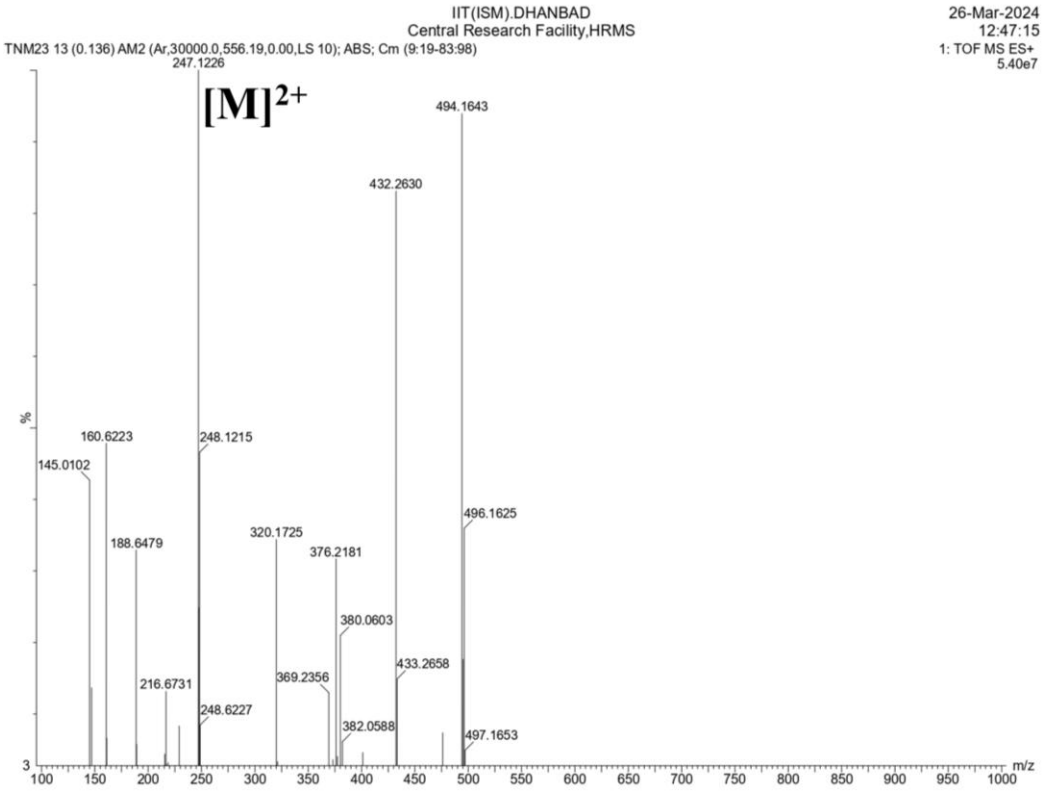

Fig. S49 ESI-MS spectrum of **[Cu1]** in acetonitrile after the CPE process at 1.4 V for 1 h (calcd, $[M]^{2+}$ = 247.1222, found, $[M]^{2+}$ = 247.1226).

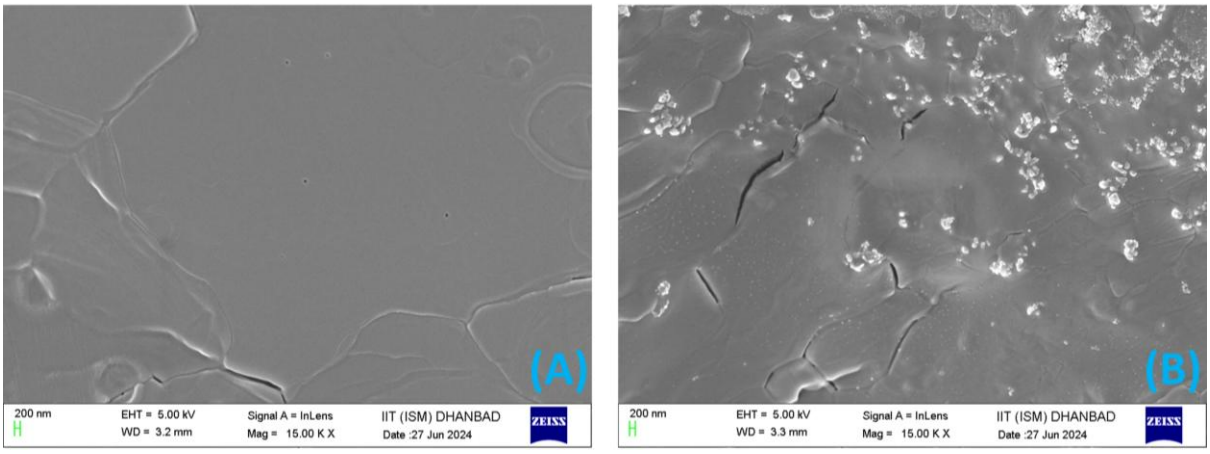

Fig. S50 FE-SEM analysis of the glassy carbon plate after the CPE process for 1 h at an applied potential of 1.4 V vs SCE (A) Blank experiment ($NH_{3(aq)}$ only) (B) In the presence of 0.5 mM **[Cu1]** in 0.84 M aqueous ammonia recorded in acetonitrile.

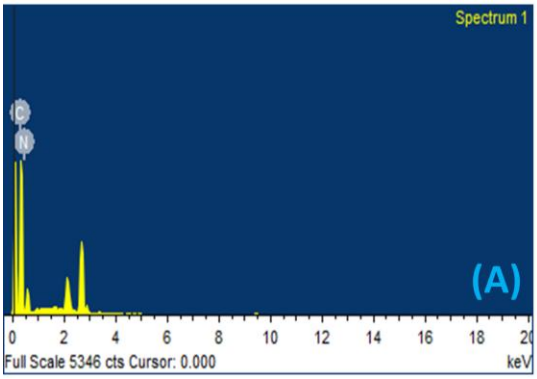

Element	Weight %	Atomic %
C K	74.69	77.48
N K	25.31	22.52
Total	100.00	

(B)

Fig. S51 (A) EDX data of glassy carbon plate after the CPE process for 1 h at an applied potential of 1.4 V vs SCE in the presence of 0.84 M $NH_{3(aq)}$ only (B) Elemental composition of working electrode surface area.

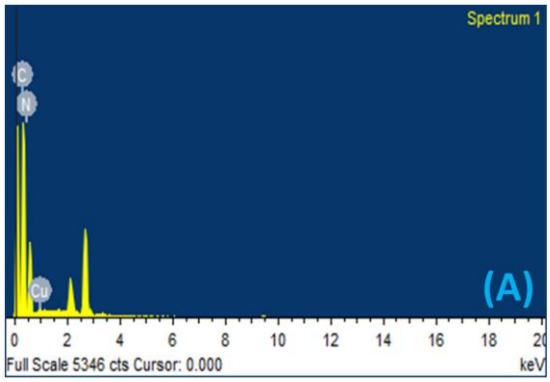

Element	Weight %	Atomic %
C K	84.06	86.35
N K	15.38	13.54
Cu L	0.56	0.11
Total	100.00	

(B)

Fig. S52 (A) EDX data of glassy carbon plate after the CPE process for 1 h in the presence of 0.5 mM **[Cu1]** in 0.84 M aqueous ammonia recorded in acetonitrile at an applied potential of 1.4 V vs SCE. (B) Elemental composition of working electrode surface area.

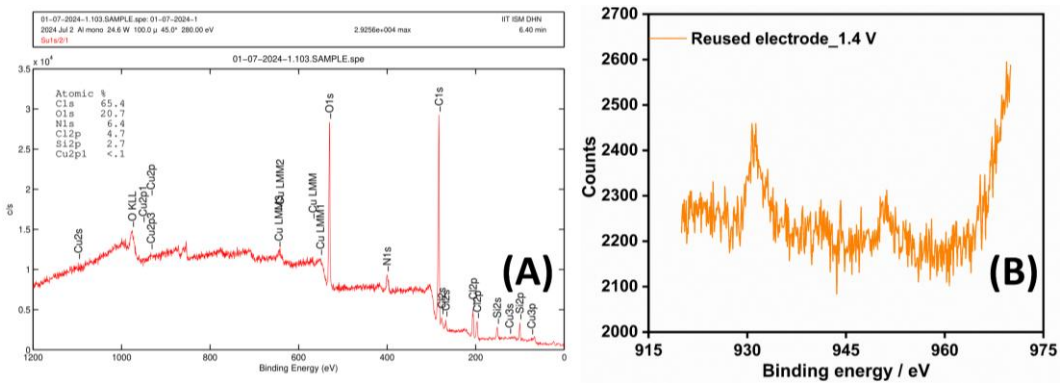

Fig. S53 (A) The full XPS survey spectrum of glassy carbon plate, (B) High-resolution spectra centered on the region characteristic Cu 2p after controlled potential electrolysis of **[Cu1]** at 1.4 V vs SCE for 1 h in 0.84 M aqueous ammonia with 0.1 M [^{n}Bu$_4$N]ClO$_4$ supporting electrolyte.

26. Electrochemical oxidation of hydrazine by [Cu1].

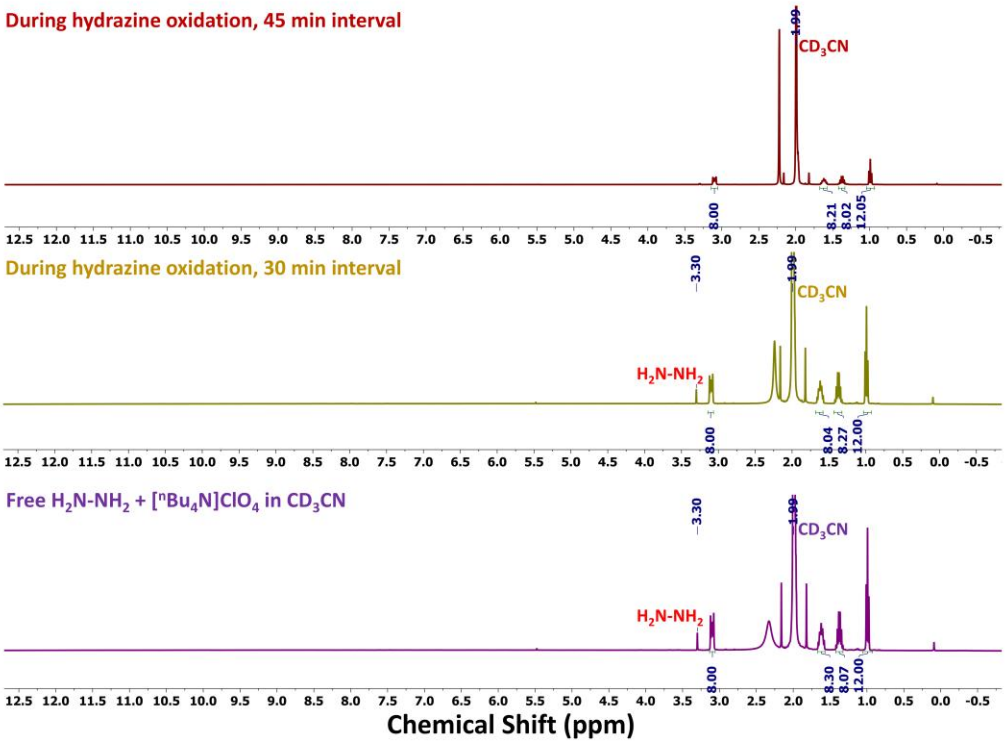

Fig. S54 Stacked ^{1}H NMR spectra (400 MHz, CD_3CN, 298 K) of free hydrazine in supporting electrolyte (bottom), during CPE with the reaction of **[Cu1]** in 0.16 M hydrazine in CH_3CN at 1.0 V vs SCE, 30 mins interval (middle), 45 mins interval (top).

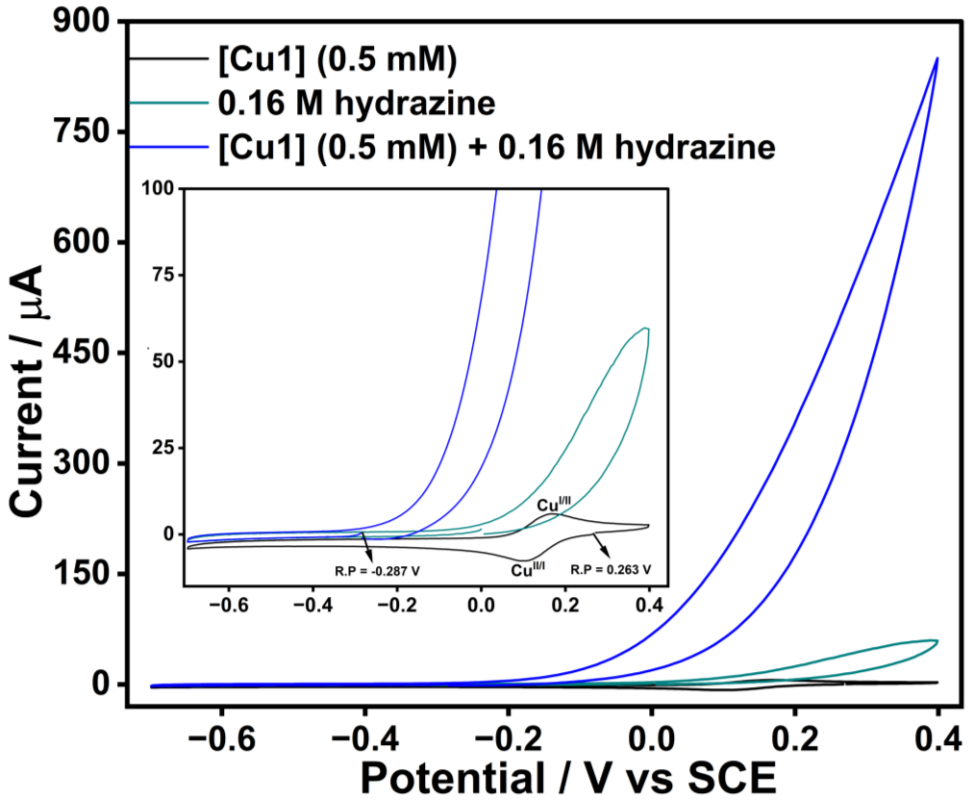

Fig. S55 Electrocatalytic oxidation of hydrazine using 0.5 mM **[Cu1]** in CH_3CN with 0.1 M $[^nBu_4N]ClO_4$ supporting electrolyte at a scan rate of 100 mV s^{-1}. Inset: metal region showing the resting potential shift.

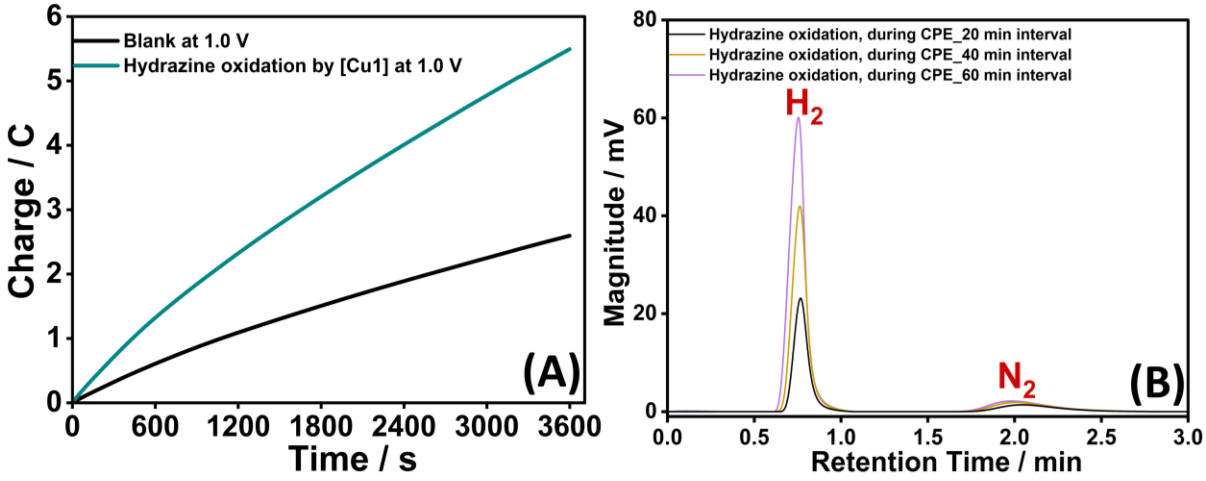

Fig. S56 (A) Controlled potential electrolysis (CPE) comparing hydrazine oxidation by [Cu1] with

a blank experiment at an applied potential of 1.0 V vs SCE for 1 h under an argon atmosphere. (B) Gas chromatograms showing a time-dependent increase in the intensities of H_2 and N_2 (20, 40, and 60 min) during hydrazine oxidation catalyzed by [Cu1] (0.5 mM) at 1.0 V vs SCE. Experimental conditions: 0.1 M $[nBu_4N]ClO_4$ supporting electrolyte; glassy carbon plate working electrode, platinum plate counter electrode, and saturated calomel reference electrode.

27. Computational Details.

We calculated the pK_a of $[Cu\text{-}NH_3]^{3+}$ in MeCN through **eq S1-S4**.

$$[Cu - NH_3]^{3+} + py \rightarrow [Cu - NH_2]^{2+} + pyH^+ \quad \textbf{(eq S1)}$$

$$\Delta G_{pK_a} = -RTln(\Delta K_a) \quad \textbf{(eq S2)}$$

$$ln(\Delta K_a) = -\Delta G/\mathrm{RT} \quad \textbf{(eq S3)}$$

$$\Delta K_a = \exp[-(4.04 \times 10^3)/(1.987 \times 298)$$

$$\Delta K_a = 1.08 \times 10^{-3}$$

$$\Delta pK_a = -\log(\Delta K_a) \quad \textbf{(eq S4)}$$

$$\Delta pK_a = -\log(1.08 \times 10^{-3}) = 2.96$$

The calculation showed that $[Cu - NH_3]^{3+}$ has lower pK_a than the pyH^+ by 2.96. The pK_a of the pyH^+ in MeCN is 12.53.

So, pK_a of $[Cu - NH_3]^{3+}$ is 12.53 – 2.96 = 9.57

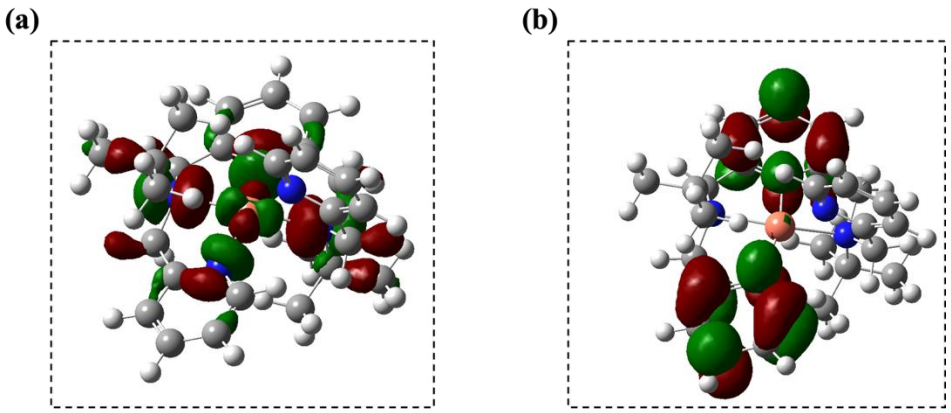

Fig. S57 The frontier molecular orbital (FMO) density distributions of the studied complex [Cu1]: (a) Highest Occupied Molecular Orbital (HOMO) and (b) Lowest Unoccupied Molecular Orbital (LUMO). The red and green surfaces represent the positive and negative phases of the orbitals, respectively, with an isovalue of 0.03.

Table S8 The selected bond angle of the initial copper complex (Int-I).

Atom	**Atom**	**Atom**	**Angle / °**
N1	Cu1	N2	82.37°
N1	Cu1	N3	158.64°
N1	Cu1	N4	106.48°
N1	Cu1	N5	78.86°
N2	Cu1	N4	126.51°
N2	Cu1	N5	155.17°
N3	Cu1	N2	82.84°
N3	Cu1	N4	94.69°
N3	Cu1	N5	110.04°
N5	Cu1	N4	74.91°

Table S9 The selected bond length of the initial copper complex (Int-I).

Atom	**Atom**	**Length / Å**
N1	Cu1	1.941
N2	Cu1	2.169
N3	Cu1	1.999
N4	Cu1	2.282
N5	Cu1	2.251

Table S10 The Cu complex (Cu1) 3d-orbital occupancy and energy of the complex.

Atom	**Orbitals**	**Energy (in Hartree)**
Cu	dxy	-0.30100
	dxz	-0.26976
	Dyz	-0.26923
	dx^2-y^2	-0.28139
	dz^2	-0.26463

Table S11 The DFT calculated energy of the Cu^{2+} and Cu^{3+}

Species	**Energy**
Cu^{2+}	-2965.417
Cu^{3+}	-2965.198

28. References.

1. R. K. Saunthwal, J. Mortimer, A. J. Orr-Ewing and J. Clayden, *Chem. Sci.*, 2022, **13**, 2079–2085.
2. A. Y. Chen, P. W. Thomas, A. C. Stewart, A. Bergstrom, Z. Cheng, C. Miller, C. R. Bethel, S. H. Marshall, C. V. Credille, C. L. Riley, R. C. Page, R. A. Bonomo, M. W. Crowder, D. L. Tierney, W. Fast and S. M. Cohen, *J. Med. Chem.*, 2017, **60**, 7267–7283.

3. C. J. Clarke, L. Bui-Le, J. P. Hallett and P. Licence, *ACS Sustain. Chem. Eng.*, 2020, **8**, 8762–8772.
4. Silverman, *US Pat.*, 2013, US2013/0040359 A1.
5. M. E. Ahmed, M. Raghibi Boroujeni, P. Ghosh, C. Greene, S. Kundu, J. A. Bertke and T. H. Warren, *J. Am. Chem. Soc.*, 2022, **144**, 21136–21145.
6. D. F. Evans and D. A. Jakubovic, *J. Chem. Soc., Dalton Trans.*, 1988, **12**, 2927–2933.
7. D. F. Evans, *J. Chem. Soc.*, 1959, 2003–2005.
8. D. H. Grant, *J. Chem. Educ.*, 1995, **72**.
9. R. K. Birdwhistell and E. M. Schubert, *J. Chem. Educ.*, *Textbook Forum: Utilizing the Evans Method with a Superconducting NMR Spectrometer in the Undergraduate Laboratory*.
10. M. Raj, K. Makhal, D. Raj, A. Mishra, B. S. Mallik and S. K. Padhi, *Dalton Trans.*, 2023, **52**, 17797–17809.
11. S. S. Akhter, D. Srivastava, A. Mishra, N. Patra, P. Kumar and S. K. Padhi, *Chem. Eur. J.*, 2024, **30** ,e202403321.
12. B. M. Lindley, A. M. Appel, K. Krogh-Jespersen, J. M. Mayer and A. J. M. Miller, *ACS Energy Lett.*, 2016, **1**, 698–704.
13. M. Kolen, W. A. Smith and F. M. Mulder, *ACS Omega*, 2021, **6**, 5698–5704.
14. L. D. Field, N. Hazari and H. L. Li, *Inorg. Chem.*, 2015, **54**, 4768–4776.
15. S. Dey, M. E. Ahmed and A. Dey, *Inorg. Chem.*, 2018, **57**, 5939–5947.
16. P. L. Dunn, S. I. Johnson, W. Kaminsky and R. M. Bullock, *J. Am. Chem. Soc.*, 2020, **142**, 3361–3365.
17. S. Feng, J. Chen, R. Wang, H. Li, J. Xie, Z. Guo, T. C. Lau and Y. Liu, *J. Am. Chem. Soc.*, 2024, **146**, 21490–21495.
18. C. Costentin, S. Drouet, M. Robert and J. M. Savéant, *J. Am. Chem. Soc.*, 2012, **134**, 11235–11242.

29. Cartesian coordinates used for the DFT study.

Int-1 (catalyst)

Cu	-0.05845133	0.09697003	-0.13058958
N	0.33802430	-1.27154161	1.65197323
N	1.07630033	1.65481400	0.10745063
N	-1.60848640	1.60780942	-0.27854250
N	1.97687675	-0.78544204	-0.51103175
N	-1.47181562	-1.07320296	-0.92404736
C	1.24580309	-2.23227374	1.37075542
C	2.36681568	-0.76723034	-1.99729324

C	0.51961638	2.87875387	-0.01210741
C	-2.35647376	1.12844958	-1.47645895
H	-3.35187125	1.59252996	-1.55719174
H	-1.78375080	1.43451992	-2.36622197
C	2.38444198	1.49272827	0.38873826
C	1.51109423	-3.29161344	2.25057935
H	2.26227177	-4.03851916	1.98328800
C	-2.47985183	-0.37376186	-1.50383223
C	1.97343371	-2.15466674	0.04574706
C	2.55022222	0.67926982	-2.48277572
H	1.63026355	1.26749822	-2.35283502
H	3.38165802	1.19698347	-1.98215438
H	2.78331908	0.64763583	-3.55784326
C	-0.32083256	-1.33975866	2.82982632
H	-1.03176018	-0.53813058	3.03448028
C	1.23061689	-1.39182121	-2.81952907
H	1.01038496	-2.43084543	-2.53415857
H	0.31163380	-0.79634338	-2.72433342
H	1.52861462	-1.39885096	-3.87925884
C	2.86144695	0.06765352	0.34726620
H	2.83296918	-0.33729603	1.37116165
H	3.91139617	0.01917357	0.01712355
C	-0.12189594	-2.36412384	3.75597829
H	-0.68385276	-2.36869273	4.69182434
C	0.81088129	-3.36523614	3.45625018
H	0.99768974	-4.18280344	4.15658151
C	-2.46245879	1.71331013	0.99853347
C	-0.88380570	2.88776329	-0.55796347
H	-0.80164691	3.00413953	-1.65014598
H	-1.43960187	3.76108629	-0.18956017
C	1.27212426	4.02501836	0.25113743
H	0.81238688	5.01112129	0.16384471
C	-1.52656145	-2.42227547	-0.90004422
H	-0.71060869	-2.93488812	-0.39098084
C	3.67532307	-1.55142442	-2.22769840
H	4.50021314	-1.17081444	-1.60499300
H	3.55138084	-2.62632225	-2.02931951
H	3.97368364	-1.43693645	-3.28100957
C	3.19188637	2.59889866	0.66185427
H	4.25031043	2.45868472	0.88883278
C	-1.52715034	2.10200350	2.15472191
H	-0.66994898	1.41502058	2.21612165
H	-1.14531026	3.12900357	2.05353833
H	-2.08748263	2.04822384	3.09985374
C	2.61758055	3.87505257	0.61121726
H	3.22564614	4.75650193	0.82745329

C	-3.12488853	0.36242244	1.30499409
H	-3.88599354	0.09476071	0.55728963
H	-2.38954928	-0.45006687	1.36388495
H	-3.63207433	0.44210573	2.27818032
C	-3.55586488	-1.02231125	-2.11707414
H	-4.35202005	-0.42912891	-2.57104637
C	-3.59912174	-2.41886877	-2.11730648
H	-4.43269098	-2.94460166	-2.58838429
C	-2.57160730	-3.13217975	-1.48724275
H	-2.57475835	-4.22249218	-1.44521973
C	-3.57324992	2.77297907	0.84714400
H	-3.17881899	3.78398584	0.66774795
H	-4.28084015	2.51997732	0.04305138
H	-4.14244695	2.80506734	1.78905963
H	3.00148132	-2.53139927	0.18675722
H	1.48337316	-2.82962107	-0.67144076

Int-2 (catalyst + NH_3)

Cu	-0.20737021	0.12211788	-0.31436324
N	2.60850197	-0.75407870	-1.94804241
N	-0.00781875	0.15148170	1.61844827
N	-1.36357790	-1.74627386	0.23093706
N	1.37729139	1.72746864	-0.14262710
N	-2.59235617	0.62002941	-0.53746814
C	3.15546197	0.19542821	-1.15584829
C	0.72250401	3.11925627	-0.29807656
C	-0.85442355	-0.58007730	2.37469872
C	-2.54895256	-1.83764909	-0.64916312
H	-2.23651873	-2.20843325	-1.63517344
H	-3.27565477	-2.56943384	-0.25382549
C	0.94370218	0.92394498	2.18392610
C	4.33508603	-0.03970553	-0.42895248
H	4.77346989	0.76129656	0.17092610
C	-3.26157573	-0.51379223	-0.82963588
C	2.49181144	1.55638221	-1.14203359
C	-0.27362049	3.32961602	0.85238815
H	-0.98981814	2.49885993	0.92364289
H	0.22881588	3.44882563	1.82371823
H	-0.83769105	4.25418289	0.65815793
C	3.21047839	-1.95669141	-2.02282556
H	2.73852761	-2.69011080	-2.68311226
C	-0.03742248	3.18331081	-1.62911925
H	0.61270389	3.02117397	-2.50143569
H	-0.85925305	2.45637392	-1.65110222
H	-0.47711777	4.18701154	-1.73257130
C	1.92535115	1.54136743	1.23354039
H	2.76865424	0.83661561	1.17317636

H	2.33337402	2.47934187	1.63931229
C	4.37073838	-2.27965352	-1.31162727
H	4.81469027	-3.27261115	-1.40731884
C	4.94410207	-1.29737471	-0.49768648
H	5.85815720	-1.50081913	0.06543355
C	-0.49883136	-3.01692871	0.16955639
C	-1.83162484	-1.43038773	1.61725699
H	-2.77532927	-0.86914242	1.53898352
H	-2.05917831	-2.34609016	2.18412967
C	-0.80298572	-0.51781461	3.76895852
H	-1.49243129	-1.11946452	4.36404056
C	-3.23764866	1.79697289	-0.69377875
H	-2.67820224	2.69551239	-0.42630170
C	1.77290592	4.25008180	-0.26560256
H	2.41824241	4.20300662	0.62524220
H	2.40752509	4.25604985	-1.16387002
H	1.23697508	5.21110370	-0.23203960
C	1.04313638	1.03525957	3.57283972
H	1.81209797	1.67345082	4.01188442
C	0.71342139	-2.85163587	1.09921872
H	1.31135159	-1.97163674	0.81766708
H	0.42868169	-2.76376245	2.15833865
H	1.34893202	-3.74452293	1.00134094
C	0.14923955	0.31272993	4.37048426
H	0.20550592	0.38367855	5.45914797
C	0.02937407	-3.21046917	-1.25913207
H	-0.76423638	-3.41326930	-1.99295231
H	0.60615211	-2.33546567	-1.58019750
H	0.70553025	-4.07838878	-1.26220352
C	-4.58481569	-0.50675952	-1.29960843
H	-5.08863246	-1.45280881	-1.51273349
C	-5.23451588	0.71561247	-1.47941328
H	-6.26283312	0.74811228	-1.84741211
C	-4.54870330	1.89569996	-1.16272727
H	-5.01875561	2.87541620	-1.26895863
C	-1.30255545	-4.26831247	0.58103398
H	-1.68916274	-4.20534974	1.60959435
H	-2.14357881	-4.45961251	-0.10236969
H	-0.63153797	-5.13990756	0.53581810
H	3.27044303	2.30858968	-0.93581856
H	2.08235317	1.75661822	-2.13926090
N	-0.16996861	-0.06243788	-2.29763874
H	-0.37325888	0.81627493	-2.78451886
H	0.81109734	-0.34517432	-2.51532695
H	-0.80868100	-0.77069893	-2.67280721

Int-3 (catalyst + NH_2)

Cu	-0.10365551	0.00841852	-0.24498967
N	-2.69639417	0.65193363	-0.37994679
N	0.09089495	-0.08940968	1.63480134
N	1.19997472	1.71638386	0.03144410
N	-1.24475040	-1.71457565	-0.00005986
N	2.64455650	-0.64908085	-0.64034515
C	-3.19909082	-0.44020872	-0.98238420
C	-0.39428987	-3.01963645	-0.17565109
C	1.04317149	0.63612518	2.25703322
C	2.15205999	1.71319046	-1.10412346
H	1.54321848	1.72346172	-2.02473130
H	2.76657778	2.62657766	-1.08153595
C	-0.75957348	-0.89962941	2.30111497
C	-4.42076078	-0.43208195	-1.67571240
H	-4.78352136	-1.34680853	-2.15098442
C	3.06173661	0.51252924	-1.18124535
C	-2.42564834	-1.73769872	-0.90617708
C	0.66750585	-3.09544645	0.92835002
H	1.30582984	-2.20209204	0.93953502
H	0.23080844	-3.24559715	1.92614684
H	1.30284356	-3.96829969	0.71766847
C	-3.41996331	1.79278232	-0.43053849
H	-2.99679876	2.65720779	0.08513027
C	0.29920563	-3.00263400	-1.54137082
H	-0.41032877	-2.97412869	-2.38178951
H	1.00096156	-2.16274438	-1.61800487
H	0.87712370	-3.93371840	-1.63991399
C	-1.75717453	-1.58092524	1.42203646
H	-2.66510953	-0.96176261	1.39372763
H	-2.04183332	-2.56887878	1.80974633
C	-4.64330741	1.89318240	-1.09403837
H	-5.18630155	2.84032907	-1.09978075
C	-5.14880706	0.75620291	-1.74006814
H	-6.09965099	0.79450431	-2.27690925
C	0.39670759	3.04563015	0.08769772
C	1.89855170	1.45179163	1.34226276
H	2.82037757	0.89003808	1.14144811
H	2.19545652	2.39589459	1.81851139
C	1.17604409	0.56148536	3.64464626
H	1.94161420	1.15297241	4.14898756
C	3.45986479	-1.71996550	-0.74281274
H	3.09988915	-2.64455542	-0.28414346
C	-1.30457222	-4.26314313	-0.08876985
H	-1.89814179	-4.29495578	0.83737508
H	-1.97948832	-4.34690849	-0.95203028
H	-0.64900057	-5.14696120	-0.08919603

C	-0.67702753	-1.01091014	3.68834718
H	-1.36094505	-1.67087854	4.22376706
C	-0.58170049	2.98229905	1.26822119
H	-1.22555415	2.09429231	1.20499815
H	-0.06535057	2.98167201	2.23928866
H	-1.21789859	3.87897739	1.23698628
C	0.30481558	-0.26991292	4.35884950
H	0.39109458	-0.34111214	5.44532253
C	-0.37939968	3.25196217	-1.21866935
H	0.28088753	3.34731717	-2.09172252
H	-1.09749916	2.44499039	-1.39599461
H	-0.94486055	4.19135978	-1.12758854
C	4.29160264	0.63952050	-1.84890348
H	4.58651860	1.60558287	-2.26599079
C	5.11898385	-0.47983255	-1.96057689
H	6.08111529	-0.40883512	-2.47373814
C	4.69768327	-1.68786399	-1.38962031
H	5.31547026	-2.58710182	-1.43625431
C	1.34068820	4.25502589	0.27993116
H	1.96713752	4.17952737	1.18043877
H	1.98718556	4.42442766	-0.59301413
H	0.70580540	5.14624016	0.39833900
H	-3.11757646	-2.52069643	-0.55204663
H	-2.10061696	-2.02519641	-1.91434851
N	-0.14790197	0.19072901	-2.11337029
H	-0.21245682	-0.74601633	-2.54029360
H	-1.04946442	0.62484729	-2.36733929

Int-4 (catalyst + NH)

Cu	-0.15234521	0.05426881	-0.26366252
N	-2.55552998	0.70007069	-0.63029687
N	-0.01011933	-0.07026579	1.62253019
N	1.21919683	1.71257977	0.04016531
N	-1.27895279	-1.73113743	-0.05474520
N	2.64376397	-0.70993297	-0.57302159
C	-3.19913302	-0.42022660	-1.01656169
C	-0.41644176	-3.01946202	-0.25260999
C	0.94403524	0.63399831	2.26943322
C	2.20423654	1.65584108	-1.07111552
H	1.61930180	1.65662375	-2.00892510
H	2.82297680	2.56730672	-1.06089407
C	-0.85306973	-0.90936121	2.26467762
C	-4.53049618	-0.41490735	-1.45555384
H	-5.01403468	-1.35041589	-1.74745542
C	3.10463453	0.44494615	-1.09732222
C	-2.43447744	-1.72683668	-0.99126847
C	0.63728334	-3.08939594	0.86001681

H	1.26494586	-2.18861286	0.87897235
H	0.19409977	-3.24621943	1.85405772
H	1.28091861	-3.95944278	0.66691170
C	-3.23530787	1.86760204	-0.67778058
H	-2.69865246	2.75683065	-0.34835851
C	0.26662983	-2.94747394	-1.62536500
H	-0.44373412	-3.02718547	-2.46096269
H	0.85471879	-2.02467789	-1.73601898
H	0.95467245	-3.80008689	-1.72191896
C	-1.82026697	-1.60918318	1.35458866
H	-2.74408718	-1.01166450	1.30348643
H	-2.09561511	-2.60312868	1.73816863
C	-4.55822190	1.96488090	-1.11195453
H	-5.05709974	2.93533712	-1.12513033
C	-5.21949220	0.79882790	-1.51478894
H	-6.25504368	0.83302906	-1.85970226
C	0.47237198	3.07632458	0.05266033
C	1.85461730	1.42201538	1.37558267
H	2.75631994	0.81815128	1.20014665
H	2.17598368	2.35822321	1.85395226
C	1.06043332	0.53481924	3.65777004
H	1.82710734	1.10281695	4.18776354
C	3.44564300	-1.79262354	-0.65980712
H	3.06371039	-2.71291100	-0.21248727
C	-1.30653755	-4.28029951	-0.18782696
H	-1.88469553	-4.35714428	0.74592904
H	-1.99273065	-4.36213143	-1.04202604
H	-0.64624970	-5.15915669	-0.22233802
C	-0.78767830	-1.04409419	3.65102125
H	-1.46765923	-1.71841649	4.17448490
C	-0.57013232	3.05457561	1.18146054
H	-1.25146840	2.19692305	1.10050336
H	-0.10578554	3.03352558	2.17829182
H	-1.16375155	3.97884502	1.13303621
C	0.17853618	-0.30569793	4.34905800
H	0.25060942	-0.39444562	5.43520006
C	-0.19247904	3.29455361	-1.31504325
H	0.53922136	3.51960517	-2.10285527
H	-0.78026989	2.42022973	-1.62989209
H	-0.86627568	4.16116505	-1.24968581
C	4.35901711	0.55550027	-1.71642322
H	4.69066732	1.51490076	-2.12106763
C	5.16932060	-0.57864276	-1.81216229
H	6.14861783	-0.52264304	-2.29200873
C	4.70302346	-1.78094161	-1.26914596
H	5.30384085	-2.69133590	-1.30460457

C	1.44678262	4.25074487	0.31070437
H	1.95326764	4.19496110	1.28523539
H	2.20208600	4.36298750	-0.47923603
H	0.85357723	5.17725663	0.31758414
H	-3.13362017	-2.53199565	-0.70979447
H	-2.06097625	-1.96653530	-1.99731121
N	-0.03051024	0.18983552	-2.07779103
H	-0.92880637	0.01468678	-2.57618688

Int-5 (catalyst + NH-NH_3)

Cu	0.21228783	-0.19146462	-0.28425930
N	2.61415615	-0.58769033	-0.31406551
N	0.00474054	-0.15073846	1.68672621
N	-1.44729505	-1.75996021	-0.03977633
N	1.34022286	1.79657974	0.31318637
N	-2.58335958	0.69085968	-1.88540447
C	3.26529584	0.54689262	-0.64822449
C	0.42921506	3.01558395	0.19158155
C	-0.90179309	-0.95829829	2.27624388
C	-2.63824115	-1.56420782	-0.93692407
H	-2.36569192	-1.87838152	-1.95098685
H	-3.46187292	-2.21396337	-0.59600866
C	0.82922025	0.60918962	2.44075170
C	4.58643481	0.53560883	-1.12390368
H	5.08178157	1.47979939	-1.36297788
C	-3.14542601	-0.13928949	-0.97748737
C	2.51913210	1.86291055	-0.56087614
C	-0.88349471	2.72612966	0.93814446
H	-1.37703701	1.83079102	0.52772560
H	-0.72590465	2.57468506	2.01689437
H	-1.55910811	3.58625530	0.81758207
C	3.25433720	-1.76613173	-0.47781417
H	2.69436985	-2.66311617	-0.20375246
C	0.10365882	3.26275577	-1.29158975
H	0.94167449	3.73656193	-1.82561935
H	-0.14841583	2.32201326	-1.79842314
H	-0.75506233	3.94748544	-1.35248372
C	1.77034613	1.52097959	1.70567852
H	2.75669494	1.03223467	1.67775549
H	1.91163002	2.44634978	2.28688113
C	4.55911305	-1.86682618	-0.96260932
H	5.02781930	-2.84647112	-1.07323725
C	5.24054634	-0.68653477	-1.28912679
H	6.26633674	-0.71967604	-1.66353157
C	-0.82217747	-3.15387465	-0.24293945
C	-1.91316911	-1.58480167	1.36561072

H	-2.76342496	-0.88645712	1.35849195
H	-2.29577384	-2.52618431	1.78886954
C	-0.96678322	-1.09251210	3.66536047
H	-1.70194306	-1.76558533	4.11014803
C	-3.00131135	1.96836048	-1.96319441
H	-2.51453102	2.58745902	-2.72053890
C	1.08221787	4.28941996	0.76970909
H	1.19914593	4.25039766	1.86341600
H	2.06635459	4.48252026	0.31471805
H	0.43390020	5.14977502	0.54072164
C	0.80713557	0.53537867	3.83641519
H	1.48157983	1.16527810	4.41968576
C	0.23519210	-3.37187632	0.84969929
H	0.93902186	-2.52812152	0.88595406
H	-0.21212496	-3.50120347	1.84626545
H	0.79932887	-4.28718476	0.61718117
C	-0.08913157	-0.34207128	4.45401964
H	-0.11699828	-0.42632086	5.54268485
C	-0.13300622	-3.21197363	-1.61207548
H	-0.84973532	-3.11199022	-2.44188524
H	0.64387211	-2.43728631	-1.69264561
H	0.35033025	-4.19407881	-1.72420539
C	-4.18507609	0.29887043	-0.14341365
H	-4.66305315	-0.40113267	0.54498667
C	-4.60956418	1.63044272	-0.21577252
H	-5.41040106	1.98892660	0.43475982
C	-4.00345900	2.48673529	-1.14003574
H	-4.30432551	3.53137955	-1.23451620
C	-1.87817366	-4.27502458	-0.16674522
H	-2.45424506	-4.24921344	0.77115831
H	-2.57966907	-4.23894616	-1.01347991
H	-1.35659979	-5.24360409	-0.20677332
H	3.22767426	2.65185167	-0.24463442
H	2.18548942	2.10893139	-1.57874409
N	0.61038024	0.06771849	-2.18205548
H	1.40636729	-0.53912039	-2.42096105
N	-0.39589606	-0.25421980	-3.18189332
H	-0.17548698	0.19538214	-4.08337187
H	-0.50956140	-1.26809113	-3.35394443
H	-1.33562599	0.13766783	-2.79955490

Int-6 (catalyst + NH_2-NH_2)

Cu	0.23564115	-0.10030316	-0.17618867
N	-2.48035987	0.72687951	-1.99787609
N	-0.04270699	0.23041636	1.72501737
N	1.63404907	1.65315932	0.19133365
N	-1.51390512	-1.47051342	0.20264558

N	2.47223960	-0.93927872	-0.39571676
C	-3.14782454	-0.21668359	-1.29567411
C	-1.05890749	-2.90799122	0.56665878
C	0.90846858	0.87583691	2.42899741
C	2.81937039	1.48609644	-0.67702016
H	2.58861372	1.86923132	-1.68213668
H	3.66523895	2.09058630	-0.30351334
C	-1.16752547	-0.22782129	2.31402187
C	-4.47932103	-0.03121586	-0.88869182
H	-4.98956820	-0.82154337	-0.33345280
C	3.28883473	0.05197187	-0.80731183
C	-2.42140177	-1.50806517	-1.00008025
C	0.06354999	-2.85084136	1.61586879
H	0.88520234	-2.19613536	1.29435330
H	-0.29563394	-2.50402904	2.59505559
H	0.45877428	-3.86882312	1.75314628
C	-3.11190397	1.87915621	-2.29568928
H	-2.53188573	2.61197656	-2.86474204
C	-0.52764367	-3.59235131	-0.70034798
H	-1.33808693	-3.88164996	-1.38590594
H	0.16487929	-2.94018503	-1.24738390
H	0.00292126	-4.51041285	-0.40710639
C	-2.17439649	-0.79791758	1.35968523
H	-2.75060415	0.05638016	0.96991179
H	-2.89147914	-1.45510755	1.87302036
C	-4.43072865	2.14748022	-1.91546705
H	-4.89699176	3.09788440	-2.18311501
C	-5.12849148	1.16796269	-1.19936941
H	-6.16315538	1.33369881	-0.88952509
C	0.97917073	3.03396635	-0.00818305
C	2.04911962	1.40626477	1.60763683
H	2.85114657	0.65143733	1.59925902
H	2.46913843	2.31543819	2.06723608
C	0.78693675	1.03272750	3.81173529
H	1.56641630	1.55427394	4.37008435
C	2.89477884	-2.21615835	-0.54088141
H	2.21425395	-2.99245146	-0.18665614
C	-2.21791704	-3.74965438	1.14169825
H	-2.53376235	-3.40870342	2.13883351
H	-3.09579555	-3.77496504	0.47853514
H	-1.85840261	-4.78495876	1.24962103
C	-1.36188696	-0.08314923	3.68911706
H	-2.27512244	-0.46060875	4.15229105
C	-0.10178335	3.28000552	1.05638946
H	-0.88660432	2.51104561	1.02196509
H	0.30488965	3.33569414	2.07652551

H	-0.57091331	4.25121989	0.83802916
C	-0.36021268	0.53949883	4.44433222
H	-0.48134287	0.65441206	5.52398610
C	0.28373216	3.06610025	-1.37525506
H	0.97005471	2.90245954	-2.21987955
H	-0.52271546	2.31945016	-1.40817640
H	-0.17064856	4.05862905	-1.51588272
C	4.54786270	-0.20007655	-1.37566235
H	5.17916365	0.63724058	-1.68313698
C	4.96699833	-1.52116484	-1.53899396
H	5.93855129	-1.74281679	-1.98727463
C	4.12307526	-2.55449716	-1.10991456
H	4.40913836	-3.60351264	-1.20792718
C	2.03449538	4.15644783	0.07506602
H	2.60646818	4.11779666	1.01565364
H	2.74026987	4.12400721	-0.76811982
H	1.51673179	5.12717816	0.04061360
H	-3.17778498	-2.29752372	-0.86286462
H	-1.79575419	-1.77405706	-1.86304021
N	0.26072797	-0.05060701	-2.19378922
H	-0.71705846	0.28577195	-2.37653760
H	0.91328019	0.67311185	-2.52268323
N	0.45175382	-1.28734520	-2.92080759
H	0.45744808	-1.06519921	-3.92540081
H	1.39585362	-1.62199007	-2.69582644

Int-7 (catalyst + NH-NH$_2$)

Cu	-0.23727376	0.09346715	-0.26341881
N	2.51551261	-0.89697895	-1.67045887
N	0.08294216	0.12718035	1.68014070
N	-1.36762643	-1.67757538	0.27063010
N	1.41617978	1.70175822	-0.10043394
N	-2.57684050	0.73688261	-0.43165491
C	3.14008663	0.21254123	-1.21136885
C	0.78023620	3.10556403	-0.14829075
C	-0.72828130	-0.62626334	2.44790352
C	-2.58239396	-1.71128442	-0.57604855
H	-2.28713348	-1.98463522	-1.60082226
H	-3.28626997	-2.48664098	-0.23086407
C	1.12311391	0.79828950	2.20744823
C	4.47021471	0.18092090	-0.76160728
H	4.94371354	1.10083259	-0.41052437
C	-3.30468852	-0.38281802	-0.62995983
C	2.36520204	1.51089383	-1.23897223
C	-0.18881298	3.25052374	1.03701801
H	-0.92413979	2.43451547	1.06107092
H	0.33773880	3.27579796	2.00310608

H	-0.72860880	4.20367131	0.93249927
C	3.19709580	-2.05933495	-1.68240648
H	2.65730507	-2.92965246	-2.06568244
C	0.00016938	3.27291190	-1.46153473
H	0.66264289	3.30882372	-2.33911169
H	-0.72104086	2.45926825	-1.60383722
H	-0.54526179	4.22820291	-1.42190244
C	2.05731843	1.44142093	1.21626089
H	2.88446101	0.72973154	1.06777962
H	2.50860132	2.34950338	1.64529834
C	4.51849451	-2.17798229	-1.24024738
H	5.02277309	-3.14587698	-1.27295464
C	5.16834905	-1.03108541	-0.77140105
H	6.20298883	-1.07717947	-0.42311272
C	-0.56596402	-2.99620363	0.16861321
C	-1.78657972	-1.37417603	1.68697737
H	-2.68553736	-0.74119429	1.64270574
H	-2.07315552	-2.29248097	2.21859804
C	-0.56389241	-0.67856762	3.83328277
H	-1.22878605	-1.29359629	4.44249649
C	-3.20581609	1.92845687	-0.51342618
H	-2.59193004	2.81302651	-0.33449798
C	1.84139450	4.22390568	-0.05780824
H	2.46558926	4.14544169	0.84547293
H	2.49828978	4.25026446	-0.93988915
H	1.31594802	5.19051992	-0.01031486
C	1.34706712	0.79394359	3.58820227
H	2.18775640	1.35119846	4.00632712
C	0.71711421	-2.87213109	1.00275640
H	1.32590181	-2.01697212	0.67471342
H	0.51149036	-2.77043177	2.07826949
H	1.30965511	-3.78911087	0.86475091
C	0.48205447	0.05769702	4.40586199
H	0.63580182	0.03935713	5.48741096
C	-0.17046927	-3.24607607	-1.29343569
H	-1.03215826	-3.45684977	-1.94311042
H	0.39612730	-2.39721396	-1.69767752
H	0.48527337	-4.12856165	-1.32544446
C	-4.67712741	-0.34714050	-0.91751977
H	-5.22583193	-1.28162214	-1.05728732
C	-5.31617719	0.89142668	-1.01406908
H	-6.38415938	0.94763519	-1.23821014
C	-4.56600297	2.05553760	-0.80483952
H	-5.02250640	3.04585849	-0.85843039
C	-1.38665950	-4.20314364	0.66964156
H	-1.63395736	-4.13502403	1.73946967

H	-2.31580390	-4.34174638	0.09710379
H	-0.77596122	-5.10891083	0.53409607
H	3.08738624	2.34182133	-1.27970846
H	1.76328002	1.53951136	-2.16068258
N	-0.11756599	0.08929287	-2.19474843
H	0.74239776	-0.50877868	-2.30783660
N	-1.05444039	-0.32610056	-3.00898772
H	-1.91511992	0.22135920	-3.08112750
H	-0.96422321	-1.18858242	-3.55658625

Int-8 (catalyst + NH-NH)

Cu	-0.20414960	0.15562884	-0.25832792
N	2.62268827	-0.59396356	-1.97911104
N	0.00349146	0.17488163	1.68428577
N	-1.20485580	-1.78244448	0.25928012
N	1.33600821	1.81226788	-0.08078217
N	-2.57327133	0.51320349	-0.56429440
C	3.12050783	0.29080664	-1.08182294
C	0.62136586	3.16667132	-0.28098608
C	-0.76251866	-0.65021896	2.43027596
C	-2.37958882	-1.93020842	-0.63158415
H	-2.02879239	-2.15406058	-1.64885179
H	-3.01826644	-2.77303942	-0.31525075
C	0.91656338	0.98680596	2.25300304
C	4.21850608	-0.03325182	-0.26993121
H	4.64050375	0.71707860	0.40176283
C	-3.21637271	-0.67109632	-0.68213299
C	2.48817783	1.66557913	-1.04295746
C	-0.41472208	3.33905068	0.83981218
H	-1.08319974	2.46844020	0.89633216
H	0.05104475	3.49436547	1.82422328
H	-1.02361046	4.22787870	0.61778117
C	3.16870290	-1.82334042	-2.05371085
H	2.72894429	-2.49973726	-2.79094346
C	-0.10855710	3.16749074	-1.62923242
H	0.56853872	3.03013359	-2.48422862
H	-0.88137540	2.38999610	-1.65849222
H	-0.60410374	4.14187940	-1.75556590
C	1.85693408	1.68029601	1.31292794
H	2.75868904	1.05115700	1.28580195
H	2.17522811	2.65269200	1.71798019
C	4.23831726	-2.23225341	-1.25320215
H	4.64102726	-3.24183409	-1.35101888
C	4.77608325	-1.31414571	-0.34652853
H	5.62471319	-1.58431898	0.28579833
C	-0.23155322	-2.97044449	0.16398393
C	-1.69216791	-1.53336607	1.65376565

H	-2.66558827	-1.02203941	1.58829109
H	-1.87592062	-2.47320365	2.19412578
C	-0.67770056	-0.63960783	3.82312764
H	-1.29999550	-1.31715542	4.40994659
C	-3.30274416	1.64721565	-0.64618857
H	-2.75704240	2.58631677	-0.53753311
C	1.61781534	4.34288857	-0.24748778
H	2.23093973	4.35233575	0.66659841
H	2.28462265	4.34369925	-1.12210315
H	1.03998820	5.27949782	-0.26706696
C	1.03935933	1.05861061	3.64333095
H	1.77325853	1.73262299	4.08828323
C	1.07598044	-2.60969499	0.88614253
H	1.52844779	-1.70563580	0.45042289
H	0.92934443	-2.44704942	1.96401032
H	1.78273766	-3.44437920	0.76808178
C	0.22220451	0.24287679	4.43270917
H	0.30153101	0.27881551	5.52136726
C	0.08355202	-3.26010034	-1.31114739
H	-0.75527394	-3.74247999	-1.83337361
H	0.36209241	-2.34972562	-1.85738609
H	0.94052536	-3.94795453	-1.35210184
C	-4.60066192	-0.75423169	-0.88381546
H	-5.07632472	-1.73442174	-0.95921259
C	-5.34457983	0.42450341	-0.97958236
H	-6.42451121	0.38570466	-1.13911896
C	-4.68315046	1.65201603	-0.85527979
H	-5.22196024	2.59928639	-0.91339505
C	-0.82965654	-4.24720004	0.79219732
H	-0.89525573	-4.18583278	1.88843307
H	-1.82562193	-4.47940881	0.38527140
H	-0.16497275	-5.09087220	0.55133197
H	3.26849435	2.39649057	-0.77436674
H	2.12355561	1.91135331	-2.04705964
N	-0.04056371	-0.02694440	-2.19056607
H	0.96971841	-0.28435293	-2.45439195
N	-0.80807930	0.12484535	-3.15440145
H	-1.75029274	0.39769378	-2.78786493

Int-9 (catalyst + N-NH)

Cu	-0.13527283	0.03775261	-0.20370465
N	2.49376066	-0.77851164	-0.89842081
N	0.17156459	-0.12585297	1.70467107
N	-1.36367428	-1.70517124	0.13988578
N	1.33094002	1.67842335	0.07065664
N	-2.60255738	0.75795613	-0.21529314
C	3.07812479	0.39460912	-1.21801274

C	0.62727112	3.04993442	0.18762362
C	-0.65944448	-0.92049134	2.40627372
C	-2.60770683	-1.66660129	-0.65830636
H	-2.40541215	-2.04996486	-1.66880513
H	-3.35363508	-2.35280176	-0.22146553
C	1.18834804	0.53993425	2.28347183
C	4.39116843	0.47666312	-1.70815795
H	4.82302387	1.45318624	-1.93918491
C	-3.24508420	-0.29421899	-0.75899532
C	2.26690461	1.65974268	-1.08215542
C	-0.31024910	3.01762540	1.40313053
H	-0.99917373	2.16364418	1.35858267
H	0.24595267	2.97078225	2.35122174
H	-0.90032730	3.94583536	1.41315678
C	3.21657081	-1.90551228	-1.06174760
H	2.72449966	-2.84118128	-0.78584006
C	-0.17649852	3.31775739	-1.09109064
H	0.46867639	3.45747979	-1.96991486
H	-0.88967049	2.51067345	-1.29655998
H	-0.75188576	4.24498780	-0.95249719
C	2.05154688	1.32668601	1.34102981
H	2.92183022	0.70378619	1.08734673
H	2.44676755	2.22593324	1.83458048
C	4.52526112	-1.91984172	-1.55190034
H	5.05845878	-2.86625298	-1.66064775
C	5.12434922	-0.69935917	-1.88488499
H	6.14811585	-0.66281949	-2.26433897
C	-0.59697179	-3.02850174	-0.12780184
C	-1.74688579	-1.55460920	1.59046440
H	-2.62767175	-0.89648645	1.63547701
H	-2.04890413	-2.52632883	2.00791886
C	-0.49883686	-1.07058359	3.78412916
H	-1.17208640	-1.71931769	4.34639032
C	-3.20515707	1.96727315	-0.27850010
H	-2.67582769	2.79871957	0.18881588
C	1.63860554	4.20217456	0.37400965
H	2.27898689	4.06932936	1.25829703
H	2.27486264	4.35052184	-0.51025695
H	1.06213366	5.12763013	0.52435780
C	1.40537094	0.43292072	3.65909311
H	2.22574084	0.97986705	4.12631401
C	0.56502164	-3.15562068	0.86572954
H	1.22913310	-2.28203505	0.82559624
H	0.21666643	-3.29737714	1.89928855
H	1.14844467	-4.04705007	0.59208278
C	0.54745264	-0.38013955	4.40988919

H	0.69671037	-0.47929895	5.48725168
C	-0.04188364	-2.99828352	-1.55711173
H	-0.83013778	-2.95259529	-2.32295556
H	0.63967708	-2.14837989	-1.69254326
H	0.52627078	-3.92449135	-1.72857068
C	-4.48667345	-0.17473258	-1.40647321
H	-4.96104000	-1.06094068	-1.83421998
C	-5.08729474	1.08178606	-1.48393091
H	-6.04857216	1.20618688	-1.98724582
C	-4.43830016	2.17558000	-0.89549884
H	-4.87464397	3.17573903	-0.91546534
C	-1.53019532	-4.24569489	0.03256843
H	-2.01164462	-4.27791900	1.02189249
H	-2.30693702	-4.28131353	-0.74463866
H	-0.91686920	-5.15396524	-0.06603469
H	2.96021698	2.51344580	-1.02755793
H	1.67135824	1.78513650	-2.00147378
N	-0.15107258	0.24313965	-2.09800262
N	-1.02451174	0.12901696	-2.88629068
H	-2.02020313	-0.12117036	-2.61843277

Int-10 (catalyst + N-N)

Cu	-0.18275709	0.08859295	-0.28574924
N	2.55928604	-0.84152650	-1.31822235
N	0.05040870	-0.03278338	1.63413200
N	-1.40338294	-1.70709988	0.09892462
N	1.36472175	1.66807451	-0.03303950
N	-2.56552175	0.76880883	-0.60150150
C	3.22020815	0.31014564	-1.07299020
C	0.67735751	3.05363896	-0.04777144
C	-0.80242077	-0.80697828	2.33785062
C	-2.61029394	-1.67485780	-0.76835295
H	-2.31198353	-1.89975524	-1.80224327
H	-3.32265903	-2.45620467	-0.45786538
C	1.03825839	0.66670395	2.22896150
C	4.60031024	0.34929820	-0.81906883
H	5.08838553	1.30654425	-0.62292074
C	-3.31796570	-0.34342764	-0.74208470
C	2.42137426	1.58910768	-1.09859070
C	-0.33902809	3.11017926	1.10171701
H	-1.04584378	2.27026209	1.05329905
H	0.14829386	3.10681097	2.08797576
H	-0.90770601	4.04778751	1.01732376
C	3.26547746	-1.98847944	-1.29381955
H	2.70402231	-2.90603600	-1.48961890
C	-0.04296154	3.23720467	-1.38937498
H	0.65574985	3.30821233	-2.23472250

H	-0.74693010	2.41591888	-1.57603215
H	-0.61718623	4.17478446	-1.35421892
C	1.97766048	1.37498986	1.30313513
H	2.83663043	0.70270370	1.14786670
H	2.37876581	2.28544784	1.77164757
C	4.64191843	-2.04437688	-1.04834410
H	5.15942066	-3.00567536	-1.04793704
C	5.32436468	-0.84734355	-0.80976007
H	6.39899571	-0.84389409	-0.61334425
C	-0.59767136	-3.01039796	-0.10849146
C	-1.83587847	-1.52406344	1.52429654
H	-2.75484927	-0.91694514	1.52811118
H	-2.09461580	-2.48846697	1.98619121
C	-0.70278608	-0.88235046	3.72739984
H	-1.39284988	-1.51689171	4.28556462
C	-3.19643946	1.96308435	-0.60484244
H	-2.57089846	2.84738115	-0.47955906
C	1.69399195	4.20190958	0.12729110
H	2.30153039	4.09949223	1.03863111
H	2.36374286	4.30295110	-0.73840398
H	1.12359016	5.13888725	0.21658535
C	1.18413686	0.63607837	3.61758998
H	1.98061344	1.21245087	4.09056388
C	0.58045587	-3.04720183	0.87560794
H	1.23171760	-2.16948539	0.76098808
H	0.25119187	-3.11640666	1.92303290
H	1.17709519	-3.94530861	0.65815713
C	0.29841088	-0.14389881	4.36904060
H	0.39475557	-0.18490372	5.45602038
C	-0.04734226	-3.04490454	-1.53975900
H	-0.83923031	-3.07576021	-2.30175359
H	0.60928753	-2.18433375	-1.72499968
H	0.55047306	-3.96122086	-1.65509202
C	-4.71146917	-0.29745844	-0.89100293
H	-5.27418065	-1.22868488	-0.98516819
C	-25.35172970	0.94349088	-0.90789926
H	-6.43597785	1.00682955	-1.02420548
C	-4.57731878	2.09967383	-0.75821711
H	-5.02854757	3.09338858	-0.75357958
C	-1.49084890	-4.24922360	0.11514090
H	-1.96706299	-4.25639597	1.10716451
H	-2.27001287	-4.33986687	-0.65543398
H	-0.85046468	-5.14169721	0.04937216
H	3.11806455	2.43268837	-0.97860093
H	1.93294785	1.69641622	-2.07538524
N	-0.25287780	0.05157615	-2.33209661

N	-0.39162617	0.06959672	-3.43200400